ADAPTATION OF LOCOMOTOR CONTROL IN ABLE AND IMPAIRED HUMAN WALKING

A Dissertation
Presented to
The Academic Faculty

by

Megan E. Toney

In Partial Fulfillment
of the Requirements for the Degree
Doctor of Philosophy in the
School of Applied Physiology

Georgia Institute of Technology
August 2014

ADAPTATION OF LOCOMOTOR CONTROL IN ABLE AND IMPAIRED HUMAN WALKING

Approved by:

Dr. Young-Hui Chang, Advisor
School of Applied Physiology
Georgia Institute of Technology

Dr. Lena Ting
Wallace H. Coulter Department of Biomedical Engineering
Georgia Institute of Technology

Dr. Richard Nichols
School of Applied Physiology
Georgia Institute of Technology

Dr. Randy Trumbower
Department of Rehabilitation Medicine
Emory University

Dr. Boris I. Prilutsky
School of Applied Physiology
Georgia Institute of Technology

Date Approved: June 13, 2014

To anyone, past, present, or future with a limb deficiency or mobility impairment.

Do or do not. There is no try. – Yoda

ACKNOWLEDGEMENTS

I enjoy reading the Acknowledgements more than any other section in dissertation documents. I like to witness the love and support behind every endeavor. Now that I sit to write mine, I am struck by how inadequate words are to describe my gratitude to everyone who made this journey with me. I only hope that my attempt to capture these feelings will begin to convey the depth my appreciation.

I first need to thank my advisor, Young-Hui Chang. Thank you for all of your support the last five years. Thank you for pushing me and constantly questioning my assumptions. I did not always appreciate these lessons when they were administered, but in retrospect, I know I am a more critical and better scientist than I was when I started thanks to your guidance.

I have been fortunate to work with some incredible intellectuals in my time at Georgia Tech, foremost of all are my committee members. Richard, thank you for always being available to tackle even the smallest of questions. I do not see how anyone could be a better department chair than you. Thank you for all your guidance and genuine interest in my research. Boris, thank you for all your detailed comments on every aspect of this body of work. I believe that I will walk away with no loose ends because of your feedback. Thank you also for the albeit brief experience working in an animal lab. I have not yet told my cats what you and Richard do for a living. Lena, thank you for your insightful and always constructive feedback. I have always been a little nervous whenever I show you my data because if there is a flaw, I know you will find it. Thank you for inevitably pushing me to constantly rethink and improve my results and

conclusions. Randy, thank you for letting me sit in on your class for a whole semester. I value all I learned from you both in that class and outside of it. Thank you for reminding me to consider both the practicality and the validity of my clinical conclusions.

For members of the Neuromechanics Lab members who helped with data collections, processing, etc. Emily L., Alli G., Tyler P. Katie B., and Gloria C. Much of this work would have been incomplete without your help.

Chris Hovorka, thank you for never keeping it brief. I have considered immeasurable other dimensions of my research because of our meandering conversations.

To Lee Childers, thank you for the continuous support and feedback regarding all aspects of amputee locomotion and for showing me how not to completely melt down at the end of the journey.

To Bill C. Thank you for being a tremendous and loyal friend. I appreciated all of our carpool complain fests. Thank you for listening, for cheering me on right to the end, and providing your dissertation for format and content reference.

To Jasper and Arick, thank you for providing so much of the foundation of the UCM analysis, creating new questions, and always being available to talk science. I am honored to have attempted to follow-up on your work and hopefully advance it some. I am forever indebted to both of you for foraging this path before me.

To Ploy, thank you for establishing the foundation for much of the adaptation work. I would not have completed as much of this work as I would have without you. Your thoughtful comments and motivating sentiment helped me over many hurdles.

Brian, thank you for sharing cube space, listening to me talk to my computer, collaborating on Matlab problems, and generally being way smarter than me.

To Tracy. Words are not enough. Thank you for being an incredible friend and an even better human being. You are someone I look up to, admire, and aspire to be more like every single day. Thank you for being there to bounce ideas back and forth. Thank you for being support and not competition. Thank you for taking time to listen to me freak out about my dissertation, research, and life in general. I have no doubt that you will succeed in everything you choose to do because you are a rock star. If you ever need a reminder just call me and I will provide it. Thank you for being the voice of reason more times than I can count, especially in hard times when I needed it most. I would not have made it through this adventure called grad school without you. I am going to miss you terribly, but I take comfort knowing that I can always pick up the phone and call you.

To MOyer. Thank you for being my sounding board for life issues these last five years. I know we will always be there for each other when we need to psychoanalyze each other's crazy. To all of my girlfriends: Beth, Anne, Kate, Rachel, Liz, Kalyn, Lauren, etc. I am so lucky to have such amazing, strong, inspiring women in my life and I appreciate every lesson and experience we have shared.

To Darren. Thank you for being my support at home. I will always appreciate coming home to dinner and a hug when I have to work late. Thank you for caring about my well-being, making me laugh, and holding me close when I need a hug more than anything. Thank you for believing in me even when I began to doubt myself. You constantly challenge me in every aspect of life, which is something I desperately need, even if I don't always appreciate it. Thank you for listening to me talk about my research and pretending to care about it more than I think you really do. I love you tons.

To Brother Brian. Thank you for being a partner in crime throughout life for as little trouble as we ever managed to get ourselves into. I appreciated being able to have someone else to complain to and commiserate with about grad school life and especially writing these last few years.

Finally, I have to thank my parents, without whom I would not have made it through this process. Thank you for being such amazing role models for how to succeed in life both personally and professionally. I cannot begin to express how much it meant to me knowing that you understood what I was going through during this process. I must thank you both more than anyone else for getting me here today. Thank you for raising me to be adventurous, curious, and stubborn. I think those traits contributed to me getting to grade 22. Thank you for help with math and chemistry homework throughout the years. Thank you for sending me to the college of my choice. Thank you for always listening and doing your best to understand my research. More than anything else, thank you for loving me through thick and thin. I love you both so much and hope that I always make you proud.

TABLE OF CONTENTS

LIST OF TABLES

LIST OF FIGURES

SUMMARY

Extensive research has documented the stereotypical kinematic and kinetic patterns in healthy human walking, but we have a limited understanding of the neuromechanical control principles that contribute to their execution. Furthermore, the strategies used to adapt human walking to morphological or environmental constraints are poorly understood. After a traumatic injury, like amputation, regaining independent mobility is a primary goal of rehabilitation. Without a clear understanding of the neuromechanical principles governing locomotion, monitoring and quantitatively improving gait rehabilitation outcomes is challenging. The purpose of this doctoral work was to identify controlled variables in able and impaired human walking and to compare the control strategies used to adapt to a novel walking environment both with and without amputation.

I apply an uncontrolled manifold (UCM) analysis to test whether likely goal variables of human walking are selectively stabilized through step-to-step variability structure. I found that both able-bodied subjects and subjects with an amputation maintain consistent whole body dynamics and leg power production by exploiting inherent motor abundance. Consistent leg power production is accomplished primarily through step-to-step leg force corrections that are driven by variable timing of ankle torque production. Covariance between ankle and knee torques enable robust motor control in able-bodied individuals, but this stabilizing mechanism is absent in individuals with a transtibial amputation. This coordinated joint torque control also appears to assist able-bodied short-term adaptation, invoked by split-belt treadmill walking. However, loss

of ankle motor control and distal sensory feedback due to amputation appears to limit reactive, feedback driven adaptation patterns in subjects with an amputation. Ultimately, this work highlights the role of intact distal sensorimotor function in locomotor control and adaptation. The major findings I present have substantial implications for gait rehabilitation and prosthetic design.

CHAPTER 1

INTRODUCTION

Independent locomotion is an essential component of daily living and loss of this ability has a profoundly deleterious effect on one's quality of life. Lower-limb loss is an especially debilitating impairment, resulting in slower walking speeds, higher metabolic costs, and reduced ability to live independently (Hermodsson, Ekdahl et al. 1994; Waters and Mulroy 1999; Nolan, Wit et al. 2003). Returning impaired individuals to lives of functional independence and community involvement is the ultimate goal of gait rehabilitation (Munin, Espejo-DeGuzman et al. 2001). However, only 36% of individuals with a lower-limb amputation are community ambulators one year post-surgery (Davies and Datta 2003). Those who are independent walkers often ambulate with noticeable deviations and compensation strategies, which can lead to further injury and permanent disability (Geertzen, Martina et al. 2001; Munin, Espejo-DeGuzman et al. 2001). Current gait rehabilitation strategies do not effectively restore complete function to impaired walkers.

Because we lack a complete understanding of the higher-level neuromechanical control principles, gait rehabilitation strategies cannot be quantitatively validated or advanced. Gait rehabilitation strategies are currently based on trial and error attempts to mimic able-bodied movement patterns and rely primarily on subjective evaluation of gait quality (Bosco and Poppele 2000; Bosco, Poppele et al. 2000; Geertzen, Martina et al. 2001; Munin, Espejo-DeGuzman et al. 2001). Identifying the specific task goals and controlled variables in both able and impaired human walking will improve gait rehabilitation techniques by providing explicit, measurable rehabilitation goals and target variables for focused improvement. Associating quantifiable outcomes with gait

rehabilitation efficacy will also allow more complete data monitoring and establish a basis for more evidence based practice by tracking clinical outcomes.

Neurological and/or biomechanical deficits associated with impaired walking likely also affect how these individuals are able to adapt their walking mechanics to new or changing environments. Measuring how both able and impaired individuals adapt identified task goals over a short period of time within an altered walking environment will provide a basic framework for how the control of able and impaired gaits change to adapt to novel environmental constraints. Quantifying short-term adaptation will also provide a window into how impaired individuals may learn and adopt new walking strategies differently from able-bodied individuals. Identifying differences in adaptation and learning strategies will provide insight into how individuals with particular impairments might be trained differently to better personalize and optimize their therapy.

The purpose of this dissertation is to identify controlled variables of intact and impaired human locomotion and to identify the strategies used to adapt these variables when walking in an unfamiliar environment. I will show that joint-level coordination strategies are disrupted in the amputated legs of walkers with an amputation, but amputation does not affect execution of higher-level task goals. I also present evidence from split-belt treadmill walking experiments suggesting that amputation limits reactive adaptation strategies that contribute to leg power generation.

1.1 Dynamic Walking and Likely Controlled Variables in Able-bodied Human Walking

Human walking is a complex task that requires coordination of muscle activity, joint torques, and leg forces at various levels of neuromuscular control. This neuromuscular challenge can be simplified by focusing higher level control onto a smaller number of important control variables, or task goals, at particular periods within the gait cycle (Bosco and Poppele 2000; Bosco, Poppele et al. 2000). Exploiting underlying walking dynamics can also reduce the number of variables that must be monitored and controlled in order to achieve bipedal walking (McGeer 1990; Garcia, Chatterjee et al. 2000; Collins, Ruina et al. 2005; Su and Dingwell 2007; Kurz, Judkins et al. 2008; Verdaasdonk, Koopman et al. 2009; Chvatal, Torres-Oviedo et al. 2011; Chvatal and Ting 2012; McKay and Ting 2012; Chvatal and Ting 2013). In fact, actuation of only a few variables can initiate and influence independent bipedal robotic walking without any controller input (Collins, Ruina et al. 2005; Collins 2008). Principles from these passive dynamic walkers may provide possible candidates for controlled variables in human bipedal walking.

Dynamic walking is a popular model that provides "a theoretical approach to [describe] legged locomotion which emphasizes the use of simple dynamical models and focuses on behavior over the course of many steps, rather than within a single step" (Collins 2008). Dynamic walking principles propose that the primary metabolic cost of bipedal walking arises from the energy exchanged in step-to-step transitions when both feet are on the ground and the center of mass trajectory must be redirected between the inverted pendular arcs of single support. During this transition, mechanical energy is dissipated by leading leg heel strike collisions which is then returned to the system through propulsive work generation of the trailing leg (Kuo 2002; Donelan, Kram et al.

2002a; Donelan, Kram et al. 2002b); (Donelan, Kram et al. 2002; Donelan, Kram et al. 2002; Kuo 2002; Kuo, Donelan et al. 2005; Ruina, Bertram et al. 2005; Kuo 2007; Collins and Kuo 2010). These principles suggest that minimal energetic loss during step-to-step transitions are important for achieving metabolically efficient walking and that supplying consistent trailing leg power may be an implicit task goal for steady-state walking (Kuo 2002; Ruina, Bertram et al. 2005).

Leg force profiles influence leg power production and contribute to walking economy, so I focus much of my analysis on joint torque organization and its influence on the timing and magnitude of leg force application. Energy loss during leading leg collisions can be reduced by controlling the specific timing of trailing leg force impulse and/or power production (Kuo 2002; Ruina, Bertram et al. 2005). Leg power is explicitly determined by force along the leg (**Eq. 3.1**; (Donelan, Kram et al. 2002a; Donelan, Kram et al. 2002b), and is therefore likely determined by how and when leg force is applied. Peak leg forces are stabilized in bouncing gaits (Yen, Auyang et al. 2009; Yen and Chang 2010; Yen 2011), demonstrating that the neuromuscular system monitors and controls leg force output in locomotor tasks. I expect that the physiological structures underlying this control may persist in other locomotor tasks and contribute to the control of walking mechanics as well.

1.2 Trans-tibial Amputation is a Morphological Constraint that Limits Motor Abundance

Lower limb amputation impairs mobility and reduces the ability to recover from a fall, suggesting that these individuals have motor control deficiencies (Kepple, Siegel et al. 1997; Vrieling, van Keeken et al. 2007; Curtze, Hof et al. 2010; Curtze, Hof et al. 2012; Wurdeman, Myers et al. 2013). A transtibial amputation eliminates active ankle control and extinguishes much of the sensory feedback typically available during

locomotor tasks. Specifically, transtibial amputation eliminates active control of the triceps surae, which are the largest contributor to trailing leg force production in human walking (Kepple, Siegel et al. 1997; Neptune, Kautz et al. 2001). Controlled ankle actuation alone is sufficient to power dynamic walking robots and is the primary contributor for generating propulsive leg power in human walking (Zajac, Neptune et al. 2002; Zajac, Neptune et al. 2003). The loss of proprioception through deafferentation also appears to eliminate inter-joint coordination in upper extremity reaching (Ghez and Sainburg 1995; Sainburg, Ghilardi et al. 1995). Amputation therefore effectively eliminates an active degree of freedom within the locomotor system, which likely affects the power production capacity and joint level coordination controlling leg force output. Studying individuals with amputations provides the unique opportunity to investigate the role of ankle function (motor control and sensory feedback) and the effect morphologically constraining the locomotor system has on locomotor control of walking *in vivo*.

1.3 Methodology for Understanding Locomotor Control: The Uncontrolled Manifold Analysis

The inherent motor abundance of the neuromuscular system presents a challenge for controlling locomotion (Bernstein 1967; Latash 2012). Rather than controlling all of these degrees of freedom at once, numerous motor tasks demonstrate specific organization of elemental variables (e.g. joint torques) such that they compensate for one another to maintain consistent execution of a particular task variable (Scholz and Schoner 1999; Scholz, Schoner et al. 2000; Latash, Scholz et al. 2001; Domkin, Laczko et al. 2002; Domkin, Laczko et al. 2005). Organizing lower-level elements in a relatively self-regulating way offloads demand on the neural system by simplifying control to a few influential task variables (Schoner and Kelso 1988). Elemental variables can then remain

more variable than the task variable they combine to produce, making it difficult to empirically observe such neuromotor organization and control. However, the uncontrolled manifold (UCM) analysis was developed to test how elemental variables of periodic movements are organized to influence a hypothesized goal variable (Scholz and Schoner 1999). No work has yet specifically sought to identify possible implicit kinetic goals of walking using the Uncontrolled Manifold analysis.

The uncontrolled manifold analysis was developed to test whether hypothesized task goals were indeed made more consistent through specific organization of elemental variables (Scholz and Schoner 1999). Specific details of the mathematics contributing to this analysis can be found in Chapter 2, Appendix A, and (Yen, Auyang et al. 2009). The analysis projects the small deviations of elemental variables during repeated movements onto the hypothesized task space using a mathematical representation (Jacobian matrix) of the relationship between the elemental variables (e.g. joint torques) and the hypothesized task (e.g. leg force). The uncontrolled manifold is the null space of this mathematical relationship between joint torque deviations and leg force output, which isolates joint torque deviations that do not affect leg force. Joint torque variance is then separated into components either parallel or orthogonal to this linear manifold. Variance parallel to the manifold does not change leg force, while orthogonal variance directly moves leg force away from the desired trajectory. By comparing the relative amounts of parallel and orthogonal variance, we can determine whether joint torques tend to stabilize (make more consistent) or modulate (change with each step) leg force output. The UCM analysis has traditionally been used to identify stabilized goals in various motor tasks, but it can also be used as a tool to quantify how elemental variables tend to influence task variables over the duration of a repeated movement, such as a gait cycle.

In my analysis, I apply a modified UCM analysis to identify the source of the task level control observed using the traditional UCM analysis. Joint torques can influence leg force output in two ways: (i) through individual joint torque actuation where each joint

torque separately influences leg force or (ii) through inter-joint covariation where joint torques work together to stabilize or modulate leg force output. The contribution of each of these elements is isolated by modifying the statistical covariance matrix used in the traditional UCM analysis (Yen and Chang 2010; Yen 2011). The resulting computations indicate what proportion of variance structure is due to individual or coordinated joint torque control. From these proportions we can determine whether a particular joint torque (e.g. ankle torque) dominates the motor control of leg force output or if coordinated action across two or more joints generate the observed leg force variability. These results help inform how a particular joint or set of joints may influence walking mechanics.

1.4 Motor Control Adaptation and Learning with Split-belt Treadmill Walking

Acquiring new motor strategies requires extended practice in which one must re-adapt movement strategies over multiple exposures (Sawers, Hahn et al. 2012). Investigating how individuals adapt over short periods of time within a single training session could illuminate the motor control strategies used to adopt new walking patterns in response to a novel environment. Studying short-term adaptation provides a window into the strategies utilized to achieve long-term motor learning.

I specifically use the term locomotor adaptation to indicate a change in response to some persistent perturbation that does not alter the fundamental characteristics of walking (e.g. 1:1 step sequence, distinct double support period is maintained) (Martin, Keating et al. 1996; Bastian 2008). Split-belt treadmill walking is a unique intervention that sufficiently perturbs locomotion without disrupting basic walking characteristics (Dietz, Zijlstra et al. 1994; Prokop, Berger et al. 1995; Jensen, Prokop et al. 1998; Reisman, Block et al. 2005; Choi and Bastian 2007; Reisman, Bastian et al. 2010; Vasudevan and Bastian 2010; Roemmich, Stegemoller et al. 2012; Finley, Bastian et al. 2013; Mawase, Haizler et al. 2013; Roper, Stegemoller et al. 2013; Ogawa, Kawashima

et al. 2014). Split-belt walking involves walking on side-by-side treadmills as one leg moves at twice the speed of the other. The details of this approach are provided in Chapter 5. Sudden introduction of split-belt treadmill walking was used to initially disrupt walking patterns so I could then record the evolution of consistent, periodic walking mechanics as subjects walked for an extended time in this novel environment.

Two distinct locomotor adaptation patterns with different suspected neural origins have been identified in response to sudden split-belt treadmill introduction (Lam, Anderschitz et al. 2006; Morton and Bastian 2006; Smith, Ghazizadeh et al. 2006; Reisman, Wityk et al. 2007; Choi, Vining et al. 2009; Jayaram, Tang et al. 2012; Ogawa, Kawashima et al. 2014). Predictively controlled parameters adapt more slowly, demonstrating large initial deviations that gradually return to baseline and distinct negative aftereffects when the perturbation is removed. Alternatively, parameters that are more reactively adapted change very quickly after initial introduction of the split-belt condition and have aftereffects that are either absent or in the same direction as the initial change. Predictive control mechanisms require intact cerebellar function, while reactive mechanisms are regulated by more distal, feedback driven, reflexive pathways and do not require central function (Lam, Anderschitz et al. 2006; Morton and Bastian 2006; Smith, Ghazizadeh et al. 2006; Choi, Vining et al. 2009; Jayaram, Tang et al. 2012)

Impaired walkers likely utilize different adaptation strategies than able-bodied individuals. Amputation in particular limits active ankle motor control, extinguishes a substantial amount of distal sensory feedback, and disrupts inter-joint coordination. Ankle actuation largely determines propulsive forces and power generation in both able-bodied individuals (Kepple, Siegel et al. 1997; Neptune, Kautz et al. 2001; Zajac, Neptune et al. 2002), which are regulated and adapted through reactive, feedback driven mechanisms (Nielsen and Sinkjaer 2002; Hohne, Stark et al. 2011; Ogawa, Kawashima et al. 2014). It is therefore likely that transtibial amputation will affect feedback regulation of propulsion in locomotor adaptation.

Studying short-term locomotor adaptation in able and impaired populations could illuminate differences in how these populations navigate difficult or unfamiliar terrain and may provide insight into possible methodological improvements for gait rehabilitation protocols. Most of the research on gait adaptation of individuals with amputations focuses on the final walking strategy after complete adaptation has occurred (Gates, Darter et al. 2012; Gates, Dingwell et al. 2012; Buckley, De Asha et al. 2013; Gates, Scott et al. 2013; Beurskens, Wilken et al. 2014; Hak, Dieen et al. 2014) and/or how prosthetic design alters walking mechanics (Selles, Bussmann et al. 1999; Lin-Chan, Nielsen et al. 2003; Selles, Korteland et al. 2003; Zmitrewicz, Neptune et al. 2006; Ventura, Klute et al. 2011; Zelik, Collins et al. 2011; Ferris, Aldridge et al. 2012; Fey, Klute et al. 2013; Grabowski and D'andrea 2013; Smith and Martin 2013; Toney and Chang 2013; Major, Twiste et al. 2014), rather than on the initial evolution of these walking patterns. In my dissertation work, I take the first step towards understanding how short-term adaptation in individuals with amputations differ from adaptation strategies seen in able-bodied walkers. To the best of my knowledge, no one has yet attempted to isolate the effect feedback and motor control of distal structures have on the time course of locomotor adaptation. I attempt to attain this knowledge for the first time by studying how individuals with an amputation who lack sensory feedback and motor output regulate adaptation of reactive mechanisms during split-belt treadmill walking.

1.5 Aims and Objectives

The aim of this dissertation work is to explore the kinetic motor control strategies used to execute steady-state locomotor mechanics in able and impaired individuals and to identify possible differences in locomotor strategies used to adapt able and impaired locomotion to a novel walking environment. In Chapter 2 (Toney and Chang 2013), I first identify the hierarchical structure of kinetic motor abundance able-bodied individuals use

to achieve robust walking mechanics. I show that consistent net vertical force trajectories during step-to-step transitions are an implicit gait goal in able-bodied walking and that net vertical force consistency is achieved through inter-leg force coordination. Chapter 3 looks more specifically at the role of individual joint torque control in trailing leg force application and power production. I show that trailing leg peak power production is made consistent by modulating force along the leg primarily through variable ankle torque timing, while the knee acts like a series brake to refine the effect of the ankle motor on whole leg power and center of mass dynamics.

Chapters 4 and 5 specifically investigate how these control strategies are affected by the physiological constraint of amputation (Chapter 4) and when perturbed by an unfamiliar walking environment (Chapter 5). When the ankle motor is impaired by transtibial amputation, net vertical force stabilization is preserved. Leg force is modulated by the action of the passive prosthetic device, but ankle-knee joint torque covariance is impaired, limiting the knee's ability to act as a brake and respond to refine ankle motor deviations. Split-belt treadmill walking elicits clear adaptation patterns in able-bodied leg and joint work production. Ankle work timing appears to contribute to adopting more efficient walking mechanics over the course of adaptation, while coupled knee work production follows ankle function to enable robust walking mechanics throughout adaptation. The lack of inter-joint ankle-knee coupling and reduction of distal sensory feedback and motor control in subjects with a transtibial amputation appears to limit the ability of these individuals to adapt either leg or joint work production on their amputated side over the course of adaptation. Instead these individuals appear to rely on their sound leg to compensate for deficits on their amputated side.

CHAPTER 2

HUMANS ROBUSTLY ADHERE TO DYNAMIC WALKING PRINCIPLES BY HARNESSING MOTOR ABUNDANCE TO CONTROL FORCES

This chapter was originally published in *Experimental Brain Research*:
Toney ME, Chang YH (2013) Humans robustly adhere to dynamic walking principles by harnessing motor abundance to control forces. Exp Brain Res 231:433-443. (doi:10.1007/s00221-013-3708-9).

This chapter addresses the first aim of my dissertation work: to identify hierarchical task goals that likely contribute to robust human locomotion. In this chapter, I investigate the organization of kinetic motor abundance in able-bodied human walking at a constant speed. I apply an uncontrolled manifold (UCM) analysis to test how inherent leg force and joint torque variance contributes to the stabilization of net vertical force trajectories during step-to-step transitions. I show that consistent net vertical force trajectories during step-to-step transitions is an implicit gait goal in able-bodied human walking, and that this consistency is achieved through trailing leg vertical force modulation and inter-leg vertical force coordination. These findings provide a necessary foundation for the work in later chapters that aim to better understand how robust able-bodied human walking is achieved (Chapter 3) and to determine how locomotor control is affected by lower limb amputation (Chapter 4).

2.1 Introduction

The overall energetic cost of walking can be minimized by selecting appropriate locomotion dynamics that minimize the energy dissipated between steps. Numerous models have described the relationship between legged locomotion dynamics and the

measured metabolic cost (Saunders, Inman et al. 1953; Cavagna and Kaneko 1977; Hoyt and Taylor 1981; McGeer 1990; Alexander 1992; Minetti and Alexander 1997; Lee and Farley 1998; Garcia, Chatterjee et al. 2000; Anderson and Pandy 2001; Kuo 2001). One popular model, dynamic walking, is "a theoretical approach to [describe] legged locomotion which emphasizes the use of simple dynamical models and focuses on behavior over the course of many steps, rather than within a single step" (Collins 2008; Collins and Kuo 2010). Dynamic walking principles propose that the primary metabolic cost of human walking results from the mechanical energy required to redirect the body's center of mass (COM) during step-to-step transitions (Collins and Kuo 2010). Sequential single-limb stance phases are considered as independent inverted pendular arcs (Cavagna and Kaneko 1977), but continuous, uninterrupted walking requires vertical redirection of the COM trajectory between these steps through coordinated actions of the leading and trailing legs (Fig 2.1A). During these transition phases, mechanical energy is dissipated at heel strike (collision) of the leading leg and restored with propulsive work by the trailing leg (Donelan, Kram et al. 2002a; Donelan, Kram et al. 2002b; Kuo 2002; Kuo, Donelan et al. 2005; Ruina, Bertram et al. 2005; Collins and Kuo 2010). Dynamic walking principles therefore suggest that maintaining mechanically efficient step-to-step transitions are necessary for metabolically efficient walking. Motor control principles propose that variables critical for execution of a desired task remain consistent across many repetitions while non-critical variables exhibit high variability. These patterns of directed variability reduction may reveal an organizational structure for movement control (Schoner and Kelso 1988; Scholz and Schoner 1999; Latash, Scholz et al. 2002). The principles of dynamic walking therefore describe an optimal mean behavior for

walking (Collins 2008), which implies consistent performance of some critical variables across many steps.

While accurately capturing mean dynamics and energetics of locomotion, dynamic walking principles do not address the natural kinetic deviations intrinsic to human joint torques and limb forces with each step. The principles of dynamic walking do not explain, for example, how consistent center of mass redirection is achieved despite natural physiological variation in muscle-generated joint-torques and leg forces experienced from one step to the next. It remains unclear how humans might robustly adhere to dynamic walking principles despite the effects of inherent step-to-step kinetic variability on net-force and resulting whole body dynamics.

Walking involves the use of more degrees of freedom than are strictly necessary to achieve a desired net force. Current motor control theories suggest that humans harness this inherent motor abundance of elemental variables to maintain consistent and robust performance of task variables (Scholz and Schoner 1999; Bosco and Poppele 2000; Scholz, Schoner et al. 2000; Ivanenko, Cappellini et al. 2007; Ivanenko, d'Avella et al. 2008; Auyang, Yen et al. 2009; Yen, Auyang et al. 2009; Yen and Chang 2010). For example, in bipedal walking, the sum of two leg forces determine each net force on the ground, so coordination of these individual leg forces may minimize net force deviations, thereby stabilizing (i.e. making more consistent) COM redirection for continuous walking without the need to minimize individual leg force deviations. To simplify control of the complex task of walking, the human locomotor system may actively monitor and control a select few task variables that are most important for successful locomotion (Bosco, Poppele et al. 2000; Ivanenko, Cappellini et al. 2007; Ivanenko, d'Avella et al. 2008).

Here we define motor control as "the ability to regulate or direct the mechanisms essential to movement" (Shymway-Cook and Woollacott 2001). It is worth noting that this control can act to either stabilize (ie. make more consistent) or modulate (i.e., make less consistent) a given variable, or 'goal', over many successive steps.

The uncontrolled manifold (UCM) analysis examines how the variance of system elements (e.g., individual leg-forces) is structured across cycles of periodic movements to minimize "error" in variables critical for task success (e.g., net-force) (Scholz and Schoner 1999; Yen, Auyang et al. 2009; Yen and Chang 2010). For example, a conductor may specify a particular volume level for a choir to perform. Rather than assigning a volume for each singer, which would yield an inconsistent ensemble volume, the conductor directs the ensemble volume while each singer adjusts their own contribution to account for too loud or too soft singing of their neighbors. Like a choral conductor, the UCM analysis considers system elements (singers) that self-adjust to errors (reducing one singer's volume when another sings too loudly) to maintain a particular output (ensemble volume) (after (Latash, Fanion et al. 2003). Applying the UCM analysis across periodic walking cycles allows us to test whether humans exploit their many degrees of freedom to stabilize task variables in accordance with dynamic walking principles. Stabilization of net-force by alignment of elemental leg-force variance with the proposed manifold would suggest that net-force may be an implicit goal of human walking that is actively monitored and controlled by the locomotor system. Alternatively, the UCM analysis may reveal misalignment of the elemental variance structure from the manifold, thus indicating that net force is not an implicit gait goal, but is instead modulated to stabilize another variable at a different hierarchical level (Shim, Latash et al. 2003; Gorniak,

Zatsiorsky et al. 2007; Gorniak, Zatsiorsky et al. 2009). This analysis provides a method for testing whether or not variance of elemental variables project to align with hypothesized task goals. The UCM approach can therefore provide insight into what variables may serve as implicit neuromechanical gait goals since structured kinetic variance provides a window into nervous system's structure and function (Schoner and Kelso 1988).

The aim of this study was to test whether humans structure their inherent motor variability to stabilize the vertical net-force trajectory for consistent COM redirection across many steps during walking. Dynamic walking principles predict which variables are critical for efficient gait, providing a hypothesis for what locomotor task variables are likely stabilized through elemental variance structure. Initially, the COM of the body is directed forward and downward as it enters into a step-to-step transition (Fig 2.1a). At the transition's conclusion, the COM is directed forward and upward as the body begins the next single leg support phase (Fig 2.1a). Because only the vertical COM velocity changes direction, redirection of the COM trajectory during this step-to-step transition is solely determined by the net vertical force (F_v^{net}) generated by the legs. To ensure consistent COM redirections and a COM trajectory for minimal energy expenditure, a consistent F_v^{net} trajectory over many steps may be an implicit goal of human walking (Fig 2.1b). We hypothesized that over many steps, walkers would generate leading and trailing leg force combinations that would act to stabilize (i.e., make more consistent) the trajectory of the vertical component of net-force (F_v^{net}) during double support (Fig 2.1d).

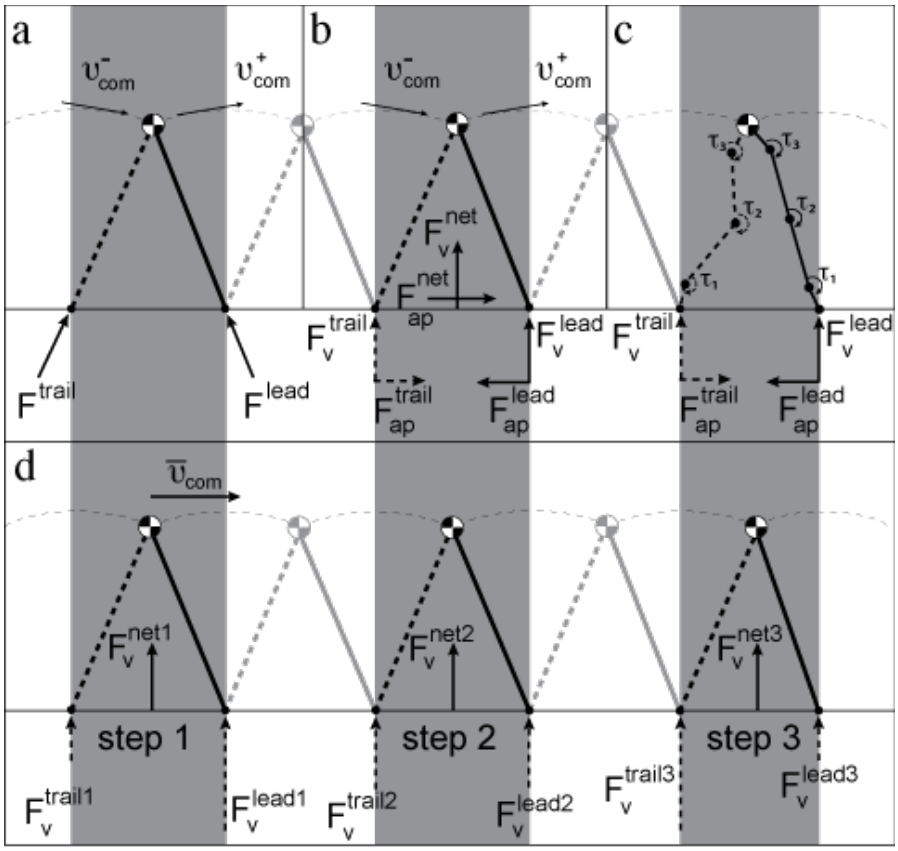

Figure 2.1: When considering naturally variable human walking, we consider steps as a cumulative behavior and not in isolation. (a) In dynamic walking, leading and trailing leg forces act together to consistently transition the center of mass from one pendular arc to the next (v_{com}^{-} at the beginning of a transition period to v_{com}^{+} at the end) (b) Individual vertical leg-forces sum to F_v^{net} while braking leading leg-forces are balanced by propulsive trailing leg-force to determine F_{ap}^{net} (c) Intra-leg joint-torques at the ankle (τ_1), knee (τ_2), and hip (τ_3) determine individual vertical and anterior-posterior leg-force components (d) Behavior within each step can vary as long as behavior over time leads to the mean behavior described by dynamic walking. For example, vertical leg forces can vary while making adjustments to maintain consistent step-to-step F_v^{net} trajectory for consistent COM transitions.

The anterior-posterior component of the center of mass velocity (v_{com}) remains oriented anteriorly (in the direction of progression) throughout the step-to-step transition. The v_{com} magnitude is adjusted using combinations of braking and propulsive forces from the leading and trailing legs, respectively (Fig 2.1b). Walking on a treadmill requires one to maintain a constant average walking velocity, thus imposing an explicit speed goal. Maintaining a consistent, steady walking speed theoretically requires the COM velocity to be the same at the beginning and end of each transition phase, $\left|v_{com}^{-}\right| = \left|v_{com}^{+}\right|$ (Fig 2.1a-

b) (Kuo, Donelan et al. 2005; Kim and Park 2012). Step-to-step transitions therefore also require balanced braking and propulsive forces but do not demand a specific target value for F_{ap}^{net} across steps. Modulating the F_{ap}^{net} trajectory with each step allows subjects to make step-to-step adjustments that counteract natural speed deviations and maintain the constant velocity required for treadmill walking. Consistent with previous work in hopping (Yen, Auyang et al. 2009), we hypothesized that individual legs would coordinate braking and propulsive leg forces to modulate F_{ap}^{net} during step-to-step transition phases of walking and maintain the required constant walking speed. Evidence of F_{ap}^{net} modulation to achieve a known explicit goal (constant walking speed) will provide support that the UCM analysis can successfully distinguish between stabilized and modulated variables.

Dynamic walking models typically consider both legs as rigid struts. In reality, individual joint torques of the hip, knee, and ankle influence the net forces that dictate COM dynamics by generating individual leg forces (Fig 2.1c). For a more complete picture of human locomotor control, we considered the role joint-torque combinations play in determining the individual leg-forces that then regulate net-force on the ground. We hypothesized that joint-torques would act in combinations that tend to stabilize individual leg-force components during step-to-step transitions. Residual variance in the two leg forces can then be coordinated to regulate the net-force trajectory for consistent COM redirection as hypothesized above. Considering *intra*-leg force control within the context of an *inter*-leg force control model is consistent with a hierarchical structure of locomotion control (Loeb, Brown et al. 1999; Shim, Latash et al. 2003; Rybak, Stecina et al. 2006; Gorniak, Zatsiorsky et al. 2007; Gorniak, Zatsiorsky et al. 2009).

2.2 Methods

2.2.1 Data Collection

Nine healthy subjects (8 male, age: 34±12.6 years, weight: 70.0±11.6 kg, leg length: 93.8±6.7 cm) gave informed consent as approved by the Georgia Institute of Technology Institutional Review Board. Each subject walked at a constant speed of 1.2m/s for three 30-second trials. Ground reaction forces were collected independently for each limb as subjects walked on a custom dual-belt instrumented treadmill (1080 Hz, Advanced Mechanical Technology Incorporated, Watertown, MA, USA). Subjects were familiar with treadmill walking, but were given as much time as desired to practice and rest prior to each trial. Simultaneous kinematics data were captured using a six-camera motion analysis system (120Hz, VICON Motion Systems, Oxford, UK). Retroreflective markers were placed bilaterally on the anterior superior iliac spine, posterior superior iliac spine, thigh segment, knee joint center, shank segment, lateral malleolus, and second metatarsophalangeal joint.

2.2.2 Data Analysis

Marker and force data were filtered with a zero-phase lag fourth-order Butterworth low-pass filter with a 10Hz cut-off frequency. Joint-torques were calculated in the sagittal plane using standard inverse dynamics calculations and estimated segment inertial characteristics based on subject specific anthropometrics (Winter 1980).

2.2.3 Uncontrolled Manifold Analysis

Uncontrolled Manifold (UCM) analysis was performed using custom Matlab code. A detailed explanation of this technique as applied to vertical and anterior-posterior force components has been provided previously (Auyang, Yen et al. 2009; Yen, Auyang et al. 2009). Briefly, the UCM analysis partitions the total variability of redundant local variables into two components either parallel or perpendicular to a linearized estimate of the goal equivalent manifold. Comparing the relative magnitude of these orthogonal variance components can reveal whether elemental variables exhibit a non-random structure that aligns with a functional goal. The goal can be implicit as identified by theoretical models like dynamic walking, or they can be explicit due to task constraints or prescribed targets. The relationship between local elemental variables and the proposed goal variable is mathematically described within the Jacobian matrix (***J***), which quantifies the effects of small local variable deviations on task variables. The null-space of J serves as a linearized approximation of the manifold against which we can test our hypotheses about the structure of elemental variance. ***J*** is derived separately for each hypothesized combination of goal and local variables.

The UCM approach is a powerful tool for using variance as a window into the nervous system function, but like all statistical analyses, the UCM approach makes several assumptions that limit the scope of its applicability and interpretation. For example, we assume that elemental redundancy exists when applying the UCM approach (i.e. there are more available degrees-of-freedom than strictly necessary to achieve the task); however, no net joint-torque redundancy exists for a particular fixed limb configuration. The system's redundancy arises from the kinematic redundancy that exists

from step-to-step as specific joint kinematics are never exactly repeated. To circumvent this limitation to study how the system utilizes step-to-step geometric redundancy and variability, we use a kinematic Jacobian that maps the corresponding joint-torques to endpoint force using an operational space formulation developed for controlling humanoid robots (Khatib 1987; Yen, Auyang et al. 2009). This conversion therefore maintains kinetic consistency between elemental (joint-torques) and task variables (leg-force), which enables more direct analysis and interpretation of the underlying neuromechanical control. Using the UCM approach to investigate coordination of joint-torques for leg-force production therefore provides a necessary foundation from which to study the underlying neuromuscular structure and function more deeply. The requirement of redundancy also limits when in the gait cycle the UCM analysis can be used to evaluate kinetic redundancy. Because inter-leg kinetic redundancy exists only when both limbs generate force on the ground, we restricted the scope of our analysis to the double support periods when both feet are in contact with the ground. Our intent was to investigate how subjects account for natural deviations during step-to-step transitions through the use of inherent redundancy across the legs. So limiting our analysis to the double support period remains consistent with our purpose and provides a better understanding of the hierarchical organization of human locomotor control.

2.2.4 Inter-leg Uncontrolled Manifold Analysis

In walking, forces applied by the leading and trailing legs on the ground determine the net-force (Eq 2.1). This simple arithmetic relationship defines a two degree-of-freedom (2-DOF) system, and a 1x2 ***J*** matrix describes the influence of each

individual leg-force on the net-force. We performed a 2-DOF uncontrolled manifold (UCM) analysis to quantify how inter-step leg-force variance is structured to generate consistent (i.e., stable) net-force values during step-to-step transitions (Scholz, Schoner et al. 2000). The manifold describes a set of leg-force combinations that satisfy a single F^{net} value, so all leg-force deviations parallel to the manifold have no effect on F^{net} and are thus collectively called goal equivalent variance (GEV, Eq 2.2). Leg-force deviations perpendicular to the manifold cause divergence from the desired F^{net} value, so this variance component is defined as non-goal equivalent (NGEV, Eq 2.3), where C is the covariance matrix of leg-forces, d is the number of global degrees of freedom (1 net-force component), and n is the number of local degrees of freedom (2 leg-forces).

$$F^{lead} + F^{trail} = F^{net} \quad \text{(Eq 2.1)}$$

$$GEV = \frac{trace(null(J)^T \cdot C \cdot null(J))}{n - d} \quad \text{(Eq 2.2)}$$

$$NGEV = \frac{trace((J \cdot J^T)^{-1} \cdot J \cdot C \cdot J^T)}{d} \quad \text{(Eq 2.3)}$$

We used the normalized difference between these two variance components, called the index of motor abundance (IMA, Eq 2.4), to characterize the use of motor abundance to stabilize net-force at every 1% of the gait cycle, where TOTV (Eq 2.5) is the total measured leg-force variance (Yen, Auyang et al. 2009).

$$IMA = \frac{(GEV - NGEV)}{TOTV} \quad \text{(Eq 2.4)}$$

$$TOTV = \frac{trace(C)}{n} \quad \text{(Eq 2.5)}$$

For inter-step behavior, each stride cycle was normalized to right heel strike. Transition phases were identified as periods of double support when both the right and left leg forces exceeded 10% of body weight (shaded region, Fig 2.2). Average double support across all subjects was used to identify the transition phases for pooled data.

2.2.5 Intra-leg Uncontrolled Manifold Analysis

We conducted a 3-DOF UCM analysis to quantify how joint-torque variance is structured to generate consistent (stable) leg-force components during transition phases. Derivation of ***J*** relating joint-torques to leg-force results from the dynamically consistent generalized inverse of the kinematic Jacobian relating joint angles to end-point position (see Appendix A for additional detail) (Yen, Auyang et al. 2009). For this intra-leg model, the ankle, knee, and hip joint-torques were the local variables and the vertical and anterior-posterior force components of individual leg-forces (F_v^{lead} and F_{ap}^{trail}) were the two tested goal variables. Similarly to the inter-leg analysis described above, the variance of intra-leg joint-torques was partitioned into GEV and NGEV components, and the IMA was used to characterize leg-force stabilization for each 1% of the gait cycle. For this intra-leg analysis, each leg's stride cycle was normalized relative to its own heel strike (ie. left leg data were normalized to left heel strike and right leg data to right heel strike). Self-normalized data from both legs were then pooled so the variance structure could be considered relative to leg function (leading or trailing) rather than by anatomical side.

2.2.6 Statistical Analysis

Mean IMA trajectories across all subjects were evaluated for significant differences from zero using a one-tailed Student's t-test (α=0.005). An IMA significantly greater than zero indicates the local variables (individual leg-forces or intra-leg joint-torques) were coordinated to generate the same net-force trajectory in each transition, which we interpret as stabilization of a controlled implicit neuromechanical goal of walking. In other words, a positive IMA indicates that only task-relevant deviations are reduced, which is consistent with a minimum intervention principle of motor control (Todorov and Jordan 2002). An IMA significantly less than zero indicates active modulation such that the local variables combined to produce a different net-force trajectory with each successive step, indicating that task-relevant deviations are not restricted, but instead contribute directly to net-force modulation. A negative IMA is therefore interpreted to mean that net-force is not an implicit gait goal, but is instead modulated to stabilize some alternative gait goal.

2.3 Results

2.3.1 Joint Moments and Ground Reaction Forces

Across all subjects, the first double support step-to-step transition period occurred during 1-13% (±0.73%) of the gait cycle. The second transition period began with contra-lateral heel contact at 50% (±0.29%) and lasted until 62% (±0.69%) of the gait cycle. The general trajectories of the recorded ground reaction forces and joint-torques were consistent with previously published work on human walking (Winter 1980; Nilsson and Thorstensson 1989). Despite the characteristic mean shapes of the trajectories, we

observed a substantial amount of step-to-step variability in all force and joint-torque data for each subject (Fig 2.2).

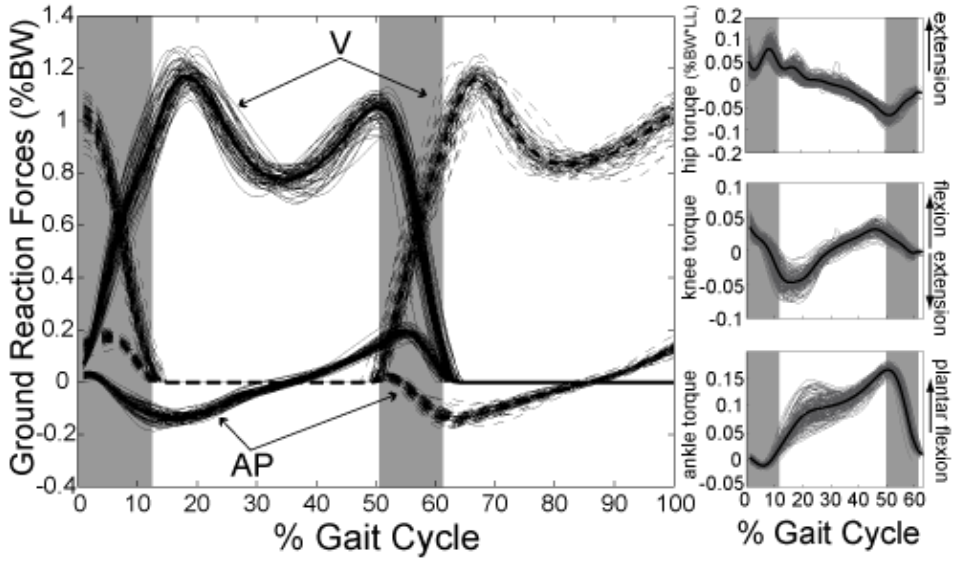

Figure 2.2: Sagittal plane kinetics as a percent of the gait cycle for each step (thin, grey lines) and mean behavior across all steps (thick, black lines) from one representative subject. Body weight normalized vertical and anterior-posterior ground reaction forces (GRF) (left panel) for a complete gait cycle and joint-torques (right column) during stance are shown. Shaded areas depict transition periods where the first occurs from 1-13% (±0.80%) of the total gait cycle as the right leg (solid lines) leads and the second from 51(±0.71)-61%(±0.83%) as the left leg (dashed lines) leads.

2.3.2 Inter-leg Model for Net-force Control

IMA values for net vertical forces (F_v^{net}) were significantly greater than zero for 1-13% and 50-62% of the normalized gait cycle, corresponding to each double support period (Fig 2.3a, double support periods shaded). These results indicate that F_v^{net} is stabilized using leading and trailing leg-force variance structure to generate net-force equivalent combinations throughout step-to-step transitions. IMA values for net anterior-posterior forces (F_{ap}^{net}) were significantly less than zero from 7-13% and 56-61% of the gait cycle (Fig 2.3b). These results indicate that structure of braking and propulsive force variance resulted in net anterior-posterior forces that were highly inconsistent during the latter part of each step-to-step transition.

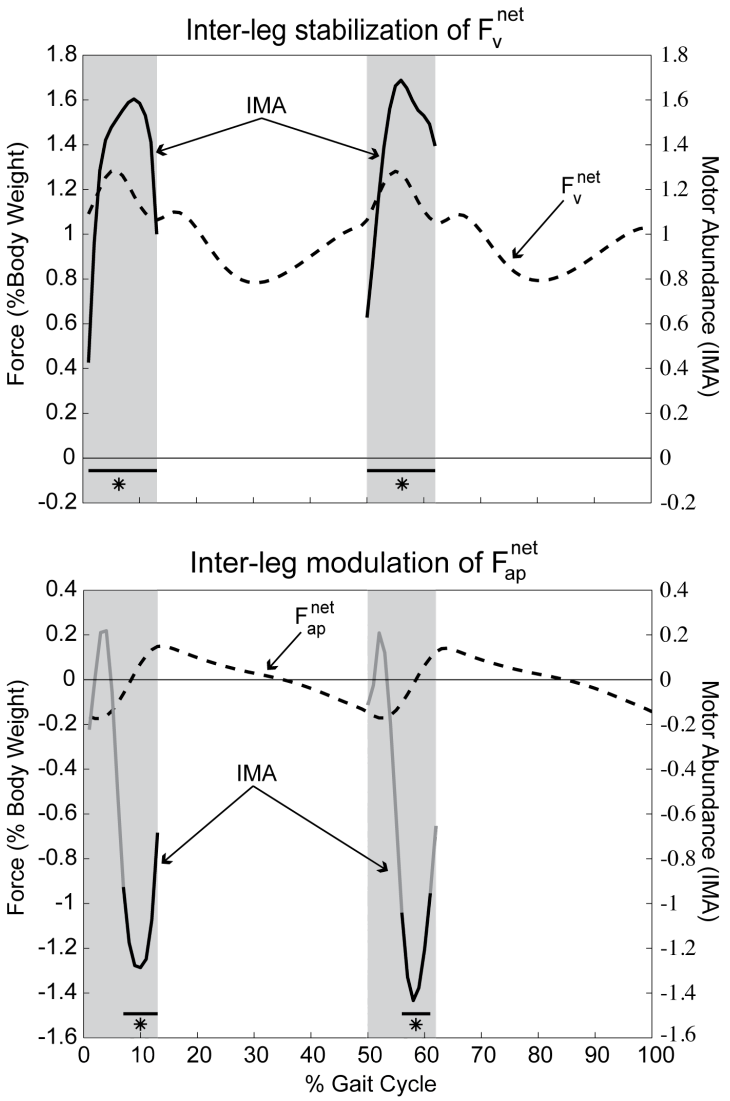

Figure 2.3: Inter-limb stabilization of net vertical force (top) and modulation of net anterior-posterior force (bottom). IMA values (solid) significantly greater than zero (horizontal bar, black line shading) indicate that net vertical force (dashed) is stabilized during inter-step transitions due to selection of net-force equivalent leg-force combinations. IMA values significantly less than zero (horizontal bar, black line shading) indicate that leading and trailing leg anterior-posterior forces are coordinated to vary net anterior-posterior forces with each step.

2.3.3 Intra-leg Model for Leg-force Control

IMA values for leading leg vertical force (F_v^{lead}) were significantly greater than zero from 1-5% and 11-13% of the complete gait cycle. In contrast, IMA values for the trailing leg vertical force (F_v^{trail}) were significantly less than zero from 56-60% (Fig 2.4a). For vertical forces, leading leg GEV exceeded NGEV throughout double support (Fig

2.4c). Trailing leg vertical force modulation resulted from a dramatic increase in NGEV while GEV remained relatively constant and small throughout double support (Fig 2.4e). IMA values for leading leg anterior-posterior force (F_{ap}^{lead}) were significantly greater than zero from 1-7% of the complete gait cycle, and IMA values for trailing leg vertical force (F_{ap}^{trail}) were significantly greater than zero from 50-61% (Fig 2.4b). Despite a slight increase in NGEV of the leading leg in late double support, GEV was greater than NGEV for both F_{ap}^{lead} and F_{ap}^{trail} (Fig 2.4d and 2.4f).

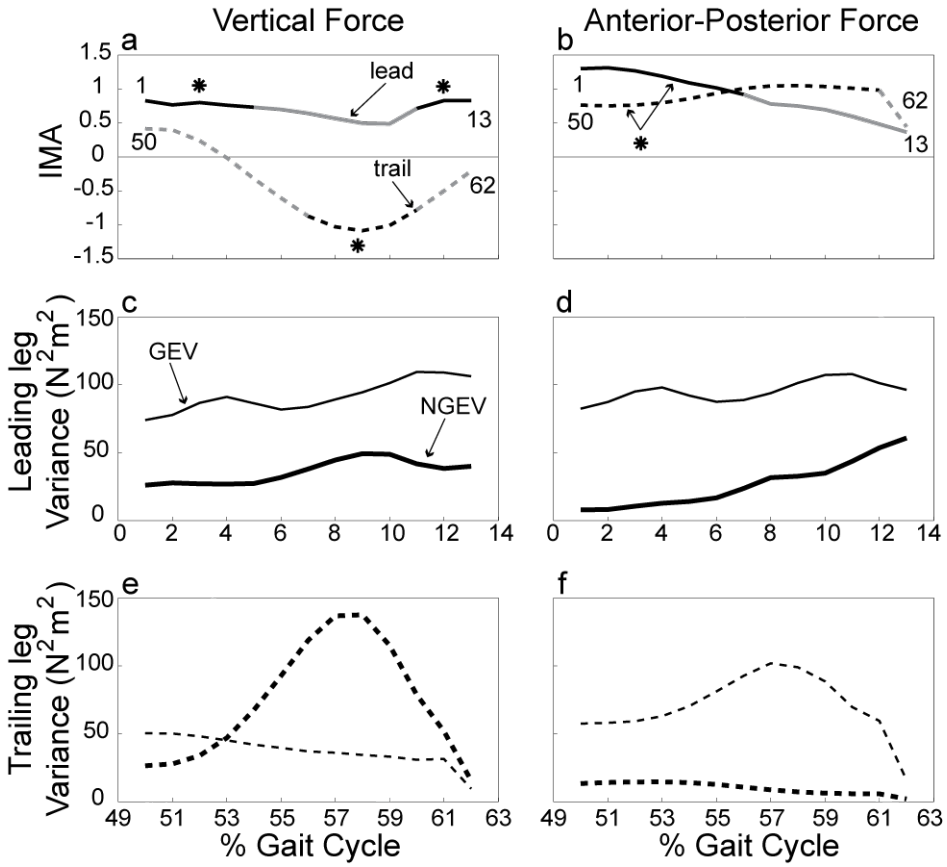

Figure 2.4: Intra-limb variance structure selectively modulates trailing leg vertical forces. IMA values for the vertical (a) and anterior-posterior (b) components of leg-forces when the leg is leading (solid line) or trailing (dashed) during the transition phase. Note that the transition period for the trailing leg begins at 50% and ends at 62% of the complete gait cycle, while leading leg transition begins at 1% and ends at 13%. During each transition, one leg leads while the other trails, so each of these behaviors occur simultaneously during each transition phase. The GEV (thin line) and NGEV (thick) components of variance for the transition phase when the leg is leading (c-d) and trailing (e-f).

2.4 Discussion

Appropriate coordination of joint-torques and leg-forces can lead to robust, stable walking behavior by harnessing inherent motor abundance to accommodate natural step-to-step inconsistencies. We applied the UCM analysis to test whether human walkers selected combinations of joint-torques and leg-forces that led to consistent locomotor goals. Positive IMA values indicate stabilization of the tested goal variable through the selection of net-force equivalent leg-force combinations to apply consistent net-force during each transition period. Negative IMA values, on the other hand, signify selection of leg-force combinations that result in variable net-force with each step to stabilize a different gait goal.

2.4.1 Inter-leg Forces Stabilize Net Vertical Force

We hypothesized that consistent vertical net-force trajectories would be necessary for maintaining the optimal step-to-step COM transitions suggested by dynamic walking principles. Motor performance is naturally variable, so individual leg-forces will not be identical with each step, creating an apparent challenge to achieving stable net forces. Our UCM analysis revealed that structure of F_v^{lead} and F_v^{trail} variance stabilized F_v^{net} trajectory throughout each transition period. These results indicate that rather than generating identical vertical leg-forces with minimal variance across steps, humans exhibited considerable step-to-step variability while selecting combinations of lead and trail leg-forces that resulted in a consistent net-force trajectory. Because they are stabilized through these strategic leg-force combinations, a consistent vertical net-force trajectory during the step-to-step transition may therefore represent an implicit goal of

walking that the human neuromuscular system is likely to monitor and control. Robust human gait as described by dynamic walking principles is thus accomplished by taking advantage of the flexible control enabled by inherent step-to-step leg-force variability to stabilize this implicit gait goal.

2.4.2 Inter-leg Forces Modulate Net Anterior-posterior Force

Coordinated application of lead (braking) and trail (propulsive) leg-forces varied F_{ap}^{net} trajectory from one step to the next. This modulation of F_{ap}^{net} trajectory indicates that, as expected, consistent net anterior-posterior force application is not an implicit goal of treadmill walking and may instead contribute to the stabilization of a different goal (Gorniak, Zatsiorsky et al. 2007; Gorniak, Zatsiorsky et al. 2009). Changing the F_{ap}^{net} trajectory with each step adjusts step-by-step COM accelerations that maintain the constant walking speed dictated by the treadmill. Requiring a particular walking speed in the experiment created an explicit goal of speed control that likely corresponds to an implicit goal of natural, overground walking. Evidence of direct F_{ap}^{net} trajectory modulation therefore provides some validation for the ability of the UCM analysis to identify and distinguish implicit locomotor goals from secondary variables that serve to stabilize other goals, such as speed.

2.4.3 Intra-leg Joint-torques Stabilize Vertical Leading Leg-force and Modulate Vertical Trailing Leg-force

Joint-torque variance is structured to control the vertical component of leg-force as required for leg function. Our results show that the F_v^{lead} trajectory is stabilized

through the selection of force-equivalent joint-torque combinations in steady state walking. Because the mechanics of a collision are by nature passive (Kuo, Donelan et al. 2005), F_v^{lead} collisional forces are unpredictable. Lead limb forces generated on the ground during the step-to-step transition are, however, largely generated by muscular forces and therefore require some motor control. Our subjects negotiated the variability of each heel strike by stabilizing leading leg vertical force as much as possible, albeit imperfectly as some leg-force variance was retained. In contrast, trailing leg-force generation involves no collisional forces and is therefore more predictable, allowing the trailing leg to effectively respond to deviations in F_v^{lead}. We observed that trailing leg joint-torques coordinate to actively modulate the trajectory of F_v^{trail} during each step-to-step transition. Rather than trying to match the values of leading leg forces, the modulation of the F_v^{trail} trajectory allows the trailing leg to make step-to-step adjustments that compensate for unexpected F_v^{lead} deviations, thereby maintaining a consistent F_v^{net} trajectory. Dynamic walking principles predict that the timing of trailing leg force application is important for minimizing the energetic cost of walking (Kuo 2002; Kuo, Donelan et al. 2005; Ruina, Bertram et al. 2005; Collins and Kuo 2010). Our UCM analysis of human walking further revealed that the trailing leg is also important for making step-to-step adjustments that stabilize the F_v^{net} trajectory, perhaps to ensure consistent COM transitions in the face of natural variability. These results provide evidence that the locomotor control system may actively monitor and modulate trailing leg forces in coordination with leading leg force deviations to redirect the COM trajectory consistently between steps.

2.4.4 Intra-leg Joint-torques Stabilize Anterior-posterior Leg Forces

Leg-force equivalent combinations of intra-leg joint-torques generate consistent braking (F_{ap}^{lead}) and propulsive (F_{ap}^{trail}) force trajectories throughout step-to-step transitions. During step-to-step transitions, the leading leg provides anterior-posterior braking forces to slow the COM velocity. Propulsive forces generated by the trailing leg offset the kinetic energy lost during these braking impulses (Kuo 2002; Ruina, Bertram et al. 2005; Collins and Kuo 2010). The consistent F_{ap}^{lead} and F_{ap}^{trail} trajectories we observed agree with the dynamic walking prediction that propulsive forces will counterbalance leading leg braking forces in each transition. This leg-force stabilization is imperfect, however, and some small anterior-posterior leg-force deviations still occur. The resulting deviations in leg-forces then become the source of inter-leg force variance that is structured to modulate the net anterior-posterior force for speed regulation.

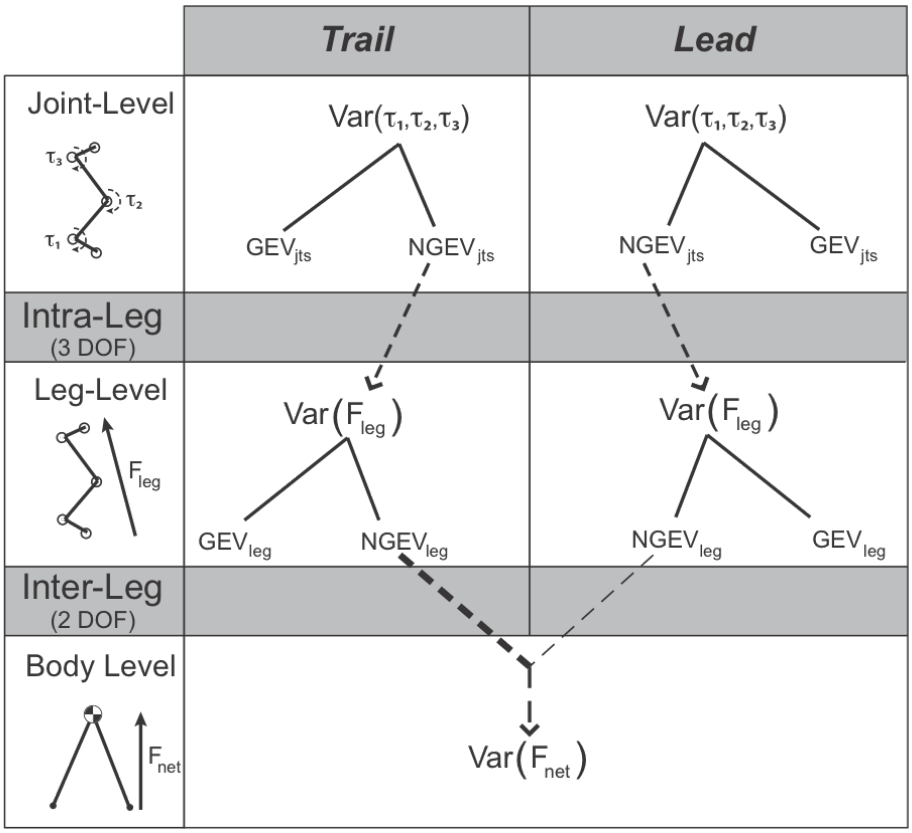

Figure 2.5: Postulated hierarchical control to achieve robust walking as described by the dynamic walking model. Intra-leg joint torque combinations modulate F_v^{trail}. Different F_v^{trail} values with each transition inflate leg-level NGEV, dominating the inter-leg variance available for inter-leg coordination to stabilize F_v^{net}, an implicit goal of human gait. A similar structure also holds for F_{ap}^{net} modulation, where leg-level NGEV is equally small in the leading and trailing legs and variable step-to-step F_{ap}^{net} is achieved through timing differences in leg-force application.

2.4.5 Joint-torques Influence Net-force Stability Through Locomotor Control Hierarchy

Considering intra-leg force stabilization within the context of inter-leg net-force control implies a dependency of body-level force control on leg-level and joint-level variability (Fig 2.5). Intra-leg joint-torques determine individual leg-forces, which are then coordinated to regulate net-force trajectories. Our results revealed how deviations at one level can be structured to attenuate or amplify the variability at another hierarchical level. Force-equivalent joint-torque deviations, by definition, do not manifest as leg-force

deviations and do not contribute to total inter-leg force variability (Gorniak, Zatsiorsky et al. 2007; Gorniak, Zatsiorsky et al. 2009). In contrast, joint-torque deviations that are not force-equivalent are directly transformed into leg-force deviations with each step. These remaining step-to-step deviations in leading and trailing leg-forces can be further structured through inter-leg coordination to directly affect the consistency of the net-force (Fig 2.5). Directing variance into goal-equivalent (GEV) or non-goal equivalent (NGEV) components at each hierarchical level allows the locomotor system to attenuate F_v^{net} and amplify F_{ap}^{net} trajectory variability with each step as required by the walking task.

Interactions between step-to-step joint-torque and leg-force deviations describe a hierarchical organization for locomotor control of human walking. In our walking data, non-force equivalent joint-torque variance (NGEV) is present in the intra-leg control of all leg-level task variables (Fig 2.4c-f, thick lines). For stabilized leg-force trajectories (F_v^{lead}, F_{ap}^{lead}, F_{ap}^{trail}), GEV exceeds NGEV to result in IMA values greater than zero, but some deviations in each of these leg forces inevitably remain. The large amount of joint-torque NGEV in the trailing leg (Fig 2.4e, thick dashed line) results in F_v^{trail} modulation. The resulting negative IMA (Fig 2.4a, dashed line) indicates that the trailing leg makes leg-force adjustments from one step to another to counteract unexpected deviations in the leading leg-force. Such coordination of leg-force deviations ultimately stabilizes the F_v^{net} trajectory for consistent COM redirection (Fig 2.5, thick dashed line). Modulation of the F_{ap}^{net} trajectory is similarly achieved by coordinating leg-force deviations that remain after F_{ap}^{lead} and F_{ap}^{trail} stabilization. These results delineate a hierarchical locomotor control strategy for stabilizing implicit (e.g., consistent F_v^{net} trajectory) and explicit (e.g., constant walking speed) locomotor goals. This hierarchical strategy attenuated kinetic

deviations from joint-torques to leg-force and ultimately minimized vertical net-force deviations. This same strategy specifically amplified the cascade of deviations that modulated net anterior-posterior force to control walking speed.

2.4.6 Potential Mechanisms for Stabilization of Hierarchical Forces

The evidence presented here supports a hierarchical organization of human locomotor control, but the mechanisms governing control within this organization remain less clear. Passive mechanics could account for some of the observed force stabilization. Dynamic walking principles use simple dynamical models (Collins 2008) that have guided the construction of passive robots requiring no active control to walk down an incline (McGeer 1990; Garcia, Chatterjee et al. 1998). Though they demonstrate the potential for walking to be driven solely by passive mechanics, these robots only walk successfully over a limited range of initial conditions. For example, Garcia et al. (1998) found that simple walkers with rigid struts for legs were stable only on slopes less than 0.019 rad (<1.1 degrees). More sophisticated robot walkers that include a knee joint still only demonstrate "stable, persistent walking" on slopes with less than 6 degrees of decline (Garcia, Chatterjee et al. 2000). Even on acceptably shallow slopes, stability of these robots remains highly sensitive to initial conditions. While they can establish the minimal requirements for locomotor control, passive dynamics alone do not explain the scope of adaptability and robust performance across the range of typical conditions observed in human walking. Unlike passive robots, human walkers must negotiate joint-torque and leg-force interactions that are not rigidly coupled and coordinate multiple active degrees-of-freedom to achieve consistent vertical net-force trajectories across large

time scales. Negotiating these complicated interactions suggests contribution from some neuromuscular controller.

While the observed vertical net-force stabilization and anterior-posterior net-force modulation could be due to some inherent mechanical properties of the biomechanical system, passive mechanics are unlikely to be the sole determinant of human walking stability. Previous work has shown that following peripheral nerve injury, hip-to-toe leg length and leg orientation parameters are preserved despite disruption of normal joint angle trajectories, suggesting that neural circuits exist to coordinate joint-level local variables to maintain whole limb-level function (Chang, Auyang et al. 2009; Bauman and Chang 2013; Boeltz, Ireland et al. 2013). Leg length trajectories are, however, disrupted following the disruption of central neural circuits despite intact biomechanical connections (Stahl and Nichols 2011). The central nervous system may, therefore, also be required to maintain the coordination of joint-level variance structure that stabilizes limb-level performance across step cycles.

Inherent properties of the neuromuscular system may contribute to achieving consistent, stable leg- and net-force production. Heterogenic reflex pathways mediate intra-leg coordination of joint-torques and may contribute to joint-torque adjustments in response to small perturbations, resulting in consistent leg-force production (Nichols 1999; Wilmink and Nichols 2003). Recent investigations demonstrate that humans adapt temporal-spatial parameters and muscular activation patterns to achieve inter-leg symmetry when forced to walk with an asymmetric walking pattern (Dietz, Zijlstra et al. 1994; Prokop, Berger et al. 1995; Reisman, Block et al. 2005). Such inter-leg coupling, coordination, and control may be informed by load receptors (Jensen, Prokop et al. 1998)

and achieved through central inhibitory pathways active during bilateral but not in unilateral tasks (Ting, Raasch et al. 1998). Actions of multi-articular muscles and/or interaction torques could also contribute to maintaining consistent leg forces through passive mechanics (Cabel, Cisek et al. 2001; Kurtzer, Pruszynski et al. 2006; Sangani, Starsky et al. 2007). For example, adopting a more extended leg posture leads to stable leg-force production despite high joint-torque variability in hopping tasks (Yen and Chang 2010). Although the aforementioned pathways may regulate the coordinated intra- and inter-leg action during gait, identification of the relevant mechanisms requires further study and focused investigation. Nevertheless, the results presented here support the idea that human walkers use a hierarchical strategy to harness inherent motor variance to achieve flexible and robust control of bipedal locomotion.

2.5 Conclusion

We studied dynamic walking principles in human subjects within the general framework of the uncontrolled manifold concept to identify implicit control targets the neuromuscular system may actively monitor and control to achieve robust walking. The results presented here collectively demonstrate that human locomotor control harnesses step-to-step kinetic variability to achieve robust, steady state walking. Human walkers take advantage of their inherent motor abundance by structuring joint- and leg- level variance to stabilize implicit intra- and inter-leg hierarchical goals. Because dynamic walking principles make predictions about individual leg power and work, future studies should also test these as potential goal variables within the framework already

constructed here. Future investigation may also explore how these implicit goals are adapted in response to changing environmental conditions or neuromuscular pathologies.

CHAPTER 3

THE MOTOR AND THE BRAKE DURING PROPULSION IN HUMAN WALKING I: LEG FORCE CONTROL THROUGH ANKLE TORQUE MODULATION AND KNEE TORQUE COVARIANCE

In this chapter, I focus more specifically on how trailing leg force modulation observed in Chapter 2 is achieved and how it contributes to robust able-bodied walking mechanics. I found that peak trailing leg power production is made consistent through step-to-step adjustments of force along the trailing leg. I then applied a modified uncontrolled manifold (UCM) analysis to test how both individual and coordinated joint torque control contributes to trailing leg force application. The observed modulation of trailing leg force for maintenance of consistent peak power was achieved primarily through variable timing of ankle torque production, while simultaneous knee torques refined the effect of ankle torque variance on leg force application. The knee appears to act as a series brake that balances the effects of the ankle motor's variance, providing a stabilizing effect and enabling more robust leg control. This chapter demonstrates that able-bodied human walkers appear to take advantage of their inherent motor abundance to achieve robust walking mechanics.

3.1 Introduction

Steady-state human walking is a complex task that requires coordination of muscle activations, joint torques, and leg forces at various levels of neuromuscular

control. Control of bipedal walking is likely simplified by exploiting the underlying dynamics (McGeer 1990; Garcia, Chatterjee et al. 2000; Collins, Ruina et al. 2005; Su and Dingwell 2007; Kurz, Judkins et al. 2008; Verdaasdonk, Koopman et al. 2009). Focusing higher-level control to a specific set of influential task parameters (e.g. limb force) during particular gait phases (e.g. double support) could reduce the number of variables and the duration over which control is required, thus simplifying the motor control problem (Bosco and Poppele 2000). Quantitative models of bipedal walking may suggest possible candidates for such controlled variables. Dynamic walking principles have established that step-to-step transitions are critical periods of the gait cycle where energetic demand originates (Donelan, Kram et al. 2002a; Donelan, Kram et al. 2002b; Kuo 2002). Negative work absorbed by the leading leg results in mechanical energy loss that must be supplied to the system by generation of positive work performed by the trailing leg to maintain a steady, forward gait (Donelan, Kram et al. 2002a; Donelan, Kram et al. 2002b; Kuo 2002). Achieving consistent trailing leg power production may therefore be an implicit task goal for steady state walking. How consistent leg power production may be achieved despite inherent motor variability remains unclear. The purpose of this study was to identify a possible mechanism for generating consistent leg power production despite intrinsic neuromuscular variability in steady state human walking.

Modulating trailing leg force application likely contributes to leg power consistency. Leg power is determined by leg force and center of mass velocity (**Eq. 3.1**). The timing of trailing leg force application is important for achieving minimal energetic loss (Kuo 2002; Ruina, Bertram et al. 2005). Adjustments in leg force timing may

therefore influence how trailing leg power is generated and provide a possible mechanism for stabilizing leg power. Our previous work demonstrated that trailing leg vertical forces were modulated with each step in human walking (Toney and Chang 2013). Modulation of a particular variable may reflect step-to-step corrections made to achieve consistent execution of an alternative variable at a different hierarchical level (Shim, Latash et al. 2003; Gorniak, Zatsiorsky et al. 2007; Gorniak, Zatsiorsky et al. 2009). Modulation of vertical leg forces likely enables net vertical force trajectory stabilization (Toney and Chang 2013). Modulation of force along the leg, however, affects leg power and may contribute to consistent power generation. We hypothesized that force directed along the trailing leg would be most modulated when leg power was most consistent, indicating that the trailing leg makes step-by-step force corrections to stabilize leg power for more efficient step-to-step transitions (**H1**).

Leg forces can be modulated in two ways: (i) through individual joint torque adjustments where each joint torque separately modulates leg force or (ii) through inter-joint coordination where joint torques work together to emphasize leg level destabilization. Using a modified uncontrolled manifold (UCM) analysis (Yen and Chang 2010), we can isolate the effect of each of these sources and determine their relative contribution to whole leg force control. Leg force modulation through regulation of a single joint torque would simplify the higher-level control required during steady state walking. The triceps surae are the largest contributor to trailing leg force production in walking (Kepple, Siegel et al. 1997; Neptune, Kautz et al. 2001), so ankle torque modulation could effectively manipulate leg force. However, relying on a single joint for motor control would result in an unstable system and limit one's ability to adjust to

unexpected perturbations. Using another joint to balance actions at the ankle would provide an additional level of control and enable more robust control of leg force. Previous work has revealed neuromechanical coupling between ankle and knee action, suggesting that ankle-knee coordination may refine and stabilize leg force control during steady state walking (Nichols 1999; Wilmink and Nichols 2003; Stahl and Nichols 2011). We hypothesized that individual control of ankle torques would be the greatest contributor to joint torque variance structure for modulating trailing leg force (**H2**), but that the ankle and knee would covary to provide a supplementary stabilizing effect on leg force (**H3**).

3.2 Methods

3.2.1 Data Collection

Eight healthy subjects (6 male/2 female, weight: 81.5±14.1 kg, leg length: 91.8±4.7 cm) gave informed consent prior to participating in a protocol approved by the Georgia Institute of Technology Institutional Review Board. Four participants completed a six-minute walk test prior to data collection, three participants completed the test on a separate day after data collection, and one did not complete a six minute walk test (660.2m±56.0m, ATS Statement: Guidelines for the Six-Minute Walk Test). Preferred walking speed (1.29±0.10m/s) was determined by allowing subjects to walk at a variety of speeds below their average walking speed during the six minute walk test, during which participants verbally indicated whether they would prefer the speed to be faster, slower, or if it was "just right." All participants walked on a custom dual-belt treadmill for two minutes at 75% of their preferred walking speed (PWS). Ground reaction forces

were collected independently for each limb using mechanically isolated force plates embedded beneath each treadmill (1080 Hz, Advanced Mechanical Technology Incorporated, Watertown, MA, USA). Simultaneous kinematics data were captured using a six-camera motion analysis system (120Hz, VICON Motion Systems, Oxford, UK). Retroreflective markers were placed bilaterally on the anterior superior iliac spine, posterior superior iliac spine, greater trochanter, thigh segment, knee joint center, shank segment, lateral malleolus, fifth metatarsal head, and second metatarsophalangeal joint.

3.2.2 Data Analysis

Marker and force data were filtered with a zero-phase lag fourth-order Butterworth low-pass filter with a 10 Hz cut-off frequency. Joint-torques were calculated in the sagittal plane using standard inverse dynamics calculations and estimated segment inertial characteristics based on subject specific anthropometrics (Winter 1980). Individual leg power was calculated as the dot product of the force recorded from that leg (leg force, F_{leg}) and center of mass (COM) velocity (v_{com}, **Eq. 1**). COM velocity was calculated with the integral of COM acceleration (a_{com}) as calculated from the product of subject mass (m) and net force recorded from both legs (F_{net}, **Eq. 2**). The integration constants were zero for the vertical COM velocity component and treadmill speed in meters per second for the anterior-posterior COM velocity component. All data were time normalized starting from ipsilateral heel contact.

$$P = F_{leg} \cdot v_{com} \quad \textbf{(Eq. 3.1)}$$

$$v_{com} = \int a_{com} dt = \int \left(F_{net} / m \right) dt \qquad \textbf{(Eq. 3.2)}$$

3.2.3 Uncontrolled Manifold Analysis

An Uncontrolled Manifold (UCM) analysis was performed using custom Matlab code. A detailed explanation of this technique as applied to vertical and anterior-posterior force components has been provided previously (Auyang, Yen et al. 2009; Yen and Chang 2010; Toney and Chang 2013). Briefly, the UCM analysis partitions total variability of local variables (e.g. joint torques) into two components either parallel or perpendicular to a linearized estimate of a goal equivalent manifold, where small joint-torque deviations do not affect the task goal (e.g. leg force). Comparing the relative magnitude of these orthogonal variance components can reveal whether elemental variables (joint-torques) exhibit a non-random structure that aligns with a hypothesized functional goal (leg force). The relationship between joint torques and the leg force is mathematically described within a Jacobian matrix (***J***), which quantifies the effects of small joint-torque deviations on the leg force. The null-space of J serves as a linearized approximation of the goal-equivalent manifold against which we test our hypotheses about the structure of elemental variance. Joint torque variance parallel to this manifold has no effect on leg force, so this parallel component of variance is termed goal-equivalent variance (GEV, **Eq. 3.3**), where n is the number of local degrees of freedom (3 joint torques), and d is the number of global degrees of freedom (1 leg force). We call joint torque variance perpendicular to the manifold non-goal equivalent variance (NGEV, **Eq. 3.4**) because it causes a change in the magnitude of leg force.

$$GEV = \frac{trace(null(J^T)\cdot C\cdot null(J))}{n-d} \quad \textbf{(Eq. 3.3)}$$

$$NGEV = \frac{trace((J\cdot J^T)^{-1}\cdot J\cdot C\cdot J^T)}{d} \quad \textbf{(Eq. 3.4)}$$

In each of these equations, C is the statistical covariance matrix of joint torques (**Eq. 3.5**), where σ_i^2 is individual variance of a single joint torque, σ_{ij} is covariance between two joint torques, and the subscripts denote a particular joint torque (a=ankle, k=knee, h-hip).

$$C = \begin{bmatrix} \sigma_a^2 & \sigma_{ka} & \sigma_{ha} \\ \sigma_{ak} & \sigma_k^2 & \sigma_{hk} \\ \sigma_{ah} & \sigma_{kh} & \sigma_h^2 \end{bmatrix} \quad \textbf{(Eq. 3.5)}$$

The relative amount of GEV and NGEV reveals the overall affect joint torque variance has on the leg force trajectory. To quantify this effect and compare the organization of joint torque variance across individuals, we calculate a normalized metric of variance structure, the Index of Motor Abundance (IMA, **Eq. 3.6**), for each 1% of the gait cycle, where TotV is the normalized total joint torque variance (**Eq. 3.7**).

$$IMA = \frac{GEV - NGEV}{TotV} \qquad \textbf{(Eq. 3.6)}$$

$$TotV = \frac{trace(C)}{n} \qquad \textbf{(Eq. 3.7)}$$

The analysis used here differs only slightly from our previously published approach (Yen, Auyang et al. 2009; Toney and Chang 2013). Here we again use a kinematic Jacobian that maps the corresponding joint-torques to endpoint force using an operational space formulation developed for controlling humanoid robots (Khatib 1987; Yen, Auyang et al. 2009). However, rather than decomposing the leg force vector into globally referenced vertical and anterior-posterior components, we instead geometrically rotate the local reference frame to align with the leg orientation vector (center of pressure to ASIS marker). From this transformed data, we construct our geometrically derived Jacobian matrix to project joint torque variance into task space aligned with the leg

orientation vector. In this way, we analyze how joint torque deviations contribute to variance of the force generated along the long axis of the leg.

IMA trajectories were evaluated for significant differences from zero using a two-tailed Student's t-test (α=0.005, Bonferroni corrected) to compare each percentage point of the gait cycle to zero. An IMA significantly greater than zero indicates the joint torques were coordinated to generate the same leg force at that point in the gait cycle with each step. A positive IMA means that only task-relevant deviations are reduced, which is consistent with a minimal intervention principle of motor control (Todorov and Jordan 2002). We therefore interpret positive IMA values as an indication that leg force is stabilized, and is likely a controlled, implicit neuromechanical goal of walking at that point in the gait cycle. An IMA significantly less than zero indicates active modulation such that joint torques combined to produce a different leg force trajectory with each step. In this case, task-relevant deviations are not restricted, but instead enhanced and contribute directly to leg force modulation. A negative IMA is therefore interpreted to mean that leg force is instead modulated to stabilize some alternative task variable (Shim, Latash et al. 2003; Gorniak, Zatsiorsky et al. 2007; Gorniak, Zatsiorsky et al. 2009).

3.2.4 Components of the Index of Motor Abundance

Variance structure as indicated by the IMA metric can arise from two different sources: 1) individual control of joint torques and/or 2) covariance across joints torques. We used a modified UCM analysis to isolate the effect of these two possible sources (Yen and Chang 2010). The UCM analysis uses a statistically derived covariance matrix (**Eq. 3.5**) to determine the underlying structure of the joint torques. Altering this

covariance matrix allows us to isolate the effects of individual variance and covariance. Specifically, the variance of each joint torque relative to itself (individual variance) is contained within the diagonal elements of the covariance matrix ($\sigma_a^2, \sigma_k^2, \sigma_h^2$), and the off-diagonal elements are inter-joint covariances. To determine the effect of this structure on the control of leg force, we set the off-diagonal elements to zero (C', **Eq. 3.8**), then re-calculate, GEV', $NGEV'$, and IMA'using C'.

$$C' = \begin{bmatrix} \sigma_a^2 & 0 & 0 \\ 0 & \sigma_k^2 & 0 \\ 0 & 0 & \sigma_h^2 \end{bmatrix} \quad \textbf{(Eq. 3.8)}$$

The IMA value that results from using C' reflects the amount of joint torque variance structure that results from individual joint torque control, so we call this new metric INV (=IMA'). All remaining variance structure must then result from covariance between the joints. We therefore calculate the contribution of this coordination by subtracting the individual variance structure (INV) from the overall structure (IMA) (**Eq. 3.9**). In this way, we can determine whether the source of the overall joint torque variance structure is derived from an individual (INV) or coordinated (COV) joint torque variance control. It is important to note that the statistical covariance matrix (C) and COV metric indicate two different aspects of motor control. The covariance matrix reflects the statistical covariance between joint torques, while the COV metric indicates the effect this inter-joint covariance has on the stabilization of the leg force trajectory.

$$COV = IMA - INV \quad \textbf{(Eq. 3.9)}$$

COV and INV trajectories were statistically evaluated and interpreted in the same way as IMA trajectories. We applied a two-tailed Student's t-test (α=0.005, Bonferroni correction) to test for differences significantly different than zero. INV values greater than zero indicate that individual joint torque variance is organized to stabilize leg force output, while positive COV values indicate that covariance between joint torques have a stabilizing effect. Negative values for INV and/or COV indicate that joint torques are organized to modulate the leg force trajectory through individual or coordinated control, respectively. To determine the similarity the COV and INV trajectories have to the IMA trajectory, we "fit" each trajectory to the other using the built in Matlab function "corrcoef." Larger resulting R^2 values indicate that either INV or COV account for a greater amount of inter-subject residual variance in the IMA trajectory (Bauman and Chang 2013). In other words, a larger R^2 value indicates a "better fit" of that component to the IMA trajectory.

3.2.5 Joint Torque Gain from the Jacobian Matrix

We further delineated the source of variance structure by quantifying the influence each joint torque has on leg force. Small deviations in each joint torque affect leg force variability differently depending on the leg's posture at that point in the gait cycle. For example, at the end of stance, small changes in ankle torque will have a larger impact on force along the leg than changes in knee or hip torque because the ankle is more flexed than either the knee or hip, maintaining a longer lever arm relative to the leg orientation vector. The geometric relationship between the joints and end point location is

captured in the Jacobian matrix, where each element represents the gain on each joint at that point in the gait cycle. We determined the gain on each joint torque by comparing the Jacobian elements at the time of peak power for each subject. Differences in joint torque gain at this point in the gait cycle were evaluated by applying a repeated measures ANOVA and Scheffe's post-hoc multiple comparison test (α=0.05).

3.2.6 Event Timing

We tested whether the time of identified gait events occurred at similar times. Specifically, we tested for differences in timing of peak power, local minimum of power variance, most negative IMA, most negative INV, maximum ankle torque variance, and maximum ankle torque rate of change. We applied a repeated measures ANOVA (α=0.05) with a post-hoc Scheffe multiple comparison test to identify differences in timing of identified gait events.

We also reanalyzed data provided by Farris and Sawicki (2012) to determine whether a timing dependence existed between muscle fascicle performance and power output. This data included ultrasound recordings of medial gastrocnemius fascicle length, rate of change, and power as well as calculated Achilles tendon forces for walking in 10 subjects at 0.75, 1.25, 1.75, and 2.00 m/s. We manually identified the time within the gait cycle that peak mean fascicle shortening acceleration, peak mean Achilles tendon force, and peak mean muscle tendon unit (MTU) power occurred for each subject. The linear relationship between peak tendon force, fascicle acceleration, and MTU power was determined with a first order polynomial fit using the built in Matlab command "polyfit."

3.3 Results

3.3.1 Joint Torques and Ground Reaction Forces

Individual leg forces and joint torque trajectories were consistent with previously published data (Winter 1980; Nilsson and Thorstensson 1989) when subjects walked comfortably at 75%PWS (**Fig. 3.1**). The first double support period when the leg of interest leads was initiated at ipsilateral heel strike and terminated at contralateral toe off, lasting from 1-15.8±1.4% of the gait cycle for all subjects. The second double support period from contralateral heel strike to ipsilateral toe off lasted from 51.1±0.8%-64.9±1.1% of the gait cycle (n=8).

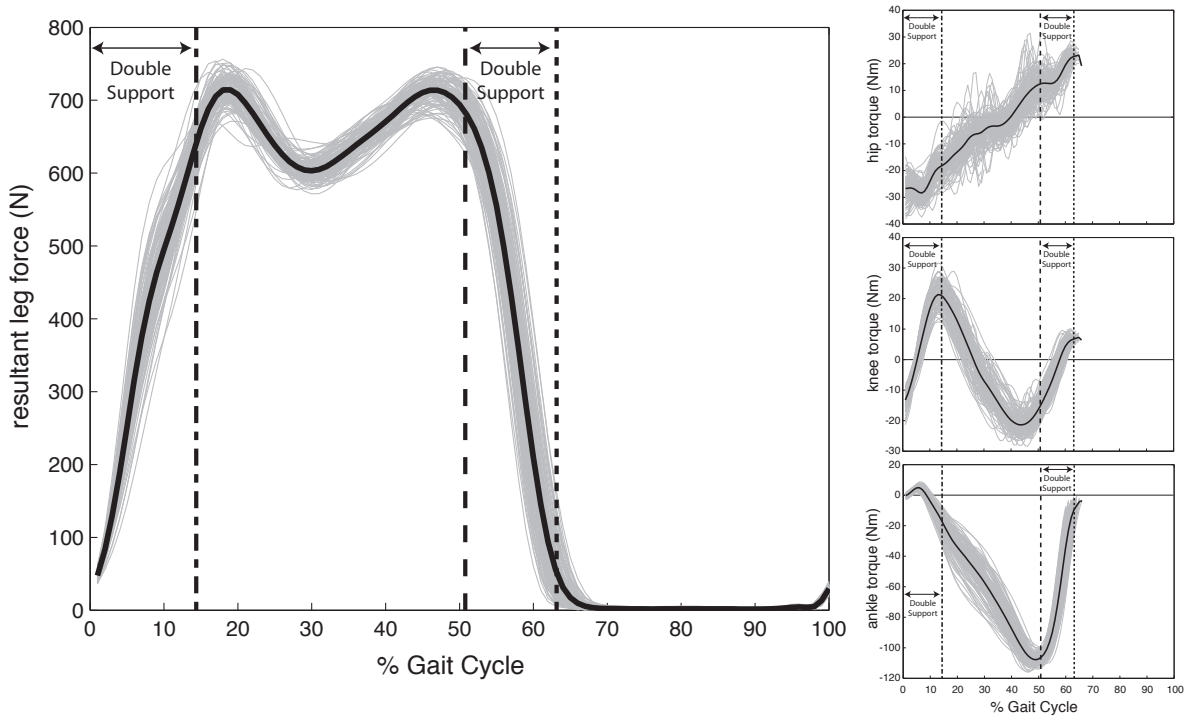

Figure 3.1: Representative subject resultant leg force (left panel) and joint torques (right column). Gray lines represent leg force and joint torque values for each step, while the thick black lines represent the mean trajectory. Double support when the leg is leading (1-14.4±0.7% gait cycle) and when the leg is trailing (50.8±1.0%-63.2±1.2% gait cycle) are bounded by the vertical lines. Gait cycles are defined from heel contact (0%) to ipsilateral heel contact (100%).

3.3.2 Leg Power

Leg power trajectories were also consistent with previously published data (Donelan, Kram et al. 2002a; Donelan, Kram et al. 2002b). Power was negative, meaning that power is absorbed by the leg, during the first double support period when the leg leads. Leg power is positive (generated) during the second double support period when the leg trails (**Fig. 3.2**). Variance of leg power is relatively constant during single limb stance, but rises as power increases during the second double support period. Variance of leg power demonstrates a local minimum (58.4±1.0% gait cycle) concurrently with the absolute maximum in leg power (**Fig. 3.2**, black arrow, 58.5±1.2% gait cycle).

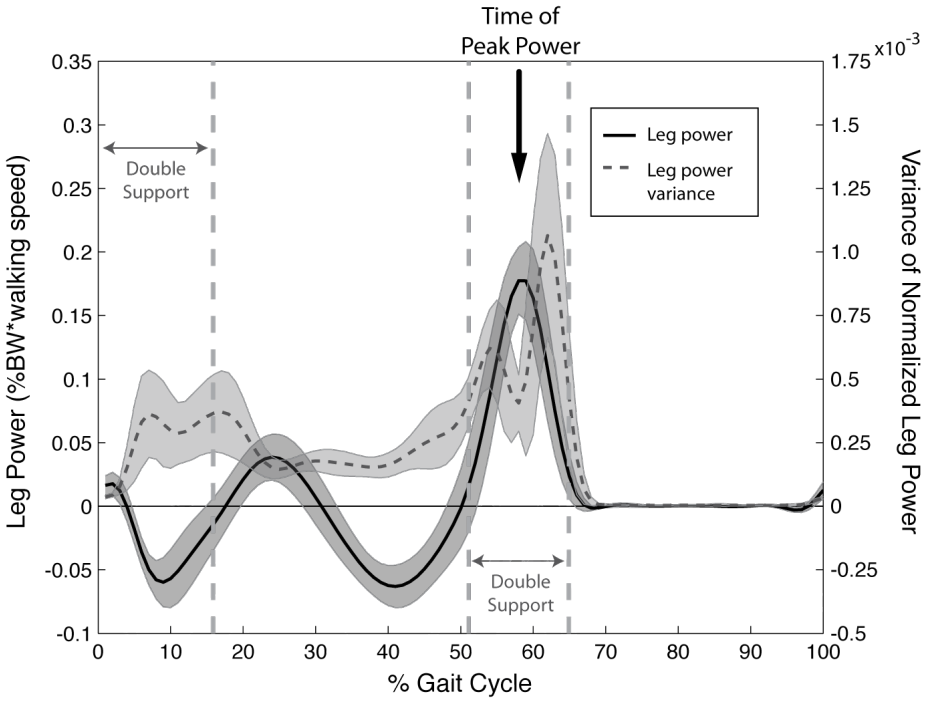

Figure 3.2: Mean and inter-subject standard deviation of leg power (solid line) and leg power variance (dashed line) for one leg of each subject throughout the gait cycle. Peak leg power occurs simultaneously a local minimum in leg power variance (large arrow). In other words, maximal leg power production is highly consistent.

3.3.3 Intra-leg UCM Analysis for Leg Force Control

The index of motor abundance (IMA) was significantly greater than zero ($p<0.005$) from 1-15% of the gait cycle, indicating that leg force is stabilized during the first double support period when the leg leads (**Fig. 3.3A**). Leg force was modulated ($IMA<0$, $p<0.005$) in a small portion of the second half of single limb stance (at 44% gait cycle) and during double support when the leg trails (59-61% gait cycle). The time of most negative IMA (58.9±1.5% gait cycle) occurs at the same time as maximal power (**Fig. 3.3**, black arrow).

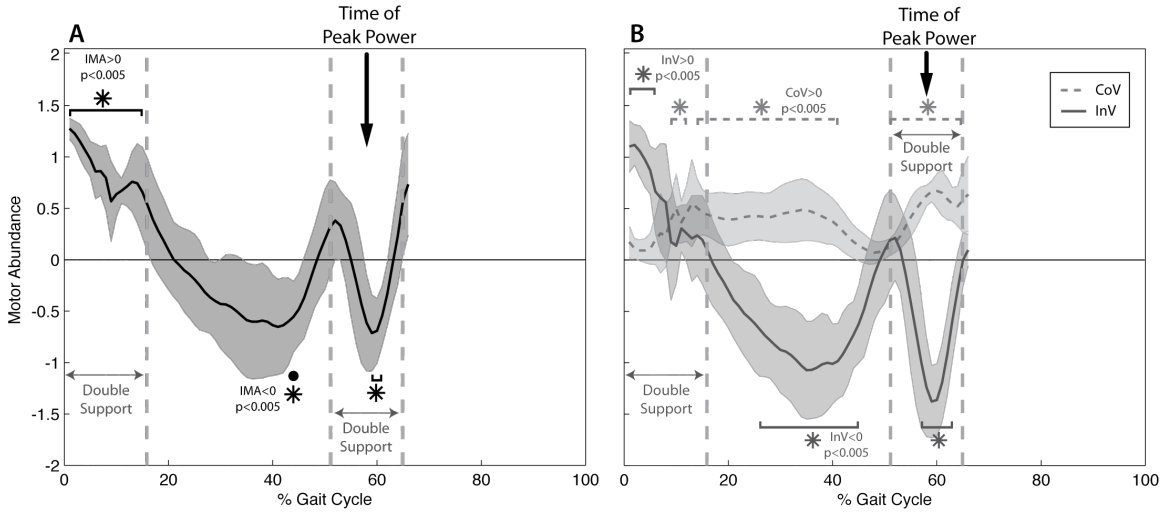

Figure 3.3: A) Mean and inter-subject standard deviation of Index of Motor Abundance of (IMA) for one leg of each subject throughout the gait cycle. Note that IMA is calculated only when the task level variable (ground reaction force) is generated when the leg is on the ground. Hip, knee, and ankle joint torques combine to stabilize leg force ($IMA\neq0$, $p<0.005$) when the leg is leading (1-15.8±1.4% Gait Cycle) and modulate leg force ($IMA\neq0$, $p<0.005$) when the leg is trailing in double support (51.1±0.8% - 64.9±1.1% GC). **B**) Variability due to individual joint torque variance structure (INV, red line) and co-variation among joint torques (COV, dashed line). Co-variation among the joints is present throughout the gait cycle ($COV\neq0$, $p<0.005$), but individual variation of joint torques appears to dominate the overall structure of joint torque variance: the trace of INV is more similar to the trace of IMA ($R^2 = 0.95$) than the trace of COV compared to IMA ($R^2 = 0.14$).

3.3.4 Contribution of Individual and Coordinated Variance to the Intra-leg Model for Leg Force Control

The trajectories of INV and COV demonstrated different patterns throughout the gait cycle (**Fig. 3.3B**). Individual joint torque control generated INV values significantly greater than zero ($p<0.005$) during the first part of double support when the leg leads (1-6% gait cycle). INV then fell to significantly less than zero during single limb support (26-45% gait cycle) and when the leg is trailing in the second double support period (57-63% gait cycle). Covariation between joint torques generated significantly positive COV values during the first double support and single limb stance (9-12% and 14-41% gait cycle) as well as throughout the second double support period when the leg trails (51-65% gait cycle). The INV trajectory accounted for 95% of the inter-subject residual variance in the IMA trajectory ($R^2 = 0.95$; $p<0.005$). The COV trajectory, on the other hand, only accounted for 14% of the residual inter-subject variance in the IMA trajectory ($R^2=0.14$; $p=0.002$).

3.3.5 Role of the Ankle in Leg Force Control

At the point in the gait cycle where peak leg power occurs, the Jacobian elements reveal a more than two-fold gain on ankle torque (6.49±0.73 gain) than either knee (2.62±0.64 gain) or hip (0.64±0.43 gain) torques ($F = 162.9$, $p<0.05$; **Fig. 3.4**).

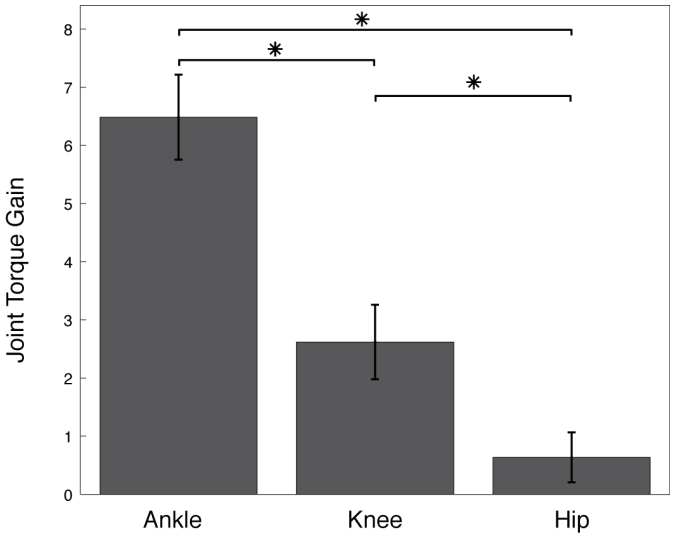

Figure 3.4: Gain of each joint torque to leg force deviations at the instance of maximum leg power. A larger gain indicates that deviations in that joint torque manifest as leg-level errors to a greater degree than joints with smaller gains. At the instance of maximum power generation, ankle torque deviations have a greater gain, and therefore a greater influence on leg force modulation, than either the knee or the hip (rmANOVA: $F = 162.9$, $p<0.05$)

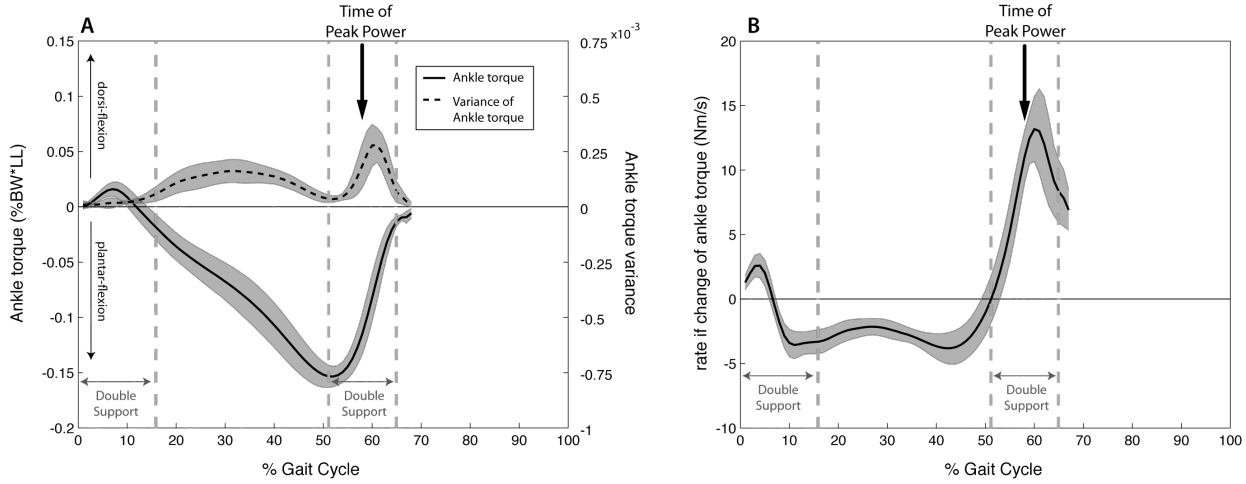

Figure 3.5: A) Mean and inter-subject standard deviation of normalized ankle torque profiles (solid line) and variability of these profiles across all steps (dashed line) for all subjects. Note that the instance of maximum plantar-flexion torque corresponds with a local minimum of ankle torque variability. In other words, maximum ankle plantar-flexion torque magnitude is more consistent than other instances in the gait cycle. **B**) Mean and standard deviation of rate of change of ankle plantar-flexion torque (blue).

3.3.6 Time of Power, Motor Control, and Ankle Torque Events

The time of maximum ankle torque variance and maximum ankle torque rate of change occurred significantly later than any tested leg power (time of peak power, time of minimum power variance) or motor control (time of minimum IMA, time of minimum

INV) event (F = 147.292, p<0.005, **Fig. 3.6**). While these observed differences were statistically significant, the absolute timing differences are likely not discernable by the nervous system. On average, maximum ankle torque variance occurred 2.1±0.7% and maximum ankle torque velocity occurred 1.4±0.6% later in the gait cycle than the average timing of the power and motor control events. A two percent difference equates to approximately 20ms in real time, which is faster than the time required for a timing error to be sensed and a reactionary force to be developed.

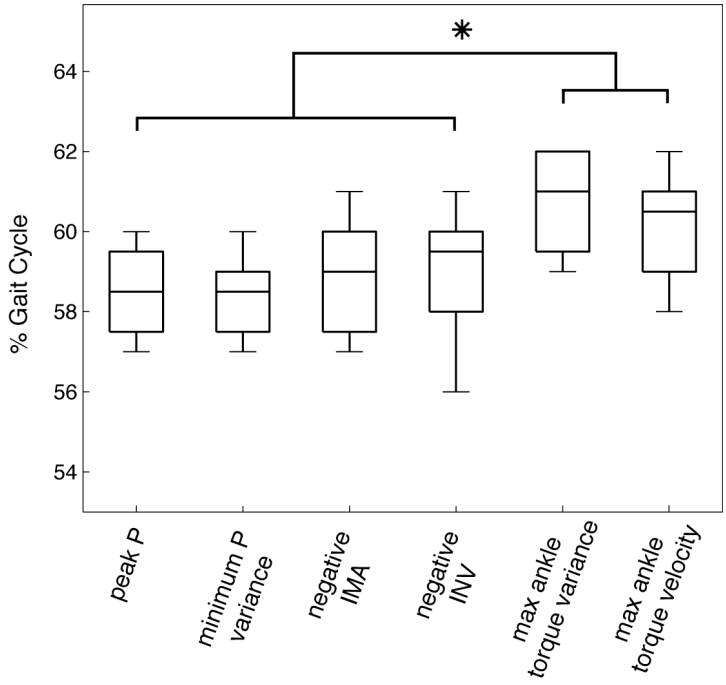

Figure 3.6: Bar and whisker plot representing the timing of identified gait events within the gait cycle: (from L to R) peak power, local minimum in leg power variance, most negative IMA value, most negative INV value, local maximum in ankle torque variance, absolute maximum in ankle torque velocity. In each box, the central line represents the median, the edges are the 25th and 75th percentiles, and the whiskers extend to the most extreme data points. A repeated measures ANOVA analysis with Scheffe post-hoc multiple comparisons revealed that maximum ankle torque variance and maximum ankle torque velocity occurred significantly later in the gait cycle (2.1±0.7% and 1.4±0.6% respectively) than the other gait events. These significant timing differences, however, are likely not a large enough delay to be detected by the nervous system.

3.3.7 Achilles Tendon Properties and Leg Force

The time at which peak Achilles tendon force occurred correlated well with when in the gait cycle peak muscle tendon unit (MTU) power was achieved (R^2 = 0.64, **Fig. 3.7A**). The slope of this relationship between peak Achilles tendon force and peak MTU power was close to unity (0.98), and the tendon reached peak force at a consistent time before peak power (intercept = 6.89). The time of peak gastrocnemius fascicle shortening acceleration was not as well correlated with when peak MTU power was achieved (R^2 = 0.397, y = 0.35x+39.12, **Fig. 3.7B**).

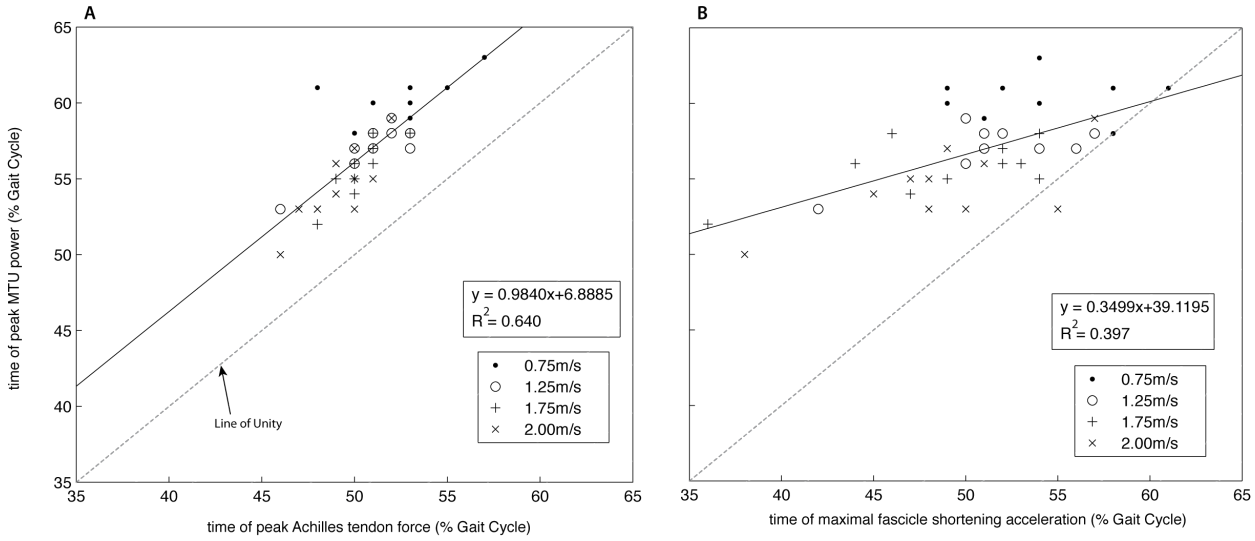

Figure 3.7: Data reproduced with permission from Farris and Sawicki (2012). Each data point indicates the time at which each event occurs for mean data of each subject. **A**) The time (% Gait Cycle) at which the Achilles tendon force is maximum is well correlated (R^2 = 0.640) with when peak muscle tendon unit (MTU) power occurs. This correlation holds across various slow and fast walking speeds. **B**) The time (% Gait Cycle) at which medial gastrocnemius fascicle shortening acceleration was the greatest was not as well correlated with the time of peak MTU power (R^2 =0.397) across various walking speeds.

3.3.8 Ankle-Knee Covariance

The magnitude of ankle-knee covariance as determined from the coefficients of the covariance matrix (**Eq. 3.8**) was greater than ankle-hip or knee-hip covariance at the time of peak power ($F=28.28 p<0.05$, **Fig. 3.8**). Positive ankle-knee covariance at the time

of peak power means that the knee tends to generate a flexion torque when the ankle generates a plantar-flexion torque, reducing the translation of ankle plantar-flexion torques directly to leg force.

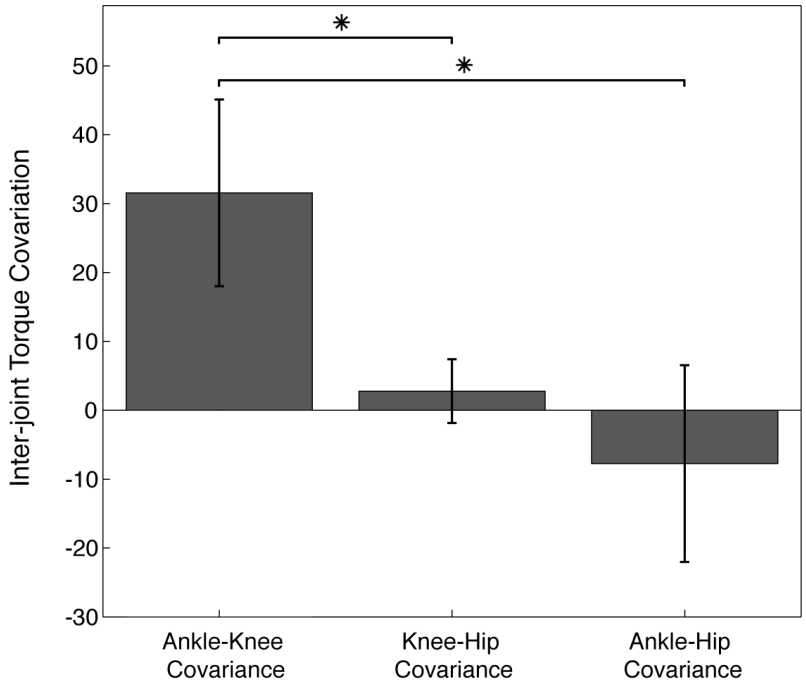

Figure 3.8: Mean and inter-subject standard deviation of covariation between ankle-knee, ankle-hip, and knee-hip joint torques at the time of peak power. The amount of covariation between joint torques depends on leg posture at each point the gait cycle. Ankle-knee torque covariation is significantly greater than either knee-hip or ankle-hip covariance (rmANOVA, $F = 28.275$, $p<0.05$). A positive relationship between ankle and knee joint torques indicates that when the ankle generates a plantar-flexion torque, the knee tends to generate a flexion torque, leading to minimally altered leg force. Ankle-knee covariation therefore likely most influence the COV contribution to leg force stabilization.

3.4 Discussion

We investigated the functional contribution of individual and coordinated joint torque control to leg force application during leg power generation in steady state walking. We found that maximal modulation of leg force coincided with the time of peak leg power production, which suggests that step-to-step corrections in leg force applications lead to consistent power generation (**H1**). Leg force modulation was achieved primarily through timing variability in ankle torque production (**H2**). We

propose a possible mechanism for how the nervous system may control and structure these timing errors by modulating when elastic recoil of the Achilles tendon is initiated. We also demonstrated that knee torque plays a key role in controlling leg force output by damping and counterbalancing the effect of ankle torque deviations on leg force (**H3**).

3.4.1 Trailing Leg Force is Modulated to Maintain Consistent Leg Power

In steady state walking, the locomotor system adopts efficient and repetitive walking mechanics, so we expected variables with a large impact on step-to-step transition efficiency to be similar with each step. We expected trailing leg power generation to be consistent because modeling studies have demonstrated the substantial influence the trailing leg has on walking efficiency, and consistent power input would lead to consistently efficient step-to-step transitions (Kuo 2002; Ruina, Bertram et al. 2005). Agreeing with our prediction (**H1**), our empirical findings show peak trailing leg power generation reaches a consistent magnitude at a consistent time in the gait cycle (**Fig. 3.2**). A local minimum in trailing leg power variance occurs concurrently with peak power and indicates that peak power is more consistent than any surrounding time point.

Our UCM analysis revealed that joint torques combine to modulate leg forces ($IMA<0$, $p<0.05$) at the same point in the gait cycle when leg power reaches its peak (**Fig. 3.3A**). In other words, joint torques combined to apply a different trailing leg force each time leg power was maximized in each step. Modulation of a particular task variable may indicate that the tested variable makes corrections with each step to stabilize a variable at a different organizational level (Shim, Latash et al. 2003; Gorniak, Zatsiorsky et al. 2007; Gorniak, Zatsiorsky et al. 2009). Leg power is determined by force along the

leg and center of mass velocity (**Eq. 3.1**), so modulation of leg force will affect the leg power profile. Our finding of negative IMA at the same instance as peak power generation suggests that joint torques are organized to generate different leg force with each step in order to maintain consistent peak power production during step-to-step transitions. The influence of leg force timing on walking mechanics has been established in robotic systems and mathematical representations (Kuo 2002; Ruina, Bertram et al. 2005), but this is the first time a similar relationship has been established in human walkers. It remains unclear, however, how joint torques are specifically controlled to modulate leg force.

3.4.2 Variable Timing of Peak Ankle Plantar-flexion Torque Leads to Leg Force Modulation

The strong agreement between INV and IMA trajectories (**Fig 3.3**) indicate that leg force control was mostly determined by a strategy of controlling individual joint torque variability throughout the gait cycle. At the instance when peak power occurs, ankle gain amplifies deviations in ankle torque much more than deviations at the knee and hip (**Fig 3.4**). In other words, at the time of peak power production, small adjustments in ankle torques will manifest as larger changes in leg force compared to adjustments in knee or hip torque. Ankle torque therefore exercises the largest influence in modulating leg force application and is largely responsible for the joint torque variance structure observed during the power generation phase at the end of stance (**H2**). As a result, leg force modulation at the end of stance is likely achieved by individually controlling ankle torque trajectories rather than through coordination of all three intra-leg

joint torques as has been seen in hopping and other phases of the gait cycle (Yen, Auyang et al. 2009; Yen and Chang 2010; Toney and Chang 2013).

Direct investigation of the ankle torque trajectory revealed that peak ankle plantar-flexion torque magnitude is consistent across strides, but variability increases when the ankle torque increases rapidly during push-off (**Fig. 3.5**). Leg force is most modulated (IMA most negative) and leg power is maximal at nearly the same time that the ankle torque is highly variable and changing rapidly (**Fig. 3.5**, **Fig. 3.6**). In congruence with the high gain on ankle torque variability at this time, these data seem to indicate that leg force is largely modulated by high ankle torque timing variability at push-off. At its peak, the magnitude of ankle torque has a high tolerance for timing deviations due to its shallow slope, but periods of rapid torque change can result in higher sensitivity to timing variability (Latash, Scholz et al. 2002; Yen and Chang 2010). As a result, small timing "errors" result in larger task level (leg level) deviations as plantar-flexion torque changes rapidly when trailing in double support. These data indicate that peak ankle plantar-flexion torque magnitudes are achieved consistently, but the timing at which these peaks occur is varied. Taken in sum, these results suggest that appropriate timing of ankle plantar-flexion torque is important for leg force modulation and ultimately, consistent leg power generation. The large influence of ankle torque on leg force output may not be surprising as the ankle has been shown to be a primary source for propelling the body forward in walking (Kepple, Siegel et al. 1997; Neptune, Kautz et al. 2001). This is the first study, however, to show the influence of the ankle joint torque on stride-to-stride variability of leg force and power. The work presented here demonstrates that, while power magnitude may be determined by ankle torque magnitude, the timing of

these ankle torques contribute to generating consistent leg power when the same power is required with each step during steady state walking.

3.4.3 Potential Passive Mechanism for Modulating Trailing Leg Forces

The evidence presented here suggests that the timing of ankle torque generation plays a critical role in modulating leg force application and, ultimately, leads to more consistent leg power output. Control of ankle torque timing, therefore, appears to be a major driver for consistently powering human walking. How the ankle is controlled in this respect requires additional investigation, but the work presented here, combined with other previously published data suggests a possible physiological mechanism for monitoring and controlling ankle torque timing with each step.

Our analysis revealed that, while the magnitude of ankle torque was relatively consistent, the timing of ankle torque production was varied to lead to consistent leg power generation. This evidence suggests that humans generate a consistent load with the ankle plantarflexor muscle tendon unit, but vary when joint power is produced. A similar mechanism has been observed in jumping frogs, where an "inertial catch" amplifies power through slow loading of passive, series elastic structures in the ankle plantarflexors, followed by rapid elastic recoil and energy release (Roberts 2002; Roberts and Marsh 2003; Roberts and Azizi 2011). This catapult mechanism amplifies peak power output with very little energetic requirements because passive structures are stretched while muscle fascicles remain at a near constant length, thus decoupling muscle fiber shortening from whole body movements and limiting the energetic demand required by cross bridge cycling to initiate movement (Roberts and Marsh 2003). A similar

decoupling of muscle fascicle shortening and Achilles tendon lengthening has been observed in human walking (Ishikawa, Komi et al. 2005; Farris and Sawicki 2012; Cronin, Avela et al. 2013), and may explain the ability to separate the control of ankle torque timing from its magnitude. Utilizing the Achilles tendon in this way would allow human walkers to employ a passive structure to amplify propulsive power and achieve more efficient step-to-step transitions. In fact, mathematical simulations reveal that series ankle elasticity aid walking economy by reducing the energy lost in leading leg collisions, consistent with dynamic walking principles and suggestive of a mechanical advantage to utilizing the Achilles tendon in this manner (Zelik, Huang et al. 2014).

The work presented here identifies an additional functional role for the control of this catapult mechanism: controlling when elastic recoil is initiated can regulate leg force output for consistent power in step-to-step transitions. Modulating the timing of ankle torque generation requires sensory feedback to make appropriate adjustments and account for ever-present inherent variability. Distal limb motor control is largely regulated by force sensory feedback (Nielsen and Sinkjaer 2002; Daley and Biewener 2006; Faist, Hoefer et al. 2006; Daley, Felix et al. 2007; Af Klint, Mazzaro et al. 2010), and Golgi tendon organs have been implicated in regulating timing of the gait cycle (Capaday 2002), making them a likely sensor for modulating initiation of Achilles tendon recoil. We reanalyzed ultrasound data from Farris and Sawicki (2012), which revealed a good correlation between the timing of peak Achilles tendon force and peak medial gastrocnemius muscle tendon unit (GM-MTU) power (**Fig. 3.7A**) but a much weaker correlation between fascicle properties (time of greatest fascicle acceleration) and GM-MTU power (**Fig. 3.7B**). These results suggest that the Achilles tendon loading inherent

to the catapult mechanism may be facilitated by force feedback. If present, force facilitation within the triceps surae group would increase muscle stiffness and provide an anchor from which the Achilles tendon can stretch as the limb is loaded. Ankle load reduction at the end of stance would result in reduction of force-mediated facilitation and possibly a complete reversal to force-mediated inhibition (Faist, Hoefer et al. 2006). Regulating when the ankle is unloaded may therefore play a critical role in controlling step-to-step leg power consistency by controlling when Achilles tendon recoil is initiated. While the potential mechanism described above is speculative, the data presented here, agrees with other previously published work, and provides an interesting framework for future investigations into the mechanism controlling the timing of ankle torque production.

3.4.4 Role of the Knee to Mediate Ankle Torque Deviations

While independent control of the ankle dominates step-to-step variability of leg force output and, ultimately leg power generation, covariation (COV) between the joints remains present and functionally significant throughout the gait cycle (**Fig. 3.3B**). The contribution of COV is largely positive throughout the gait cycle, contrasting the destabilizing effect of the ankle. Controlling leg force output with ankle torque alone would be challenging, similar to driving a car with a gas pedal and no brake. The knee may serve as an ancillary controller that adjusts the extent to which ankle torque deviations are translated up the leg to influence the COM movement, possibly regulating force translation and stabilizing leg power generation. In fact, at the time of peak leg power production, the ankle and knee covary such that plantar-flexion torques at the

ankle are balanced by flexion torques at the knee (**Fig. 3.8**). In other words, the knee is able to counteract increases in ankle plantar-flexion torque in a way that tends to lessen the effect on leg force. In this way, the ankle acts as the primary motor for leg power generation, but the knee may act as a brake to dampen the effect ankle torque deviations can have on the leg (**H3**). The knee adds an additional layer of control and allows for more robust regulation of leg force.

It remains unclear whether ankle-knee covariance results from biomechanical connections or is an active reflex mechanism to help mediate ankle torque deviations up the leg. Intra-leg and inter-muscular reflex mechanisms may contribute to the monitoring and control of ankle torque generation (Wilmink and Nichols 2003; Stahl and Nichols 2011). However, the inherent stiffness of medial and lateral gastrocnemius couples the knee and ankle, resulting in inter-joint stability (Nichols 1999), so a passive or structural mechanism for ankle-knee coupling is also possible. Ishikawa et. al. (2005) also demonstrated different functional behaviors between the bi-articular medial gastrocnemius and the mono-articular soleus muscles, suggesting that various muscles may be regulated via different mechanisms during human walking. A combination of neural and/or biomechanical ankle-knee coupling is, therefore, also be possible. While the exact mechanism for ankle-knee covariation remains unclear, the knee appears to coordinate with the ankle to mediate the effects of distal torque deviations as they translate proximally up the leg and influence center of mass mechanics. In the accompanying study, we investigate how motor control changes, specifically whether ankle-knee covariation persists with the removal of direct ankle torque control and feedback.

3.5 Conclusion

We studied the motor control of trailing leg force generation to determine how consistent step-to-step leg power production may be achieved in steady state walking. Our results demonstrate that human walkers modulate trailing leg forces primarily through variable timing of peak ankle plantar-flexion torque in order to make step-to-step leg force adjustments that maintain consistent peak leg power production. Variable timing of peak ankle torque generation may be regulated by controlled initiation of Achilles tendon elastic recoil. Utilization of the Achilles tendon in this way would not only amplify peak power output and reduce the energetic demand of power production but may also simplify motor control to regulation of a single task: timing of muscle-tendon unit unloading and Achilles tendon recoil. Our subjects maintained robust leg force control by coupling knee and ankle function. Knee torques were coordinated to dampen the effect of ankle torque deviations on leg force, providing an additional layer of control and allowing more refined modification of leg force. Our results emphasize the important roles intact ankle control, sensory feedback, and ankle-knee motor control coupling have in achieving consistently powered steady state walking. These results in healthy adults further highlight possible physiological sources of pathological gait deviations in individuals with impaired ankle function (e.g. amputation, stroke, trauma, etc.) and provide potential areas for focused improvement of walking robot and powered exoskeleton design and implementation.

CHAPTER 4

THE MOTOR AND THE BRAKE DURING PROPULSION IN HUMAN WALKING II: TRANSTIBIAL AMPUTATION LIMITS KNEE TORQUE COVARIATION

This chapter addresses the second aim of my dissertation work: to determine how the locomotor control strategies identified in able-bodied walking (Chapters 2 and 3) are affected by lower limb amputation. Transtibial amputation effectively removes active ankle control and distal sensory feedback, thus reducing the inherent motor abundance in the locomotor system. I therefore expected individuals with amputations to demonstrate locomotor control strategies that were different from their able-bodied peers. Able-bodied walkers utilized inherent motor abundance to stabilize net vertical force trajectories during step-to-step transitions (Chapter 2) and make leg power consistent through step-to-step leg force adjustments (Chapter 3). Individuals with a lower limb amputation were able to control these whole-body and leg-level variables similarly to able-bodied subjects, despite their limited motor abundance. However, unlike able-bodied subjects, subjects with an amputation did not demonstrate any significant inter-joint covariation between their knee and ankle torques. Lower limb amputation appears to limit the stabilizing effect of inter-joint covariation and impede robust control of leg force. Less robust leg force control in individuals with an amputation likely makes these individuals less able to respond to unexpected perturbations or novel walking environments (Chapter 5).

4.1 Introduction

Lower limb amputation dramatically alters leg morphology and results in step length, stance duration, joint torque and leg force asymmetries (Winter and Sienko 1988; Hermodsson, Ekdahl et al. 1994; Sanderson and Martin 1997; Donker and Beek 2002; Davies and Datta 2003; Nolan, Wit et al. 2003; Detrembleur, Vanmarsenille et al. 2005; Su, Gard et al. 2007; Houdijk, Pollmann et al. 2009; Kovac, Medved et al. 2009; Sagawa, Turcot et al. 2011; Czerniecki, Turner et al. 2012; Svoboda, Janura et al. 2012; Bonnet, Villa et al. 2014). While these mechanical differences have been well described, we lack a complete understanding of how the underlying neuromechanical control of gait may differ for individuals missing important elements of the locomotor system due to amputation. Lower limb amputation eliminates active control in at least one joint and extinguishes a wealth of sensory information, which limits typically available motor abundance and may affect lower limb motor control. Individuals with amputations are also more prone to falls (Miller, Deathe et al. 2001; Miller, Speechley et al. 2001; Curtze, Hof et al. 2010; Curtze, Hof et al. 2012), possibly because they are unable to respond to perturbations as robustly as able-bodied individuals (Nederhand, Van Asseldonk et al. 2012; Wurdeman, Myers et al. 2013). Differences in locomotor control could explain the increased fall rate of individuals with amputations because it may illuminate differences in how individuals with amputations control their limbs and respond to small step-to-step variations. Individuals with unilateral, trans-tibial amputations also provide an excellent model for understanding the role of the ankle in human walking. Insights from studying individuals with amputations can provide information about how the neuromuscular system responds to morphological constraint or injury (e.g. in response to orthosis wear,

traumatic ankle injury, etc), ultimately providing more information to improve prosthetic and orthotic design and enhance rehabilitation practices.

This work is the second in a two part series investigating the role of ankle and knee coordination in human walking. In part I, we examined the functional contribution of intra-leg joint torque coordination to maintaining consistent leg power generation in able-bodied walkers (Chapter 3). We found that variable ankle torque timing drives the step-to-step leg force adjustments that maintain consistent peak leg power, while simultaneous ankle-knee coupling provided an additional level of control to regulate how these ankle torque deviations were translated up the leg to affect center of mass dynamics. Variable ankle torque timing was achieved with mostly passive structures. Controlled timing of Achilles tendon recoil initiation may act as a physiological motor to amplify power output. Coupled knee torques enabled robust leg level function by acting as a series physiological brake that refined and balanced the effect of ankle torque timing variability on leg force application and leg power output. Controlled ankle torque timing and ankle-knee covariation therefore appear important for robust control of propulsive leg power production in able-bodied walking. In part II of this series, we aim to determine the effect of essentially eliminating active ankle control and ankle-knee neuromechanical coupling while maintaining passive ankle function by studying the motor control of walkers with a transtibial amputation. The purpose of this study was to test whether step-to-step leg force control was achieved differently in amputated legs when compared to contralateral, sound and intact, control legs.

We can test how joint torques combine to modulate leg force by applying an uncontrolled manifold (UCM) analysis to periodic walking behavior. The UCM analysis

tests whether the variance of elemental variables (joint torques) over many repetitions tends to make a hypothesized task variable (leg force) consistent over many repetitions (Scholz and Schoner 1999). Specifically, the UCM analysis partitions elemental variance into two orthogonal components that contribute to either task stabilization or task modulation. By comparing the relative amounts of each component, we can determine how the tested elemental variables coordinate to affect the hypothesized task variable. The UCM analysis was developed based on the principle of motor abundance, meaning that human walkers have more available degrees of freedom than necessary to control identified task variables (Bernstein 1967; Scholz and Schoner 1999; Latash 2012). Applying the UCM analysis to the walking mechanics of subjects with an amputation is especially pertinent because such an analysis will allow us to study how loss of active control of one degree of freedom affects the coordination of this motor abundance. Using the UCM analysis, we have previously determined that able-bodied subjects combine leg forces to stabilize net vertical force trajectories to consistently transition from one step to the next (Chapter 2), but that trailing leg forces are modulated to maintain consistent trailing leg peak power generation (Chapter 3). We generally expected subjects with an amputation to maintain consistent net vertical force trajectories and whole body dynamics, but to alter how joint torques within the leg combine to affect leg force modulation.

Trailing leg forces in able-bodied subjects are modulated with each step through careful control of ankle loading and elastic energy return from the Achilles tendon (Chapter 3). For all intents and purposes, individuals with trans-tibial amputations lack these structures and the principal muscle group (triceps surae) that controls ankle torque

generation. Many individuals with trans-tibial amputations instead rely on artificial dynamic response, elastic storage and return (ESAR) prosthetic devices to mimic an intact human ankle and provide power for walking. These mechanical feet produce less power than intact ankles-foot structures and lack a mechanism for user regulated control and response to inherent variability (Winter and Sienko 1988; Hermodsson, Ekdahl et al. 1994; Sanderson and Martin 1997; Zmitrewicz, Neptune et al. 2006; Su, Gard et al. 2007; Kovac, Medved et al. 2009; Ventura, Klute et al. 2011). Individuals with a transtibial amputation, therefore, likely compensate for motor control deficiencies on their amputated side using either their contralateral, sound limb, or more proximal joint control (Vrieling, van Keeken et al. 2007; Houdijk, Pollmann et al. 2009; Curtze, Hof et al. 2012; Gates, Darter et al. 2012; Gates, Dingwell et al. 2012; Nederhand, Van Asseldonk et al. 2012). However, deafferentation and lack of proprioception inhibit inter-joint coordination in reaching (Ghez and Sainburg 1995; Sainburg, Ghilardi et al. 1995), suggesting that individuals with an amputation may be similarly challenged on their affected side. In this study, we specifically tested whether subjects with an amputation generate consistent peak leg power in their amputated leg using a similar mechanism as observed in control subjects. We expected subjects with an amputation to generate consistent peak propulsive leg power values in both their sound and prosthetic limbs (**H1**), mirroring consistent peak power generation observed in control subjects (Chapter 3). Furthermore, we expected that prosthetic legs would modulate trailing leg forces to achieve this consistent power output, but demonstrate less joint torque covariation than either sound or control legs (**H2**).

4.2 Methods

4.2.1 Subject Characteristics

Eight subjects with a unilateral transtibial amputation (6M/2F, weight: 80.4±16.9 kg, amputated leg length: 92.2±6.6 cm, sound leg length: 92.0±6.4 cm) and eight healthy, control subjects (6M/2F, age: 34±12.6 years, weight: 81.5±14.1 kg, leg length: 91.8±4.7 cm) gave informed consent as approved by the Georgia Institute of Technology Institutional Review Board. Data collected from these control subjects were previously reported in Part I of this two part series (Chapter 3), but relevant details are presented here again. Subjects with an amputation were community ambulators (K3 and K4), able to walk for at least 15 minutes continuously without assistance or an additional walking aid; wore their own custom-made, well fitting prosthesis; had an amputation due to trauma or congenital deformity; and had no other known cardiovascular or neurological pathologies. All subjects with an amputation wore their own prosthetic feet while participating in our study. Subjects with an amputation using SACH feet and/or powered ankles were specifically excluded from this study in order to ensure a group of subjects with an amputation who have as similar ankle function to control subjects as possible without the uncertainty of an externally powered device. Control subjects were carefully selected to match recruited subjects with an amputation in regards to gender, weight, and leg length.

4.2.2 Data Collection

Four subjects with an amputation completed a six-minute walk test prior to data collection (519.3m±70.3m, ATS Statement: Guidelines for the Six-Minute Walk Test).

Four of the control subjects completed the six minute walk test of the same day as data collection, three completed the test one a separate day on a return visit, and one did not complete the test (660.2±56.0m). Preferred walking speed was determined by allowing subjects to walk at a variety of speeds, first decreasing then increasing from their average speed from the six minute walk test, during which participants verbally indicated whether they would prefer the speed to be faster, slower, or if it was "just right." Subjects who did not complete the six-minute walk test before data collection began walking at a typically comfortable walking speed, 1.3m/s, when determining their preferred walking speed. All participants walked for two minutes at 75% of their preferred walking speed. All subjects were familiar with treadmill walking. Ground reaction forces were collected independently for each limb as subjects walked on a custom dual-belt instrumented treadmill (1080 Hz, Advanced Mechanical Technology Incorporated, Watertown, MA, USA). Simultaneous kinematics data were captured using a six-camera motion analysis system (120Hz, VICON Motion Systems, Oxford, UK). Retroreflective markers were placed bilaterally on the anterior superior iliac spine, posterior superior iliac spine, greater trochanter, thigh segment, knee joint center, shank segment, lateral malleolus, fifth metatarsal head on the lateral aspect of the foot, and second metatarsophalangeal joint on the foot dorsum. Identical marker sets were used for subjects with an amputation and able-bodied subjects. Prosthetic leg foot and ankle markers were placed as closely matched to the sound side as possible.

4.2.3 Data Analysis

Marker and force data were filtered with a zero-phase lag fourth-order Butterworth low-pass filter with a 10Hz cut-off frequency. Joint torques were calculated in the sagittal plane using standard inverse dynamics calculations and estimated segment inertial characteristics based on subject specific anthropometrics (Winter 1980). Inertial characteristics of the amputated leg and the prosthetic device were determined with the same method used for intact limbs. Possible errors introduced by using cadaveric rather than measured segmental inertial properties for the amputated leg and prosthetic components likely has little effect on the calculated joint torques during stance (Miller 1987; Winter and Sienko 1988; Powers, Rao et al. 1998; Su, Gard et al. 2007; Goldberg, Requejo et al. 2008; Nguyen and Reynolds 2014).

4.2.4 Individual Leg Power Trajectories

Individual leg power was calculated in the same way for all leg types (control, sound, and amputated). Leg power was calculated as the dot product of the resultant ground reaction force and the body center of mass (COM) velocity (**Eq. 4.1**, Donelan, Kram et al. 2002a; Donelan, Kram et al. 2002b). The COM velocity was calculated as the integration of COM acceleration as calculated from the subject mass and the net ground reaction force recorded from both legs (**Eq. 4.2**). The integration constants used were zero for the vertical and medio-lateral components of COM velocity and the set treadmill speed for the anterior-posterior COM velocity component. In order to compare across subject, leg power was normalized by body weight and walking speed of each individual.

$$P = F_{leg} \cdot v_{com} \qquad \textbf{(Eq. 4.1)}$$

$$v_{com} = \int a_{com} dt = \int \left(F_{net} / m \right) dt \qquad \textbf{(Eq. 4.2)}$$

4.2.5 Uncontrolled Manifold Analysis

An uncontrolled Manifold (UCM) analysis was performed using custom Matlab code. Specific details of this approach were discussed in Part I of this series (Chapter 3; Appendix A; Yen, Auyang et al. 2009; Yen and Chang 2010). For clarity, the general approach is outlined here and differences in how the analysis was applied to the amputated legs are discussed in detail.

To apply the UCM analysis, we must first establish a mathematical relationship relating elemental variables to the task variable. This mathematical relationship then defines a task specific Jacobian matrix (J) quantifying the effects of small changes in the elemental variables on the hypothesized task variable. The null space of J is therefore a linearized approximation of the task equivalent manifold, which contains all combinations of elemental variables that yield the same task variable. The measured elemental variance can then be described by two components: one parallel to the manifold, containing all elemental variance that has no effect on the task variable (goal equivalent, **Eq. 4.3**) and one orthogonal to the manifold, containing all elemental variance that cause divergence from the task variable (non-goal equivalent, **Eq. 4.4**), where C is the statistically derived covariance matrix for the elemental variables, n is the number of local degrees of freedom (i.e. number of elemental variables), and d is the number of global degrees of freedom (i.e. number of task variables). The difference between these two components, normalized by the total elemental variance ($TotV$, **Eq. 4.6**), is called the index of motor abundance (IMA, **Eq. 4.5**) and characterizes how the structure of elemental variance affects the task-level variance (Auyang, Yen et al. 2009;

Yen, Auyang et al. 2009; Yen and Chang 2010; Toney and Chang 2013). Positive IMA values indicate that more of the elemental variance is goal-equivalent, and the elemental variables tend to combine to make the task variable more consistent. Negative IMA values indicate that more of the elemental variance is non-goal equivalent, and the elemental variables combine tend to combine to modulate the task variable from step-to-step. In this way the UCM analysis provides a window into how the nervous system regulates motor abundance towards a particular outcome.

$$GEV = \frac{trace(null(J)^T \cdot C \cdot null(J))}{n - d} \quad \textbf{(Eq. 4.3)}$$

$$NGEV = \frac{trace((J \cdot J^T)^{-1} \cdot J \cdot C \cdot J^T)}{d} \quad \textbf{(Eq. 4.4)}$$

$$IMA = \frac{(GEV - NGEV)}{TotV} \quad \textbf{(Eq. 4.5)}$$

$$TotV = \frac{trace(C)}{n} \quad \textbf{(Eq. 4.6)}$$

4.2.6 Inter-leg Uncontrolled Manifold Analysis

During double support, both legs are on the ground, each applying a vertical force component on the ground. The combination of these two components directly sum to yield net vertical force. This simple relationship defines a two degree of freedom system that affects whole body dynamics, with a 1x2 J matrix (**Eq. 4.7**).

$$J_{2dof} = \begin{bmatrix} 1 & 1 \end{bmatrix} \quad \textbf{(Eq. 4.7)}$$

4.2.7 Intra-leg Uncontrolled Manifold Analysis

We use a dynamically consistent generalized inverse of the kinematic Jacobian relating joint angles to end point position to derive a Jacobian matrix (J) relating joint torques to force along the leg (Khatib 1987; Yen, Auyang et al. 2009); Chapter 2; Appendix A). We use the same Jacobian to relate joint torques to leg force in the amputated as in the able-bodied and sound legs. In doing this, we assume that the prosthetic ankle is a meaningful degree of freedom in determining the leg force. While it cannot be directly actuated, controlling the way the prosthetic device is loaded and deflected during single support phase of walking can indirectly modify prosthetic ankle torque output. For this reason, we chose to include the prosthetic ankle in the Jacobian and resulting UCM analysis as a first step to understanding how all contributing degrees of freedom influence leg force output. A more in depth motor control model for the motor control of individuals with amputations should be addressed and further studied in future experiments.

4.2.8 Components of Covariation and Individual Joint Torque Control Contributing to Leg Force Control

Joint torque variance structure can arise from two possible sources: (i) individual joint torque control and/or (ii) covariance across joints. We can isolate the effects of these two variance sources by manipulating the covariance matrix used to calculate GEV and NGEV. The diagonal components of the covariance matrix ($\sigma_a^2, \sigma_k^2, \sigma_h^2$, **Eq. 4.8**) contain the variance of each joint relative to itself (individual variance), while the off-diagonal elements describe inter-joint covariance, where a=ankle, k=knee, and h=hip). We can

isolate the effect of individual joint torque variance on overall variance structure by setting the off-diagonal covariance components of the covariance matrix (C) to zero (C', **Eq. 4.9**) then re-calculating GEV', $NGEV'$, and IMA' using C'. The resulting IMA' indicates the influence of individual joint torque control on leg force output, so we call this new metric INV. All remaining variance structure is due to covariance between the joints, so we can calculate the contribution of inter-joint covariation to leg force output by subtracting INV from COV (**Eq. 4.10**).

$$C = \begin{bmatrix} \sigma_a^2 & \sigma_{ka} & \sigma_{ha} \\ \sigma_{ak} & \sigma_k^2 & \sigma_{hk} \\ \sigma_{ah} & \sigma_{kh} & \sigma_h^2 \end{bmatrix} \quad \textbf{(Eq. 4.8)}$$

$$C' = \begin{bmatrix} \sigma_a^2 & 0 & 0 \\ 0 & \sigma_k^2 & 0 \\ 0 & 0 & \sigma_h^2 \end{bmatrix} \quad \textbf{(Eq. 4.9)}$$

$$COV = IMA - INV \quad \textbf{(Eq. 4.10)}$$

4.2.9 Ankle-Knee Covariation

The contribution of each joint's individual control and/or between two specific joints (e.g. ankle-knee covariance, σ_{ak}) can be determined from the individual components of the covariance matrix. Notice that these values of covariance are different than the metric COV. The covariance described here are statistically derived reliance of one joint on another's action, while COV is a metric that indicates how much leg force control arises from this covariance source of inter-joint covariance.

4.2.10 Statistical Analysis

Mean IMA trajectories across all subjects were evaluated for significant differences from zero using a one-tailed Student's t-test (α=0.005, with a Bonferroni correction for 100 comparisons). An IMA significantly greater than zero indicates the local variables (individual leg-forces or intra-leg joint-torques) were coordinated to generate the same net-force trajectory in each transition, which we interpret as stabilization of a controlled implicit neuromechanical goal of walking. In other words, a positive IMA indicates that only task-relevant deviations are reduced, which is consistent with a minimum intervention principle of motor control (Todorov and Jordan 2002). An IMA significantly less than zero indicates active modulation such that the local variables combined to produce a different net-force trajectory with each successive step, indicating that task-relevant deviations are not restricted, but instead contribute directly to net-force modulation. A negative IMA is therefore interpreted to mean that net-force is not an implicit gait goal, but is instead modulated to stabilize some alternative gait goal.

We evaluated the contribution of coordinated and individual joint torque control strategies to leg force control by testing the similarity of the COV and INV trajectories to the IMA trajectory. Testing similarity of trajectories was accomplished by "fitting" each trajectory to the other using the built in Matlab function "corrcoef." The resulting R^2 value indicates the amount of inter-subject IMA variance that the COV or INV trajectory is able to explain (Bauman and Chang 2013). In other words, larger R^2 values indicate a better "fit" and a greater amount of inter-subject IMA variance explained by that source of elemental organization.

4.3 Results

4.3.1 Subject Characteristics

Matched control subjects did not differ significantly from subjects with an amputation in regards to weight or leg length (rmANOVA; $p>0.05$), but subjects with an amputation demonstrated a significantly lower preferred walking speed than control subjects (CON: 1.29±0.10 m/s; AMP: 1.17±0.09 m/s; $p<0.05$) (**Table I**).

Table 1: Subject characteristics. (*significant difference, paired ttest, $p<0.05$)

	Control legs (n=8)	Sound legs (n=8)	Prosthetic legs (n=8)
leg length (cm)	91.5±4.9	92.0±6.4	92.2±6.6
weight (kg)	81.5±14.1	80.4±16.9	
gender	6M/2F	6M/2F	
preferred walking speed (m/s)	1.29±0.10	1.17±0.09*	

4.3.2 Joint Torques and Ground Reaction Forces

Individual joint torque and leg force trajectories are consistent with previous published data (Winter and Sienko 1988; Hermodsson, Ekdahl et al. 1994; Kovac, Medved et al. 2009; Sagawa, Turcot et al. 2011) for subjects with an amputation (**Fig. 4.1** and **4.2**).

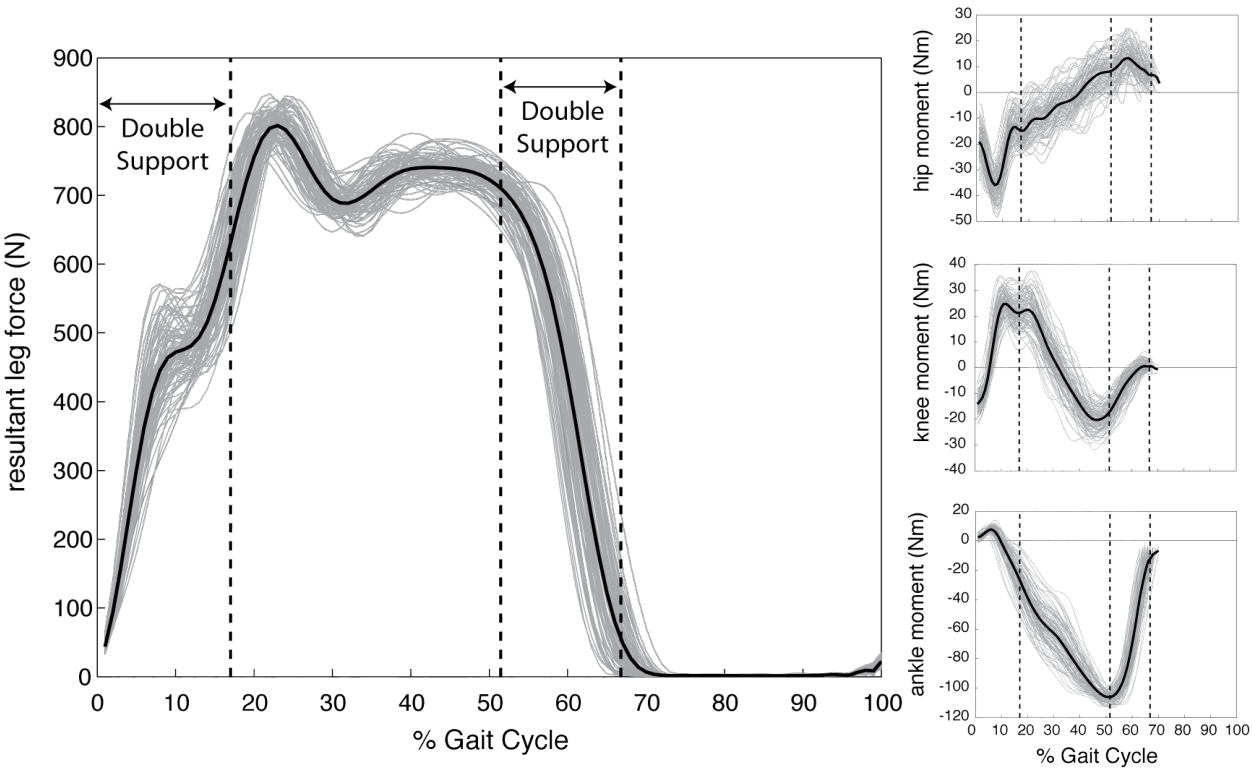

Figure 4.1: Representative subject resultant sound leg force (left panel) and joint torques (right column). Gray lines represent leg force and joint torque values for each step, while the thick black lines represent the mean trajectory. Double support when the sound leg is leading (1-17.5±1.3% gait cycle) and when the leg is trailing (50.8±3.0-66.8±1.6% gait cycle) are bounded by the dashed vertical lines. Gait cycles are defined from heel contact (0%) to ipsilateral heel contact following swing phase (100%).

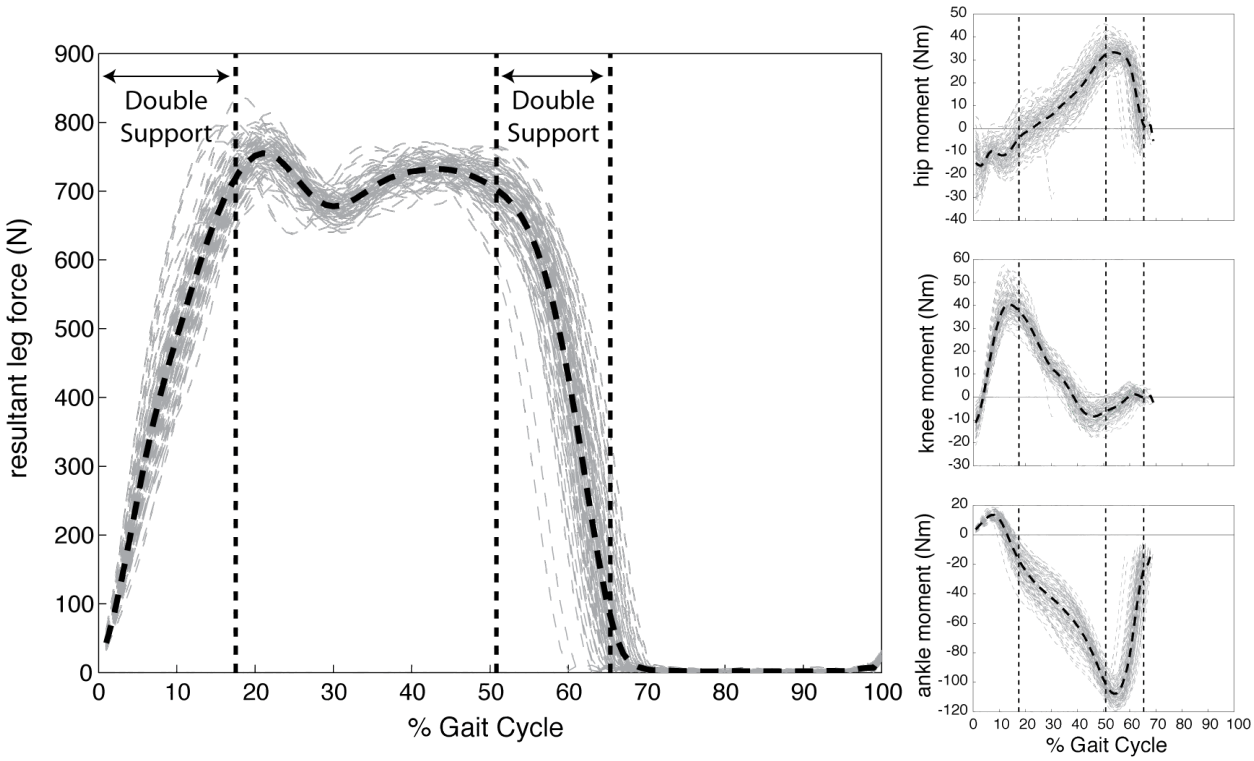

Figure 4.2: Representative subject resultant amputated leg force (left panel) and joint torques (right column). Convention is same as for **Figure 4.1**. Gray lines represent leg force and joint torque values for each step, while the thick black lines represent the mean trajectory. Double support when the sound leg is leading (1-17.0±1.1% gait cycle) and when the leg is trailing (51.5±1.3-65.4±1.8% gait cycle) are bounded by the dashed vertical lines. Gait cycles are defined from heel contact (0%) to ipsilateral heel contact following swing phase (100%).

4.3.3 Inter-leg Model for Leg Force Control

Index of motor abundance (IMA) values were significantly greater than zero during double support ($p<0.005$) when the non-preferred stance leg (controls) (**Fig.4. 3**, left column), sound leg (**Fig. 4.3**, middle), and amputated leg (**Fig. 4.3**, right) trailed, generating propulsive power and push-off forces.

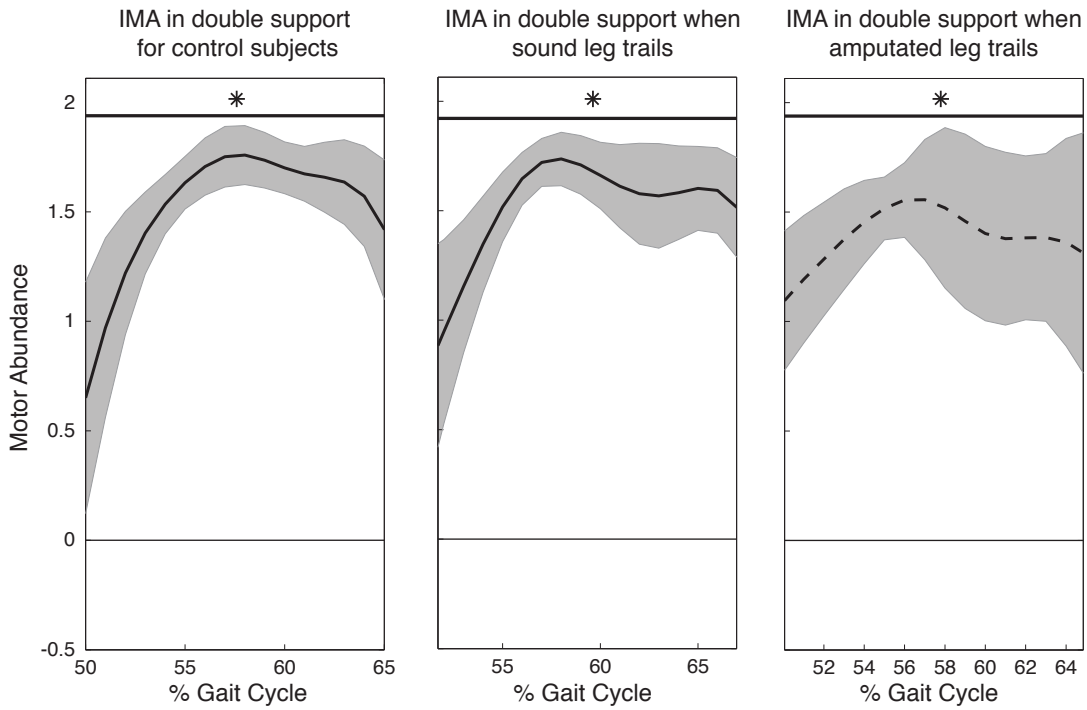

Figure 4.3: Mean and standard deviation of the Index of Motor Abundance (IMA) for the 2-dof model for inter-leg coordination to generate net vertical ground reaction forces during double support. Leading and trailing leg forces combine to generate consistent net vertical force (IMA>0,p<0.005) regardless of whether the sound (**A**) or prosthetic (**B**) trails, providing propulsive force. That subjects with an amputation generate consistent net vertical force in both transition phases suggest that they are able to control their individual limbs similarly to controls and maintain whole body mechanics. During step-to-step transitions, differences in motor control appear to be restricted to within the affected leg in experienced walkers with an amputation.

4.3.4 Leg Power

Individual leg power profiles were similar to previously published data (Donelan, Kram et al. 2002a; Donelan, Kram et al. 2002b). Peak leg power and a local minimum of leg power variance occurred at the same time in control (**Fig. 4.4A**), sound (**Fig. 4.4B**), and amputated legs (**Fig. 4.4C**). Control legs generated peak power at 58.5±1.2% of the gait cycle and a local variance minimum at 58.4±1.1% of the gait cycle, which were not significantly different in their timing (paired t-test, p= 0.35). In the sound limb of subjects with an amputation, peak power (60.0±1.3% gait cycle) occurred slightly later than the local variance minimum (59.3±0.9% gait cycle, p=0.02). However, the average timing

difference was 0.8±0.7% of the gait cycle, which equates to less than 10ms, a timing difference that would be indistinguishable by the human nervous system. The amputated legs did not have a difference in timing ($p>0.05$) between peak power (58.8±1.7% gait cycle) and the local variance minimum (58.8±1.7% gait cycle). A repeated measures ANOVA analysis of peak power magnitudes revealed a significant main effect of leg type ($F=12.614$, $p=0.001$). The magnitudes of peak power in the prosthetic legs (0.12±0.3% BW*walking speed) were significantly smaller than peak powers in either the sound (0.16±0.04% BW*walking speed; $p=0.0124$), or the control legs (0.19±0.02% BW*speed; $p=0.002$). The sound and control leg peak power magnitudes were not significantly different ($p=0.189$).

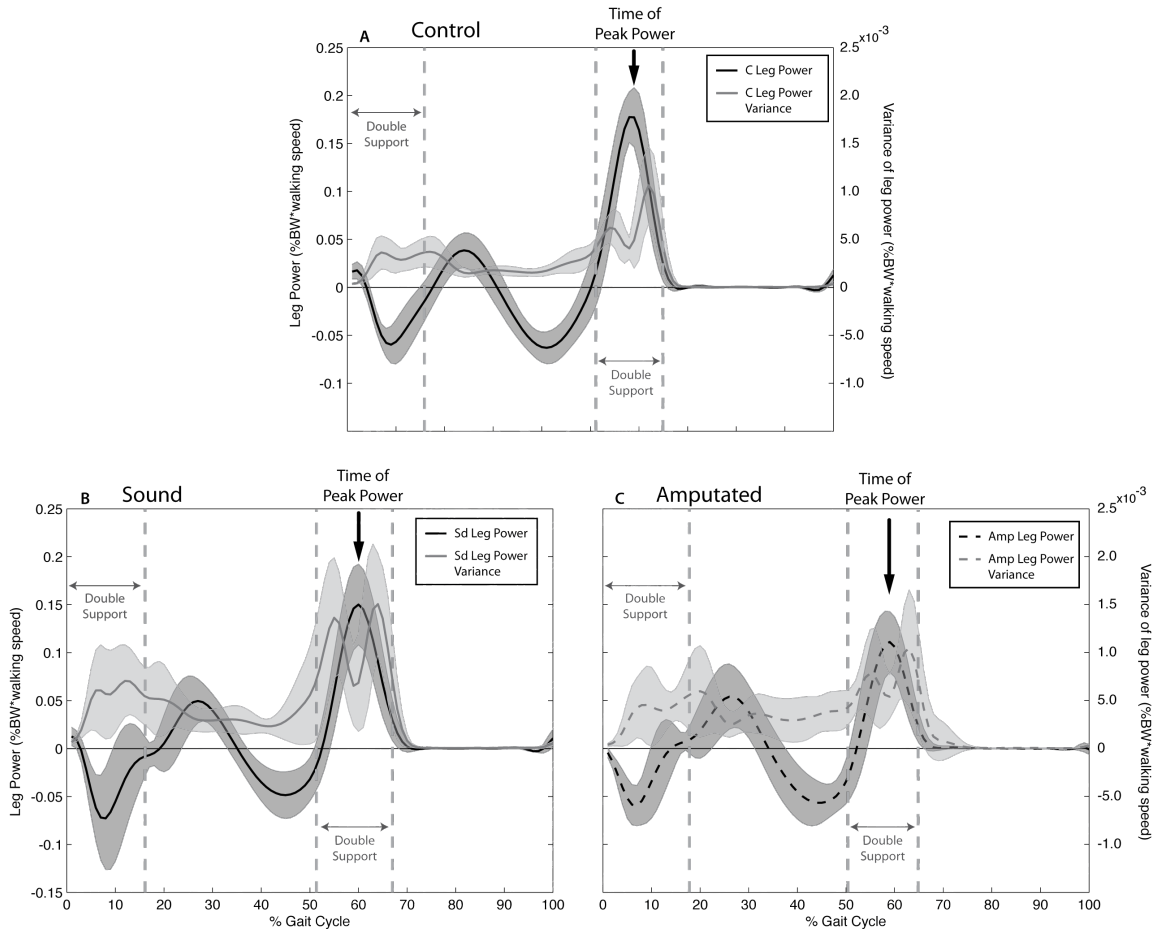

Figure 4.4: Mean and standard deviation of leg power (black) and variance of leg power (grey) for the control (**A**), sound (**B**), and amputated (**C**) legs of subjects with an amputation. Peak amputated leg power (0.12±0.3% BW*speed) is slightly smaller than the sound leg (0.16±0.04) peak propulsive power (paired t-test, t=2.4934,p=0.0207,one-tailed alpha = 0.05). However, both legs demonstrate a local minima of leg power variance when leg power is maximal (large arrow), indicating that peak leg power is consistent.

4.3.5 Intra-leg Model for Leg Force Control

The Index of Motor Abundance was significantly greater than zero (IMA>0, $p<0.005$) for all leg types (Control 1-15% gait cycle; Sound 1-6% and 9% gait cycle; Amputated 1-9% gait cycle) when the leg of interest lead (**Fig. 4.5A**, **4.5C**, and **4.5E**). Control legs demonstrated significantly negative IMA values (IMA<0, $p<0.005$) once during single leg stance (44% gait cycle) and during double support when the leg trailed (59-61% gait cycle, **Fig. 4.5A**). The sound limbs of subjects with an amputation

demonstrated negative IMA values (IMA<0, p<0.005) during the second double support period (58-64% gait cycle, **Fig. 4.5C**). Similarly to control and sound limbs, the amputated legs of subjects with an amputation demonstrated IMA values significantly less than zero (p<0.005) during double support when the amputated leg trailed and generated positive power (57-59% gait cycle, **Fig. 4.5E**). All leg types (control, sound, and amputated) demonstrated negative IMA values at the same instance as peak leg power (**Fig. 4.5**, black arrow).

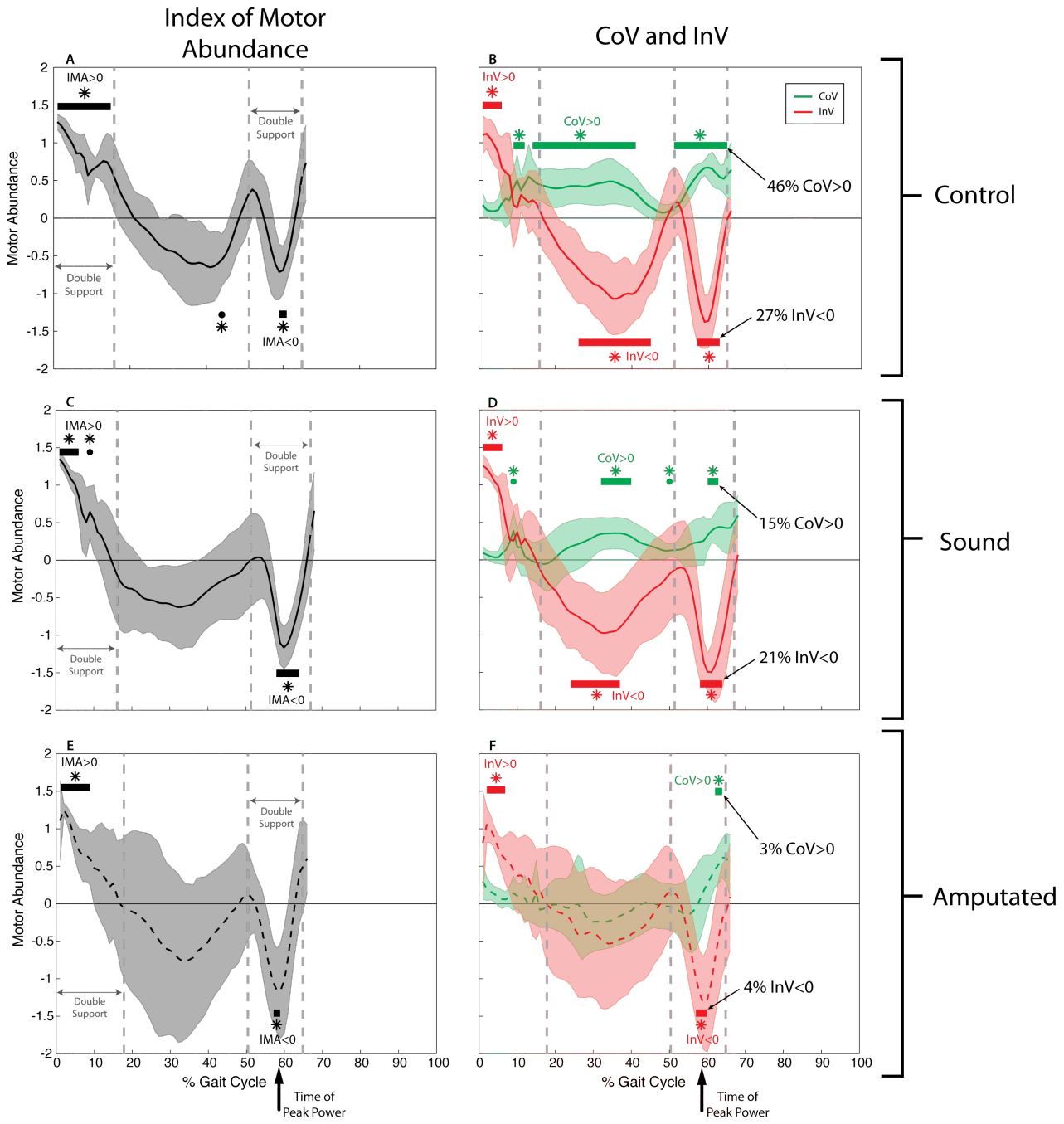

Figure 4.5: Variance structure for control (A, B), sound (C, D) and amputated (E, F) legs throughout the gait cycle. Mean and standard deviation of the Index of Motor Abundance (left column) demonstrates whether joint torques combine to stabilize (IMA>0) or modulate (IMA<0) leg force. The components of stabilization or modulation (right column) indicate to what degree the ankle, knee, and hip joint torques are coordinated together (COV, green) or individually controlled (INV, red) to create the overall IMA structure (IMA=COV+INV). A) Control subjects stabilize leg force (IMA>0, $p<0.005$) during double support when the leg is leading (1-15.9±1.4%) and modulate leg force (IMA<0,$p<0.005$) from step-to-step when the leg generates maximal power when trailing in double support (51.1±0.8%-64.9±1.1%). B) Both the stabilization and modulation of leg force reflected in IMA values arise from individual joint control (INV), despite coordination across joints acting mainly to stabilize leg force (COV>0, $p<0.005$) throughout most of the gait cycle. C-D) The sound limb of subjects with an amputation behave similarly to control legs. Leg

force stabilization (IMA>0, p<0.005) when leading in double support (1-16.1±1.3%) and modulation (IMA<0, p<0.005) when trailing in double support (51.3±1.5%-67.0±1.1%) arise primarily from individual joint torque control (INV). Covariation between joints (COV, green) does not have as persistent an effect in the sound limb of subjects with an amputation as compared to controls. E) The amputated legs of the subjects with an amputation demonstrate similar overall IMA structure as control and sound limbs. Ankle, knee, and hip joint torques combine to stabilize leg force (IMA>0, p<0.005) when the leg is leading in double support (1-17.8±1.6%) and modulate leg force (IMA<0, p<0.005) when the leg is trailing in double support (50.4±1.5%-64.8±1.9%). Subjects with an amputation appear capable of maintaining leg control similar to intact limbs despite inherent structural differences. F) Amputated legs demonstrate similar amounts of individual joint variance structure (INV, red), which primarily contribute to leg force control. However, prosthetic legs demonstrate no significant COV contribution to leg force control. The small amount of COV at the end of stance occurs immediately before liftoff, when leg force is small and has little influence on center of mass mechanics. This COV may reflect coordination between joint angles to control leg orientation at liftoff, rather than leg force. Overall, subjects with an amputation appear able to control their amputated legs similarly to sound limbs through individual joint control, but are unable to generate covariation between joint torques.

4.3.6 Contribution of Individual and Coordinated Variance to the Intra-leg Model for Leg Force Control

Control leg joint-torque structure was organized using both individual (INV, red line) and covariance (COV, green line) joint coordination (**Fig. 4.5B**). For control legs, INV was significantly positive (INV>0, p<0.005) when the leg lead in double support (1-6% gait cycle), and was significantly negative (INV<0, p<0.005) for 27% of the total gait cycle during both single limb stance and the second double support period (26-45% and 57-63% gait cycle). The time of minimum INV occurred at the same time as peak power in control legs (Chapter 3, **Fig. 3.6**). The COV component of joint torque variance organization was significantly greater than zero for 46% of the gait cycle (COV>0, p<0.005, 9-12%, 14-41%, 51-64%gait cycle), acting to stabilize to leg force control throughout the majority of stance phase. The sound leg of subjects with an amputation also demonstrated significant contributions of INV and COV at different points in the gait cycle (**Fig. 4.5D**). INV values were significantly greater that zero (INV>0, p<0.005) when the sound leg lead in the first double support period (1-6% gait cycle), and was

significantly less than zero (INV<0, p<0.005) for 21% of the gait cycle during single limb stance (24-37% gait cycle) and the second double support period (58-64% gait cycle). The COV component of variance structure was positive (COV>0, p<0.005) for 15% of the total gait cycle, generating a stabilizing effect on leg force for less total time but at similar instance in the gait cycle as control legs when the leg lead in double support (9% gait cycle), single limb stance (32-40% and 50% gait cycle), and when the leg trailed in double support (60-63% gait cycle). The most negative INV (and IMA) value occurred at the same time as peak leg power in sound limb of subjects with an amputation (rmANOVA, p=0.393, paired ttest (INV&P), p = 0.5490), similarly to what was observed in the control legs. Similarly to control and sound legs, amputated legs demonstrated positive INV values (INV>0, p<0.005) when the leg lead in double support (2-7% gait cycle). However, amputated legs demonstrated much less negative INV and positive COV contributions to leg force control throughout the gait cycle (**Fig. 4.5F**). INV values were significantly less than zero (INV<0, p<0.005) for only 4% of the gait cycle when the leg trailed in double support (57-60% gait cycle), while COV was positive (COV>0, p<0.005) for only 3% of the entire gait cycle just before prosthetic leg toe off (62-64% gait cycle). Like control and sound legs, there was no significant different in the timing of most negative INV (and IMA) values (rmANOVA, F=0.529, p=0.513).

Similarly to observations in control subjects (Chapter 3), simple regression analysis showed that INV contributed to the shape of the IMA trajectory more than COV in both sound and amputated legs. Sound leg INV accounted for 97% of the inter-subject residual variance in the sound leg IMA trajectories (R^2=0.97), while COV only accounted for 26% of residual IMA variance in sound legs (R^2=0.26). Amputated leg INV

accounted for 91% of inter-subject IMA residual variance (R^2=0.91), but COV only accounted for 20% of the residual inter-subject variance in the IMA trajectories (R^2=0.20).

4.3.7 Intra-leg Joint Torque Covariance

Components of the statistical covariance matrix (C, **Eq. 4.8**) revealed ankle-joint covariance was significantly greater than zero (p<0.005) in control legs (**Fig. 4.6**, solid line) periodically throughout the gait cycle. Positive covariance values indicate that the knee tends to generate a flexion torque when the ankle generates a plantar-flexion torque, reducing translation of ankle torque up the leg and having a stabilizing effect on leg force (Chapter 3). Amputated legs, however, did not demonstrate any significant ankle-knee covariance at any point in the gait cycle (**Fig. 4.6**, dashed line).

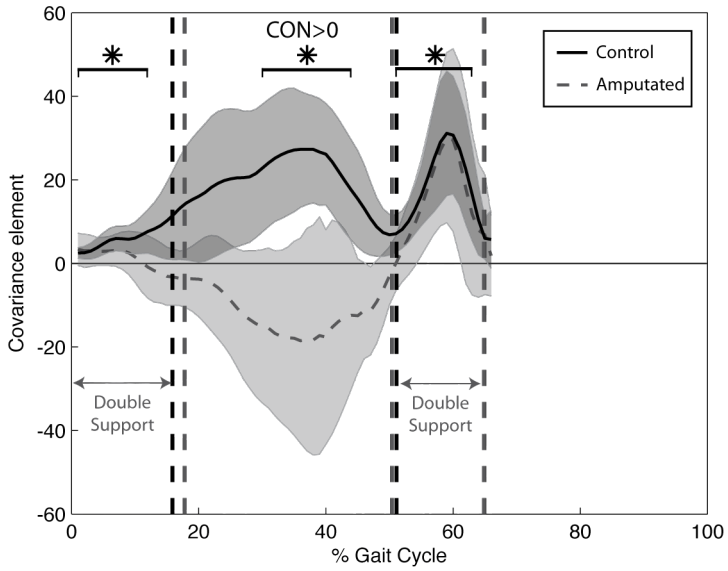

Figure 4.6: Mean and standard deviations of covariation between ankle and knee torques in control (solid) and amputated (dashed) legs. Control subjects (CON) demonstrate significantly positive ankle-knee covariation (p<0.005) throughout the gait cycle, while the amputated legs of the subjects with an amputation do not demonstrate any significant covariation.

4.4 Discussion

We investigated the underlying motor control of walking with an amputation using a modified uncontrolled manifold (UCM) analysis. We found that subjects with an amputation stabilize whole body and leg-level dynamics similarly to able-bodied controls, but differed in how they organized their joint torques to achieve similar leg force function. Subjects with an amputation demonstrated less inter-joint covariation in their amputated leg when compared to both their own contralateral sound legs and the intact legs of matched able-bodied subjects. Furthermore, amputated legs demonstrated significantly less covariation between their prosthetic ankle and knee torques than either control or contralateral sound legs. These results suggest that dynamic response prosthetic feet are able to mimic the influence of ankle torque timing variability on leg force modulation that we have observed in control subjects (Chapter 3), but the prosthetic user experiences significant motor control differences that persist even with extended use.

4.4.1 Inter-leg Forces Stabilize Net Vertical Force

Similarly to controls, subjects with an amputation demonstrated positive IMA values throughout double support, regardless of which leg (sound or amputated) provided propulsive power. These results indicate that subjects with an amputation selectively minimize leg-level force variance that leads to in-consistent net vertical force trajectories with each step. Individuals with an amputation appear able to achieve consistent center of mass dynamics by coordinating leg-level force variance similarly to control subjects. Motor control differences possibly resulting from their morphological constraint do not appear to affect leg force coordination in subjects with an amputation.

4.4.2 Subjects with an Amputation Maintain Consistent Trailing Leg Peak Power in Each Leg

Peak leg power occurred at same point in the gait cycle as a local minimum in leg power variance for each leg type (**Fig. 4.4**). These results indicate that, regardless of leg type, leg power was more consistent at its peak than at any other surrounding instant in the leg power trajectory, suggesting that peak leg powers were consistently generated with each step. Subjects with an amputation appear able to generate consistent, albeit smaller, peak leg power values similarly to control legs despite lacking direct ankle torque control.

4.4.3 Subjects with an Amputation Generate Leg Forces Similarly to Able-bodied Subjects

Leading leg forces were stabilized (IMA>0) during the first double support period in all leg types (**Fig. 4.5**). Subjects with an amputation structure their joint torque variance in both their sound and amputated legs similarly to control legs when the leg leads, suggesting that the leg forces generated during weight acceptance are not affected by a lack of direct ankle torque control. Trailing leg forces, however, were modulated from step-to-step (IMA<0) in each leg type (**Fig. 4.5**). This result shows that, like intact legs, subjects with an amputation modulated their amputated leg forces at the point in the gait cycle when leg power was maximal and the most consistent. We previously showed that control subjects stabilize trailing leg peak power through modulation of trailing leg force trajectories with each step (Chapter 3). Individuals with an amputation appear able

to modulate amputated leg force trajectories to stabilize leg power in a similar way as intact legs, despite relying on a passive ankle-foot mechanism to generate leg force and power. Any locomotor control differences resulting from use of a prosthetic ankle-foot device do not appear to affect leg forces in our subjects with unilateral, trans-tibial amputations. It is worth noting that we specifically recruited participants who were very familiar and skilled with walking using a prosthetic device. The similar leg force control we observe here may result from the considerable experience and training our participants possess. Individuals with more acute amputations might demonstrate notable differences in leg force control, which adapt to more closely resemble the control patterns observed here with training and rehabilitation. In fact, if individuals with new amputations are indeed deficient, achieving leg force modulation for consistent leg power generation might be a useful rehabilitation goal to monitor and target for improvement.

4.4.4 Amputated Legs Demonstrate Fewer Periods of Structured Joint Torque Variance Throughout the Gait Cycle

While subjects with an amputation are able to generate leg force trajectories similar to control subjects, how joint torques were combined to generate these leg force trajectories was different in the amputated legs compared to either the contralateral sound or intact control legs. Individual joint torque variance structure (INV) contributed the most to total joint torque structure (IMA) in all leg types, but the proportion of the gait cycle when INV was significantly different than zero was smaller in amputated than in either the sound or control legs (**Fig. 4.5**). While the control and sound limbs combined the effects of individual (INV) with coordinated (COV) joint torque control throughout

the gait cycle, the amputated legs of subjects with an amputation demonstrated significant contributions from INV at very limited instances within the gait cycle. INV effects were present during weight acceptance and at push off, when leg forces likely have the most influence on center of mass and whole body dynamics. Leg mechanics during weight acceptance are largely passive, determined by the preceding step's dynamics and leg posture, so leading leg forces are likely made as consistently as possible by stabilizing leg orientation and trailing leg power (Kuo, Donelan et al. 2005; Toney and Chang 2013); Chapter 2). Prosthetic ankle torque deviations are, therefore, unlikely to substantially affect leg force output when the leg is leading. During the second double support period, however, ankle torques have the greatest influence on the leg force trajectory (Chapter 3, **Fig. 3.4**). We have previously postulated that control subjects modulate ankle torque timing by altering when Achilles tendon elastic recoil is initiated (Chapter 3). Individuals with an amputation do not have an Achilles tendon on their affected side and must instead rely on their manufactured passive ankle-foot system to modulate trailing leg forces. The power generated by ESAR feet is a function of the toe lever deflection (e.g. prosthetic ankle angular displacement) achieved before push off (Ventura, Klute et al. 2011). Individuals with lower limb amputations must, therefore, somehow control how their passive device is being loaded and/or unloaded in order to initiate the elastic recoil and modulate leg forces. The specific mechanism walkers with amputations use to regulate prosthetic ankle torque remains unclear, but could involve monitoring and correcting of distal socket kinetics (Childers, Prilutsky et al. 2014), shank inclination angles, included knee angles, and/or leg orientation. Identifying the specific method of control used by individuals with amputations requires additional investigation, but the

work presented here demonstrates that prosthetic feet appear able to mimic intact ankle function well, supporting the idea that ankle joint modulation in able-bodied, control subjects may be achieved through mostly passive structures, such as the Achilles tendon (Ishikawa, Komi et al. 2005; Farris and Sawicki 2012; Cronin, Avela et al. 2013; Zelik, Huang et al. 2014).

While ankle torque modulation may originate from a passive mechanism, the effects of ankle torque deviations are mediated through mechanical and/or neural coupling with more proximal joints. Control subjects covary ankle and knee torques (**Fig. 4.6**), presumably to adjust the amount of ankle torque variance translated along the leg to influence center of mass, whole body dynamics (Chapters 2 and 3). Subjects with an amputation lack significant COV throughout the gait cycle (**Fig. 4.5**), and specifically lack any significant ankle-knee covariance (**Fig. 4.6**), suggesting that the knee is coupled (either mechanically or neurally) to ankle function via sensory feedback in able-bodied subjects. Reduced ankle-knee covariation indicates that the knee does not respond to passive prosthetic foot-ankle torque output similarly to how ankle and knee torques are related in control subjects. In other words, prosthetic ankle plantar-flexion torques are not balanced by a knee flexion torque, such as was observed in able-bodied subjects (Chapter 3). Increasing the magnitude of sensory signals via vibratory stimulation under the prosthetic foot improved feedforward, open-loop postural responses, suggesting that sensory feedback from distal structures play an important role in movement coordination (Rusaw, Hagberg et al. 2012). Some ankle plantar-flexor muscles are mechanically coupled to also cause knee flexion and provide inter-joint stability in intact legs (Nichols 1999). Following a trans-tibial amputation, however, triceps surae activation may cause

some slight knee flexion, but no longer generates ankle plantar-flexion; the neuro-mechanical ankle-knee coupling no longer exists. Regardless of the source, subjects with an amputation do not actively or passively covary knee and ankle torques. Individuals with amputations are, therefore, less able to appropriately respond to unexpected ankle torque deviations, resulting in less robust leg force control and possibly explaining the reduced stability and increased fall risk observed in walkers with amputations (Miller, Deathe et al. 2001; Miller, Speechley et al. 2001; Curtze, Hof et al. 2010; Curtze, Hof et al. 2012).

4.5 Conclusion

In this study, we applied a modified uncontrolled manifold (UCM) analysis to steady-state walking of subjects with an amputation to test how the locomotor system responds to a morphological constraint. Our results show that, despite loss of significant ankle sensorimotor function, subjects with an amputation maintain consistent whole-body dynamics and leg power production during steady-state walking. However, joint torque covariation was significantly affected by loss of ankle sensory feedback and active motor control. While subjects with an amputation were able to utilize the passive properties of their prosthetic device to modulate leg force application, they did not demonstrate significant covariation between their knee and prosthetic ankle. The lack of inter-joint covariation limits robust control of leg force and may explain why individuals with amputations are more prone to falls. Rehabilitation practices and prosthetic design may both benefit from additional attention to coordinated function of the ankle and knee. Training impaired individuals to utilize their inherent motor abundance would enable

more flexible responses to unexpected perturbations and could aid adaptation and long-term motor learning.

CHAPTER 5

DISTAL SENSORY FEEDBACK AND ANKLE MOTOR LOSS DUE TO AMPUTATION LIMITS SHORT-TERM LOCOMOTOR ADAPTATION

This chapter focuses on the final aim of my dissertation research: to determine how the physiological constraint of amputation affects short-term adaptation to walking in a novel environment. Able-bodied subjects and subjects with an amputation completed a split-belt walking adaptation protocol in which they were asked to walk on side-by-side treadmill belts moving at different speeds. This intervention revealed that able-bodied walkers adapted negative leading leg work in a pattern consistent with predictive control, while positive trailing leg generation was adapted in a more reactive, feedback mediated manner. Chapter 4 showed that transtibial amputation limits robust control of trailing leg force application, suggesting that individuals with an amputation would be less able to respond to an environmental perturbation on their amputated side. In subjects with an amputation, leading leg work of the amputated legs was adapted in a similar predictive manner as able-bodied subjects, but reactive adaptation of trailing leg work was impaired. Individuals with an amputation appear less able to respond reactively to novel walking conditions, instead using their intact, sound leg to make necessary accommodations. The results presented in this chapter may help explain why individuals with amputations are more prone to falls and has notable implications for prosthetic design and gait rehabilitation of many impaired populations.

5.1 Introduction

Navigating the world requires constant interaction with various obstacles and changeable terrain. Traversing novel environments requires one to flexibly adjust walking mechanics. Little is known about how humans adapt to cope with novel walking environments and/or acquire new walking patterns. Here, we use the term adaptation to specifically refer to locomotor changes in response to a perturbation that do not alter the fundamental characteristics of the action (e.g. a subject remains walking and does not begin running) (Martin, Keating et al. 1996; Bastian 2008). Identifying the strategies used to adapt walking mechanics over time in both able and impaired populations may inform gait rehabilitation protocols that help restore independent walking and prevent maladaptive gait patterns after an injury or pathology (e.g. stroke, trauma, amputation, etc). The purpose of this research was to compare the joint-level mechanical strategies impaired individuals (subjects with a unilateral, transtibial amputation) adopt to walk in a novel, split-belt treadmill environment, to the strategies employed by able-bodied individuals. Comparing the adaptation strategies used by individuals with an amputation to those of intact individuals will further illuminate the role ankle joint actuation and distal sensory feedback play in short-term locomotor adaptation and may identify particular adaptive joint strategies used by individuals with amputations that could be exploited or should be de-emphasized during gait training.

Split-belt treadmill walking is a unique intervention that perturbs locomotor mechanics without disrupting the basic nature of walking (1:1 stepping, distinct double support) or precipitating a fall (Dietz, Zijlstra et al. 1994; Prokop, Berger et al. 1995; Jensen, Prokop et al. 1998; Reisman, Block et al. 2005; Choi and Bastian 2007; Reisman,

Bastian et al. 2010; Vasudevan and Bastian 2010; Roemmich, Stegemoller et al. 2012; Finley, Bastian et al. 2013; Mawase, Haizler et al. 2013; Roper, Stegemoller et al. 2013; Ogawa, Kawashima et al. 2014). Able-bodied subjects adapt a variety of step parameters (e.g. step length, double support time), kinetic variables (e.g. A-P braking forces), and muscle activation patterns to reduce the metabolic demands of split-belt walking over time (Dietz, Zijlstra et al. 1994; Reisman, Block et al. 2005; Malone, Bastian et al. 2012; Finley, Bastian et al. 2013; Roper, Stegemoller et al. 2013; MacLellan, Ivanenko et al. 2014; Ogawa, Kawashima et al. 2014). Some evidence suggests that such metabolic efficiency arises from adopting more mechanically efficient walking mechanics by switching from a hip to primarily ankle strategy for generating propulsive work and power over the course of split-belt treadmill adaptation (Oh, Baek et al. 2012; Cho, Thajchayapong et al. 2013; Park and Park 2013; Thajchayapong, Cho et al. 2014). Controlled ankle torque timing plays an important role in maintaining consistent power production and mechanically efficient step-to-step transitions in steady-state able-bodied walking (Kuo 2002; Ruina, Bertram et al. 2005; Chapter 3). Appropriate ankle torque timing also appears to allow able-bodied walkers to utilize the series elastic properties of the Achilles tendon to achieve more efficient walking mechanics (Ishikawa, Komi et al. 2005; Cronin, Avela et al. 2013; Zelik, Huang et al. 2014). We therefore expected intact individuals to adapt the timing of ankle work production over the course of adaptation to adjust the extent to which series elastic ankle structures contribute to leg power generation, which would then contribute to adopting more efficient walking mechanics over the course of split-belt treadmill adaptation. In steady state walking, the knee acts as a brake to balance the effect of ankle variability on leg power generation (Chapters 2 and

3). This ankle-knee covariation thus enables more robust motor control in steady state walking, which will likely also aid responses to environmental perturbations, like split-belt treadmill walking. We therefore expected this mechanism to contribute to changes in knee work magnitude that parallel ankle work adaptation during push off and power generation at the end of stance.

Two adaptation patterns with different suspected neural origins have been observed in split-belt locomotor adaptation. Slower adapting variables with distinct initial error and aftereffects are likely under predictive, more central motor control, and require intact cerebellar function (Morton and Bastian 2006; Jayaram, Tang et al. 2012). Fast adapting variables with near immediate changes after initial exposure and limited aftereffects are more reactive and controlled primarily through more distal, feedback regulated pathways (Lam, Anderschitz et al. 2006; Morton and Bastian 2006; Smith, Ghazizadeh et al. 2006; Reisman, Wityk et al. 2007; Choi, Vining et al. 2009; Ogawa, Kawashima et al. 2014). While intact cerebellar function is necessary for predictive adaptation, cerebral damage does not affect stroke patient's ability to adapt both predictive and reactive regulated behaviors (Reisman, Wityk et al. 2007; Reisman, McLean et al. 2013). Distal load receptors have been implicated in contributing to the retention of perceived inter-leg speed asymmetries after locomotor adaptation (Jensen, Prokop et al. 1998), and may contribute to the adaptation of more reactive adaptation mechanisms. Distal reflexes also play an important role in ensuring proper responses to perturbation during gait (Nielsen and Sinkjaer 2002; Hohne, Stark et al. 2011; MacLellan, Ivanenko et al. 2014). No work has yet attempted to explicitly determine the

effects of coincident distal sensory feedback and motor control on the progression of leg- and joint-level adaptation during split-belt walking.

In this study, we have taken the first step towards understating the role of integrated peripheral feedback and motor function on split-belt treadmill adaptation by investigating adaptation of individuals with a unilateral, transtibial amputation and comparing their amputated leg adaptation to the legs of matched control subjects. Transtibial amputation effectively eliminates direct ankle motor control, significantly limits typically available distal sensory feedback, and impairs ankle-knee covariation during steady-state walking (Chapter 4). Most individuals with amputations use energy storage and return (ESAR) prosthetic devices to provide push-off power in walking, retaining passive ankle function in the absence of distal reflexes and feedback, so studying gait of individuals with amputations provides a unique opportunity to study the *in vivo* effect of distal feedback and active motor control removal in otherwise healthy human walkers. Individuals with amputations have good anticipatory but poor online (i.e. rapid) obstacle avoidance responses during walking, suggesting that they are less able to respond to an environmental perturbation when feedback integration is required (Houdijk, van Ooijen et al. 2012). Furthermore, delayed EMG responses to obstacle avoidance tasks also suggest that individuals with amputations lack or suppress feedback affecting motor control responses (Hofstad, Weerdesteyn et al. 2009). During split-belt treadmill walking, push off forces and positive work generated by the trailing leg are feedback mediated (Cho, Thajchayapong et al. 2013; Ogawa, Kawashima et al. 2014; Thajchayapong, Cho et al. 2014). Studying how individuals with amputations adapt these parameters will allow us to study how these feedback-regulated elements are controlled

in the absence of direct peripheral feedback and distal motor control. Because the sensory input and motor output necessary to adjust a feedback mediated response is limited, we expected subjects with an amputation to have slow or possibly absent trailing leg positive, propulsive work adaptation on the prosthetic side.

If prosthetic leg propulsive work adaptation is indeed limited, individuals with an amputation likely make compensatory adjustments in either their contra-lateral, sound leg or at more proximal structures on their prosthetic side to successfully walk when perturbed by a split-belt treadmill. Individuals with an amputation use their contra-lateral sound limb to recover from standing balance perturbations (Vrieling, van Keeken et al. 2007; Curtze, Hof et al. 2012; Nederhand, Van Asseldonk et al. 2012). In steady state walking, individuals with an amputation also adjust work done by their sound limb to compensate for reduced propulsive work applied by their amputated leg (Houdijk, Pollmann et al. 2009). The lack of ankle-knee covariation previously observed in individuals with a transtibial amputation indicates that inter-joint communication is impaired after amputation (Chapter 4), which will likely limit the ability of the knee to respond and adapt to deficient ankle function. We therefore expected that subjects with an amputation would demonstrate different adaptation patterns in their contralateral, sound leg to compensate for lack of adaptation and propulsive power in their amputated leg but will not significantly adapt ankle-knee function on their amputated side. While other studies have identified the adjustments individuals with amputations make to walk in various novel environments (Gates, Darter et al. 2012; Gates, Dingwell et al. 2012; Buckley, De Asha et al. 2013; Gates, Scott et al. 2013; Beurskens, Wilken et al. 2014; Hak, Dieen et al. 2014), this study is the first to investigate how individuals with an

amputation adapt their walking mechanics over time in response to perturbation by a split belt treadmill.

5.2 Methods

Eight individuals with a unilateral, trans-tibial amputation (6M/2F, weight: 80.4±16.9 kg, amputated leg length: 92.2±6.6 cm, sound leg length; 92.0±6.4 cm) and eight able-bodied, control subjects (6M/2F, weight: 81.5±14.1 kg, leg length: 91.8±4.7 cm) gave informed consent as approved by the Georgia Institute of Technology Institutional Review Board. Portions of the data from this cohort and data collection protocol have been previously reported (Chapter 4), but are included again here for completeness. Subjects with an amputation were community ambulators (K3 and K4), able to walk at various speeds and for at least 15 minutes at a comfortable speed without walking aids besides their prosthesis. Seven of the subjects with an amputation had an amputation due to trauma, while one subject had an amputation to correct congenital club foot. For this experiment, all subjects with an amputation wore their own custom-made, well-fit prosthetic devices. All subjects with an amputation and able-bodied, control subjects were free of any known cardiovascular or neurological pathologies. Able-bodied control subjects were carefully selected to match a specific recruited impaired subject's gender, weight, and leg length (Chapter 4, Table 1). All subjects with an amputation and able-bodied subjects were familiar with treadmill walking, but none had experienced split-belt treadmill walking prior to this experiment.

5.2.1 Experimental Protocol

Four subjects with an amputation completed a six-minute walk test prior to data collection (519.3m±70.3m, ATS Statement: Guidelines for the Six-Minute Walk Test). Of the able-bodied control subjects, four completed a six-minute walk test prior to data collection, three completed the test on a separate day on a return visit, and one did not complete the test (660.2±56.0m). Preferred walking speed (Control: 1.29±0.10m/s, Amputee: 1.17m/s±0.09m/s) was determined by having subjects walk on the instrumented treadmill also used for data collection (details below) at various speeds below their average six minute walk speed, while verbally indicating whether the speed felt "too fast," "too slow," or "just right." Subjects who did not complete a six-minute walk test prior to data collection walked at speeds less than 1.5m/s, beginning at a typically comfortable speed of 1.3m/s.

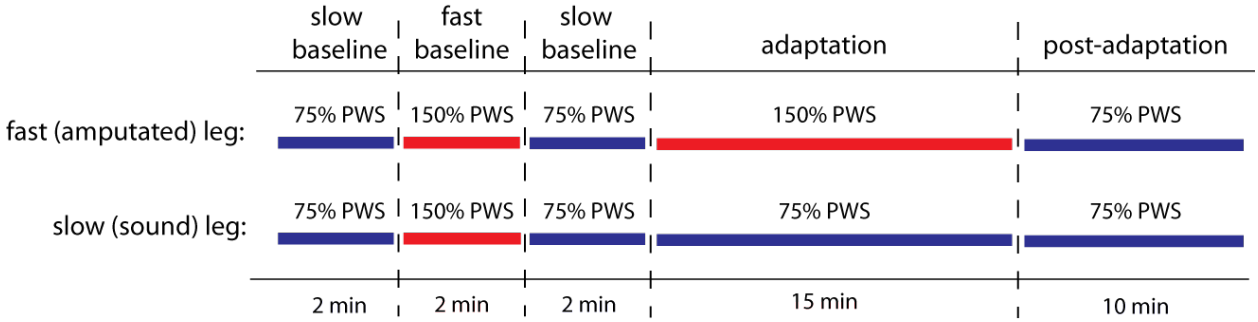

Figure 5.1: Experimental protocol. All subjects completed five consecutive experimental conditions. In baseline conditions, both the fast and slow (amputated and sound respectively for subjects with an amputation) moved at the same speed. In slow baseline conditions, the treadmill belts were tied to move at 75% (blue bars) of that subjects preferred walking speed (PWS). In the fast baseline condition, both belts moved at 150% PWS (red bars). Adaptation is when split-belt walking was introduced, where the fast (or amputated) leg stepped on a treadmill belt moving at 150% PWS and the slow (sound) leg stepped on a belt moving at 75% PWS. In post-adaptation, both belts were again tied and both moved at 75% PWS.

We used a similar protocol as previously published split-treadmill walking protocols (**Fig. 5.1**; Reisman, Block et al. 2005; Morton and Bastian 2006; Ogawa, Kawashima et al. 2014). All subjects walked on a custom, dual-belt treadmill with the treadmill belts running at the same (tied-belt) or different (split-belt) speeds. Subjects began with three two-minute baseline trials: first at 75%, then 150%, and again at 75% of their preferred walking speed (PWS). Next, subjects completed a fifteen minute adaptation period, where one leg stepped at 75% PWS and the other stepped at 150% PWS, maintaining this 2:1 speed ratio throughout the adaptation trial. Finally, subjects completed a ten minute post-adaptation trial, were they returned to a tied condition and both legs moved at 75% PWS. For control subjects, we refer to the leg stepping on the slower treadmill (75%PWS) during the adaptation trial as the slow leg and the contralateral leg stepping at 150%PWS as the fast leg. During the adaptation trial, subjects with an amputation walked with their amputated leg on the fast belt and their sound leg on the slow belt. Three out of four subjects with an amputation who attempted to walk in the opposite orientation, with their prosthetic leg on the slow belt, found it very challenging and could not complete the full 15 minutes. As a result, all remaining participants with an amputation only walked with their prosthetic leg on the fast belt. Able-bodied subjects walked with their preferred stance leg (4R/4L) on the slow belt. Preferred stance side of control subjects was determined by asking subjects to stand on one leg for three seconds.

The treadmills were stopped completely between each baseline trial and after adaptation to allow an experimenter to set the speeds required for the next trial. The treadmill belts stopped quickly, and no subjects took additional steps after the completion

of each condition. Subjects were asked to step to the side, off the treadmills, while the belt speeds were adjusted between trials, but no other walking was allowed. At the beginning of the adaptation and post-adaptation trials, subjects were instructed to wait until a researcher gave a verbal indication that the treadmills had reached their desired speed before stepping onto the moving treadmill belts. All subjects were required to hold onto a secure handrail placed at a comfortable distance in front of them at the beginning of each condition. We asked subjects to maintain contact with the handrail for the first 30 seconds of each trial and manually recorded when within the trial subjects actually let go of the handrail. We allowed some subjects to maintain contact with the handrail for longer than 30 seconds if they felt it was necessary for their safety. Subjects were given as much time as desired between baseline trials and before starting the adaptation trial. The time between the adaptation and post adaptation trial was kept to the minimal time required to adjust the treadmill belt speeds and never exceeded sixty seconds. Throughout the experimental protocol, subjects wore a safety harness that did not support body weight, but would prevent a fall if the subject were to trip at any point during the data collection. Subjects were also provided a mirror placed in their line of sight to allow subjects to track their foot placement while maintaining a forward gaze. No instructions were given specifically regarding foot placement, and subjects were reminded that they were not being evaluated based on how they looked when they walked.

5.2.2. Data Collection

Data was sampled continuously throughout all experimental conditions. Ground reaction forces were collected independently for each leg with six-degree of freedom

force plates embedded beneath each treadmill belt (1080 Hz, Advanced Mechanical Technology Incorporated, Watertown, MA, USA). Simultaneous kinematics data were collected using a six-camera motion analysis system (120 Hz, VICON Motion Systems, Oxford, UK). Retroreflective markers were placed bilaterally on the anterior posterior iliac spine, posterior superior iliac spine, greater trochanter, thigh segment, knee joint center, shank segment, lateral malleolus, fifth metatarsal head on the lateral aspect of the foot, and second metatartophalangeal joint on the foot dorsum. The same marker set was used for subjects with an amputation and control subjects. Markers placed on the prosthetic leg and foot were placed at the best approximation of comparable anatomical landmarks and were matched as closely to the sound leg as possible.

5.2.3 Data Analysis

Marker and force data were filtered using a zero-phase lag fourth-order Butterworth low-pass filter with a 10Hz cutoff frequency. Joint torques were calculated in the sagittal plane using standard inverse dynamics calculations and segment inertial characteristics estimated from subject specific anthropometrics (Winter 1980). Inertial characteristics of the residual limb and prosthetic device were calculated using the same method as able-bodied subjects. Any error resulting from these approximations likely has little effect on the calculated joint torques during stance (Miller 1987; Winter and Sienko 1988; Powers, Rao et al. 1998; Su, Gard et al. 2007; Goldberg, Requejo et al. 2008; Nguyen and Reynolds 2014). Due to the likelihood that holding the safety handrail affects leg power and work values, data from the period of handrail holding at the beginning of each trial were cropped and excluded from analysis.

5.2.4 Leg Work

Individual leg power was calculated for each leg as the dot product of leg force recorded under the leg (F_{leg}) and center of mass velocity (v_{com}, **Eq. 5.1**). The center of mass velocity was calculated by integrating the center of mass acceleration (a_{com}) as calculated from the product of subject mass (m) and the total ground reaction force summed from both legs (F_{net}, **Eq. 5.2**). The integration constants were zero for the vertical component of the center of mass velocity and the treadmill speed of that leg for the anterior-posterior component of the center of mass velocity. In the split-belt condition, fast leg power was calculated using a center of mass integrated with the fast belt speed integration constant, while the slow leg was calculated with the slow belt speed.

Leg work was determined using the same methodology established by Donelan et. al. (Donelan, Kram et al. 2002a; Donelan, Kram et al. 2002b). Leg work was calculated with a definite integral of leg power P_{leg} over a defined period of the gait cycle (e.g. double support and single support). Double support was designated as the period of the gait cycle when both feet were on the ground, from ipsilateral heel contact (a in **Eq. 5.3**) to contralateral toe off (b). During double support, one leg leads and accepts center of mass progression, while the other leg trails and provides propulsion into the next step cycle. Because the leading and trailing legs fulfill separate specific functions, work in double support was calculated for the leading and trailing legs independently. Leading leg work was calculated as the integration of negative leg power values during double support (**Eq. 5.4**). Trailing leg work was calculated as the integration of positive leg

power values during double support (**Eq. 5.5**). Positive values of leading leg power and negative values of trailing leg power are negligibly small and do not contribute substantially to leg work (Donelan, Kram et al. 2002a; Donelan, Kram et al. 2002b). Single support work was calculated from contralateral toe off (a) to contralateral heel strike (b), capturing the period in which the leg of interest was in stance while the other leg was in swing. Because single support encompasses periods of both braking and propulsion, single support work was calculated over all leg power values and not segmented based on the sign of leg power.

$$P_{leg} = F_{leg} \cdot v_{com} \qquad \textbf{(Eq. 1)}$$

$$v_{com} = \int a_{com} dt = \int \left(F_{net} / m \right) dt \qquad \textbf{(Eq. 2)}$$

$$W = \int_a^b P_{leg} dt \qquad \textbf{(Eq. 3)}$$

$$W_{lead}^{-} = \int_a^b \left(P_{lead} < 0 \right) dt \qquad \textbf{(Eq. 4)}$$

$$W_{trail}^{+} = \int_a^b \left(P_{trail} > 0 \right) dt \qquad \textbf{(Eq. 5)}$$

All work values were normalized by subject body weight and leg length to enable inter-subject comparisons. To facilitate inter-leg comparisons of work values during double support, we analyzed double support work "error." Work error was calculated as the difference from mean baseline values. Each leg's work error was computed when compared to itself in the baseline period (fast or slow) corresponding to the belt speed in that particular trial. For example, fast leg positive trailing leg work error during

adaptation was determined based on the comparison of that leg's (right or left) mean positive trailing leg work in the fast baseline trial.

5.2.5 Joint Work

Individual joint power (P_{jt}) was calculated as the product of sagittal plane joint moment (M_{jt}) and angular velocity (ω_{jt}, **Eq. 5.6**). Angular velocity was determined by differentiating the included joint angle (θ_{jt}, **Eq. 5.7**). Similarly to leg work, individual joint work was calculated with a definite integration over the gait phase of interest (double support or single support). Because we were interested in the propulsive role of the ankle, ankle work was taken only over the positive values of ankle joint power, while knee work was calculated by integrating over all values of joint power. Positive ankle work therefore indicates propulsive work generation from plantarflexion and positive knee work generation results from knee extension.

$$P_{jt} = M_{jt}\omega_{jt} \quad \textbf{(Eq. 5.6)}$$

$$\omega_{jt} = \frac{d\theta_{jt}}{dt} \quad \textbf{(Eq. 5.7)}$$

5.2.6 Statistical Analysis

In order to make comparisons over the course of adaptation, we binned data from the last five steps of each baseline trial (slow baseline, fast baseline), the first five steps of adaptation after subjects released the safety handrail (early adaptation), the last five steps of adaptation (late adaptation), the first five steps of post-adaptation after subjects

released the safety handrail (early post-adaptation), and the last five steps of post-adaptation (late post-adaptation). We performed a one-way repeated measures analysis on negative leading, positive trailing, and single support work for each leg type (able-bodied fast, able-bodied slow, amputee sound, and amputee amputated). Greenhouse-geiser corrections were applied when sphericity was violated. With the exception of the linear regressions (discussed below) all statistical analyses were performed with SPSS Statistics (IBM Corp., Version 21).

Similarly to how leg work error was calculated, we only considered pairwise comparisons relative to the appropriate baseline speed during adaptation (i.e. fast leg work values were compared to fast baseline), and post-adaptation values were only compared to slow baseline. Predictive adaptation was identified by an initial significant difference in early adaptation that returned to respective baseline values in late adaptation, followed by a negative aftereffect where early post-adaptation differed from baseline in the direction opposite from early adaptation errors. Reactive adaptation was identified by variables that were different from baseline values throughout adaptation and demonstrated either no aftereffect in post-adaptation or an aftereffect similar in direction to early adaptation. with Greenhouse-geisser correction used when sphericity assumption was violated.

We tested for inter-leg symmetry as discussed in the Results section using a Student's paired t-test with appropriate Bonferroni corrections in early and late adaptation. We tested for symmetry between: positive work error of the able-bodied fast leg and negative work error of the able-bodied slow leg, positive work error of the

amputated leg and negative work error of the sound leg, fast and slow leg single support work, and amputated and sound leg single support work.

Comparisons between single support and double support positive ankle work in the fast leg of able-bodied subjects and the amputated legs of subjects with an amputation were also done using a Student's paired t-test with a Bonferroni correction in early and late adaptation. Tests for a linear relationship between single support and double support positive ankle work as well as between positive ankle work and total knee work in double support were done for both the fast and amputated legs with a first order polynomial fit using the built in Matlab command "polyfit."

5.3 Results

Matched control subjects did not differ significantly from subjects with an amputation in regards to weight or leg length (rmANOVA; $p>0.05$), but subjects with an amputation demonstrated a significantly lower preferred walking speed than control subjects (Able-bodied: 1.29±0.10 m/s; Amputee: 1.17±0.09 m/s; $p<0.05$) (Chapter 4, **Table 1**). Leg force and joint torque trajectories were previously reported (Able-bodied: Chapter 3; Amputee: Chapter 4) and recorded data from both subject groups were consistent with previously published data.

5.3.1 Double Support Work Adaptation

<u>Able-bodied Subjects</u>

Able-bodied subjects adapted negative work error of the fast leg when leading (rmANOVA: $F=16.626$; $p=0.001$; **Fig. 5.2A&C**). Negative work errors in the first five

steps of split-belt walking (early adaptation) differed significantly from fast baseline ($p<0.05$) but did not differ from fast baseline in late adaptation. Negative fast leg work errors were not significantly different than slow baseline in early or late post-adaptation, but mean errors in early post-adaptation qualitatively appear smaller than slow baseline with large inter-subject standard deviation (**Fig. 5.2C**). Positive work errors of the slow leg when trailing were smaller than slow baseline values throughout adaptation ($F=6.597$; $p=0.006$; pairwise comparisons $p<0.05$; **Fig. 5.2D**). Slow leg positive work error difference from slow baseline approached significance in early post-adaptation ($p=0.055$) and increased during post-adaptation to values similar to slow baseline in late post-adaptation ($p=0.008$). Negative work errors in the slow leg when leading demonstrated a similar trend (rmANOVA: $F=30.824$; $p<0.001$; **Fig. 5.2B&E**). Slow leg negative work errors differed from baseline values throughout adaptation ($p<0.05$). Despite not returning to baseline values in late adaptation, slow lead work errors demonstrated negative aftereffects, initially differing from baseline ($p<0.05$) and then returning to baseline values in late post-adaptation (**Fig. 5.2E**). When trailing, positive work error in the fast leg of able-bodied subjects was significantly different than fast baseline throughout adaptation and immediately returned to slow baseline values in post-adaptation (rmANOVA: $F=8.588$; $p=0.005$; pairwise comparisons $p<0.05$; **Fig. 5.2F**).

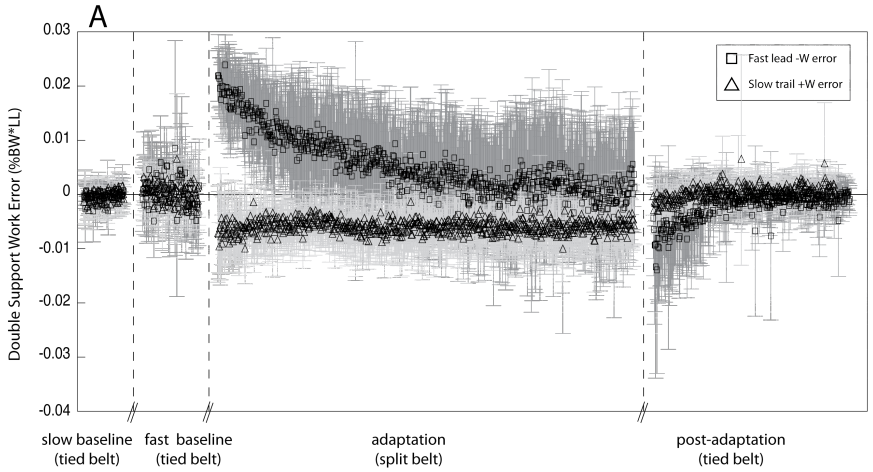
A
Fast lead -W error
Slow trail +W error
Double Support Work Error (%BW*LL)
slow baseline (tied belt)
fast baseline (tied belt)
adaptation (split belt)
post-adaptation (tied belt)

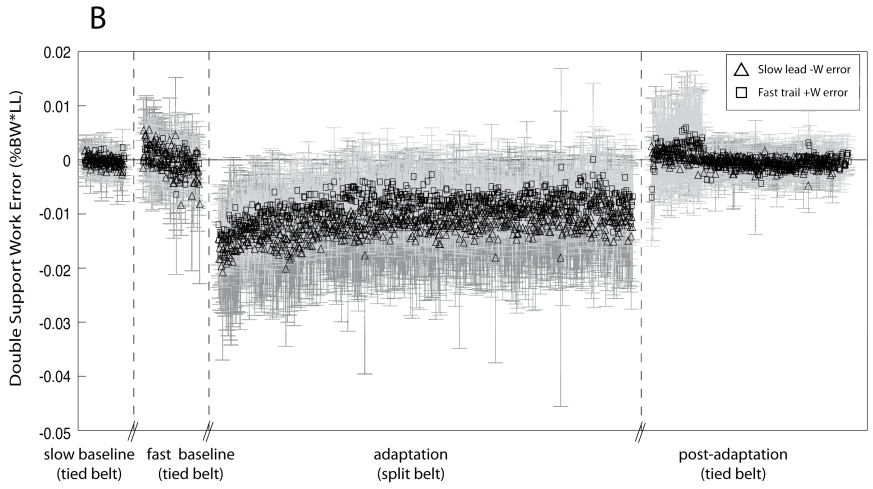
B
Slow lead -W error
Fast trail +W error
Double Support Work Error (%BW*LL)
slow baseline (tied belt)
fast baseline (tied belt)
adaptation (split belt)
post-adaptation (tied belt)

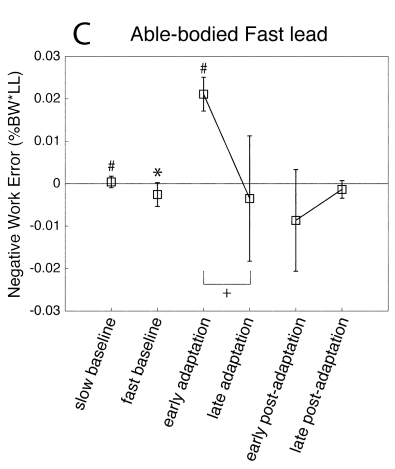
C
Able-bodied Fast lead
Negative Work Error (%BW*LL)
slow baseline
fast baseline
early adaptation
late adaptation
early post-adaptation
late post-adaptation

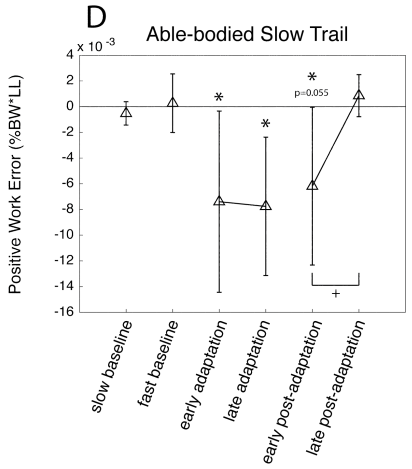
D
Able-bodied Slow Trail
x 10 -3
p=0.055
Positive Work Error (%BW*LL)
slow baseline
fast baseline
early adaptation
late adaptation
early post-adaptation
late post-adaptation

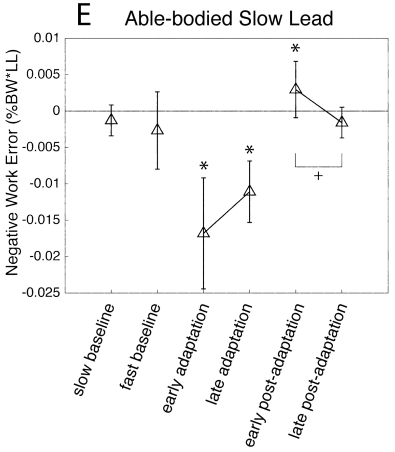
E
Able-bodied Slow Lead
Negative Work Error (%BW*LL)
slow baseline
fast baseline
early adaptation
late adaptation
early post-adaptation
late post-adaptation

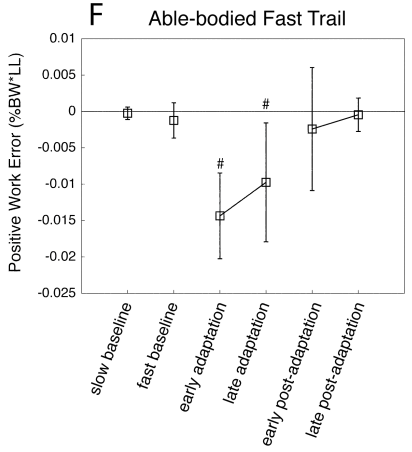
F
Able-bodied Fast Trail
Positive Work Error (%BW*LL)
slow baseline
fast baseline
early adaptation
late adaptation
early post-adaptation
late post-adaptation

Figure 5.2: Work error during double support for able-bodied subjects. **A**) Double support work error for each step when the fast leg leads and the slow leg trails. In this case, the subject is generating positive propulsive work with their slow leg (triangles) and negative braking work with their fast leg (square). Each symbol represents mean and standard deviation values for a single step across all eight subjects. Vertical dashed lines separate the different experimental conditions. All work error is referenced to the appropriate baseline trial, so the slow leg is referenced to slow baseline and the fast leg to fast baseline (see Methods). A clear initial deviation is seen in the fast leg negative work error. **B**) Double support work error for each step when the slow leg (triangles) leads and the fast leg trails (squares). Here, the fast leg generates positive work and the slow leg does negative, braking work. **C**-**F**) Data sampled from different stages of adaptation. **C** and **D** represent data sampled from **A**, and **E** and **F** are sampled from **B**. Each symbol represents data averaged across five steps for that particular stage (see Methods for detail). Inter-subject mean and standard deviation values are indicated with the symbol and error bars. The # symbol indicates significant differences ($p<0.05$) from fast baseline as determined from pairwise comparisons following a repeated measures ANOVA. Asterisks (*) indicate significant differences ($p<0.05$) from slow baseline. Bar and plus signs (+) indicate significant differences ($p<0.05$) across adaptation or post-adaptation stages (i.e. early adaptation compared to late adaptation). Only relevant statistical differences are represented (i.e. fast leg adaptation stages were only compared to fast baseline, see Methods for detail). **C**) Negative work error of the fast leg when leading. **D**) Positive work error of the slow leg when trailing. **E**) Negative work error of the slow leg when leading. **F**) Positive work error of the fast leg when trailing.

Subjects with an Amputation

Subjects with an amputation demonstrate similar trends in both sound and amputated leg negative work error adaptation to the behavior observed in control subjects (**Fig. 5.3**). Amputated leg negative work when leading initially deviates from baseline values in early adaptation, followed by a return to baseline in late adaptation (rmANOVA: $F=10.030$; $p=0.002$; pairwise comparisons $p<0.05$; **Fig. 5.3A&C**). Unlike the fast legs of able-bodied subjects, amputated legs did not demonstrate clear differences from baseline in early post-adaptation. However, the mean negative work error in early post-adaptation was smaller than the mean error of slow baseline, and did increase back towards baseline values over the course of adaptation, suggesting that small changes did occur, though the initial deviation from baseline was not large (**Fig. 5.3C**). The negative work errors of the leading sound leg of subjects with an amputation followed a similar trend as the comparable slow leg of the control subjects, remaining significantly different from baseline values throughout adaptation (rmANOVA: $F=20.935$; $p<0.001$; pairwise comparisons $p<0.05$; **Fig. 5.3E**). Post-adaptation slow leg negative work errors were not

significantly different from slow baseline in either early or late post-adaptation stages, though mean error in early post-adaptation was greater than slow baseline values (**Fig. 5.3B&E**).

Unlike the comparable fast leg in able-bodied subjects, the amputated leg of subjects with an amputation did not show any statistically significant change in positive work error when trailing over the course of the experimental protocol (rmANOVA: $F=2.956$; $p=0.094$; **Fig. 5.3F**). Amputated legs, however, did generate different absolute positive, propulsive work values between the fast and slow baseline trials (two-tailed paired t-test: $t=-3.0449$, $p=0.0187$), revealing that subjects with an amputation are capable of altering the work generated by their amputated leg based on walking speed requirement. Repeated measures ANOVA revealed that the positive work error of the sound legs of subjects with an amputation did, however, change during the experiment ($F=11.124$; $p<0.001$; **Fig.5.3D**). Positive work error of the trailing sound leg was significantly different from the slow baseline condition in early adaptation ($p=0.003$). Late adaptation positive sound leg work errors, however, did not differ from slow baseline values, though there difference did approach significance ($p=0.052$; **Fig. 5.3D**). Early post-adaptation sound leg positive work error differed from slow baseline values ($p=0.041$) and increased over the course of post-adaptation so as to not differ from slow baseline values in late post-adaptation. A paired t-test revealed that positive trailing leg work in the amputated leg was different from negative leading sound leg work error in early adaptation ($p<0.001$) but not in late adaptation ($p=0.058$).

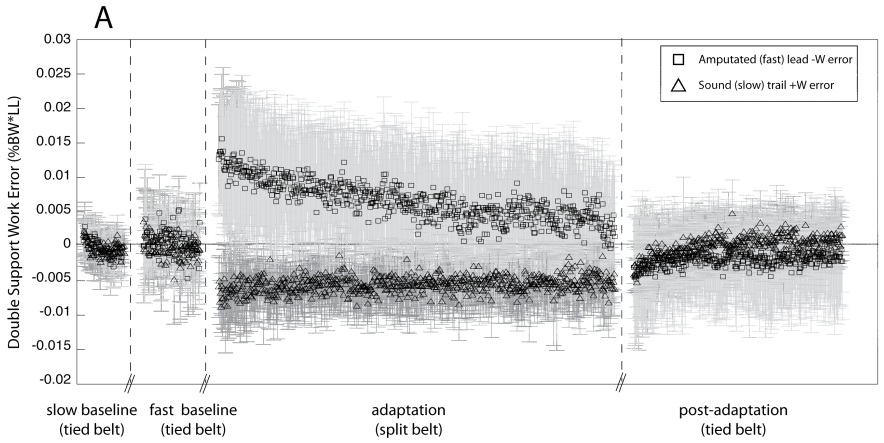
A
Amputated (fast) lead -W error
Sound (slow) trail +W error
Double Support Work Error (%BW*LL)
slow baseline (tied belt)
fast baseline (tied belt)
adaptation (split belt)
post-adaptation (tied belt)

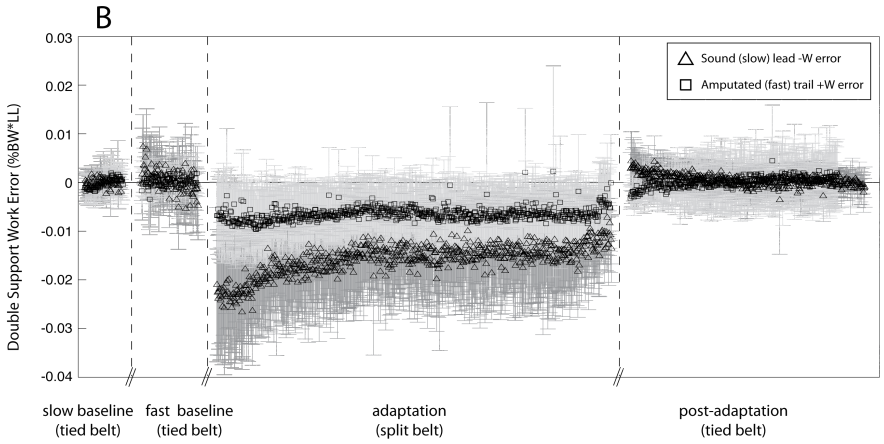
B
Sound (slow) lead -W error
Amputated (fast) trail +W error
Double Support Work Error (%BW*LL)
slow baseline (tied belt)
fast baseline (tied belt)
adaptation (split belt)
post-adaptation (tied belt)

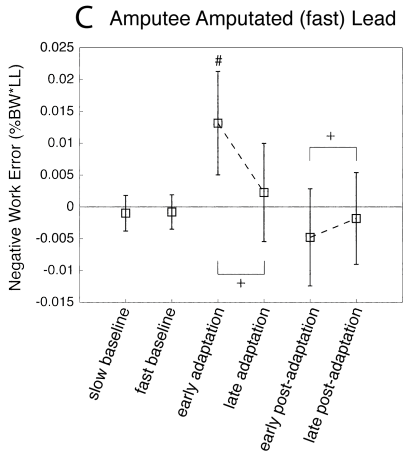
C Amputee Amputated (fast) Lead
Negative Work Error (%BW*LL)
slow baseline
fast baseline
early adaptation
late adaptation
early post-adaptation
late post-adaptation

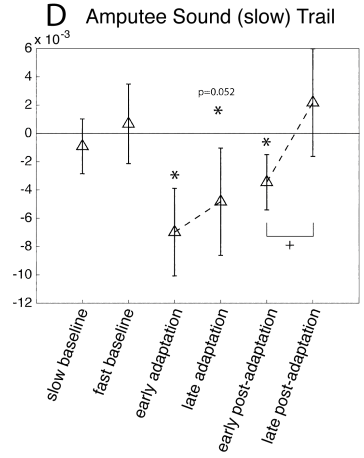
D Amputee Sound (slow) Trail
x 10-3
p=0.052
slow baseline
fast baseline
early adaptation
late adaptation
early post-adaptation
late post-adaptation

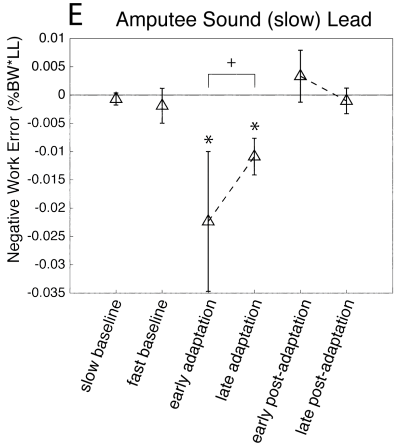
E Amputee Sound (slow) Lead
Negative Work Error (%BW*LL)
slow baseline
fast baseline
early adaptation
late adaptation
early post-adaptation
late post-adaptation

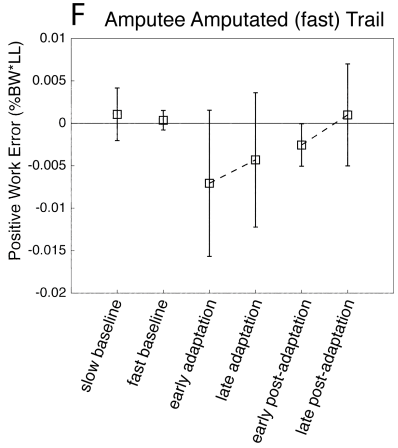
F Amputee Amputated (fast) Trail
Positive Work Error (%BW*LL)
slow baseline
fast baseline
early adaptation
late adaptation
early post-adaptation
late post-adaptation

Figure 5.3: Work error during double support for subject with an amputation. **A**) Double support work error for each step when the amputated (fast) leg leads and generates negative work (squares), while the sound (slow) leg trails and provides positive, propulsive work (triangles). Conventions here are the same as in Fig. 2. A clear initial deviation is seen in the fast leg negative work error is again observable. **B**) Double support work error for each step when the sound (slow) leg leads (-W, triangles) and the amputated (fast) leg trails (+W, squares). **C**-**F**) Data sampled from different stages of adaptation. **C** and **D** represent data sampled from **A**, and **E** and **F** are sampled from **B**. Each symbol represents data averaged across five steps for that particular stage (see Methods for detail). The # symbol indicates significant differences ($p<0.05$) from fast baseline as determined from pairwise comparisons following a repeated measures ANOVA. Asterisks (*) indicate significant differences ($p<0.05$) from slow baseline. Bar and plus signs (+) indicate significant differences ($p<0.05$) across adaptation or post-adaptation stages (i.e. early adaptation compared to late adaptation). Only relevant statistical differences are represented (i.e. fast leg adaptation stages were only compared to fast baseline, see Methods for detail). **C**) Negative work error of the amputated (fast) leg when leading. **D**) Positive work error of the sound (slow) leg when trailing. **E**) Negative work error of the sound (slow) leg when leading. **F**) Positive work error of the amputated (fast) leg when trailing. The rmANOVA did not detect any significant changes over the course of adaptation.

5.3.2 Single Support Work Adaptation

Able-bodied Subjects

Repeated measures ANOVA revealed significant changes in both the fast ($F=59.492$; $p<0.001$) and slow ($F=22.188$; $p<0.001$) leg work during single limb support (**Fig. 5.4A,C,D**). The fast leg generated more single support work during fast baseline walking than during slow baseline walking ($p<0.05$; **Fig. 5.4C**), reflecting greater propulsive work needed for faster walking (Park and Park 2013). Fast leg single support work during early adaptation was significantly different than fast baseline values, but late adaptation single support work was not (**Fig. 5.4C**). Fast leg single support work was not different from slow baseline values in early or late post-adaptation (**Fig. 5.4C**). The slow leg also generated different single support work values during fast and slow baseline conditions (**Fig. 5.4D**). In both early and late adaptation, the slow leg generated greater single support work than slow baseline values (**Fig. 5.4D**). Both early and late post-adaptation slow leg single support work values were significantly different than slow baseline values, but late adaptation work was significantly less than early adaptation work ($p=0.002$), demonstrating a clear trend back towards slow baseline values. A paired

t-test between fast and slow leg single support work revealed a significant asymmetry between fast and slow leg single support work generation in early adaptation ($t=9.090$, $p=4.0e-5$, $p<0.025$, Bonferroni correction) which was eliminated by the end of adaptation ($t=0.009$, $p=0.993$).

Subjects with an Amputation

A repeated measures ANOVA analysis indicated that subjects with an amputation also changed single support work generation in both their amputated ($F=6.614$, $p=0.004$) and sound ($F=24.744$, $p<0.001$) legs over throughout the experimental protocol. Amputated legs generated different amounts of single support work in fast and slow baseline trials ($p=0.019$, **Fig. 5.4B**). Neither of the adaptation stages (early adaptation or late adaptation) were significantly different than fast baseline, but the work generated by the amputated leg did change over the course of adaptation ($p=0.011$). None of the single support work values generated by the prosthetic leg during post-adaptation were significantly different from slow baseline either, although early and late post-adaptation values differed from one another ($p=0.036$; **Fig. 5.4B**). The sound limb of subjects with an amputation generated greater single support work during fast baseline than during slow baseline ($p=0.003$, **Fig. 5.4F**). Single support work generated by the sound leg during early and late adaptation was significantly different than the slow baseline and did not differ from one another (**Fig. 5.4F**). Values of slow leg single support work did not differ from slow baseline during either early or late post-adaptation (**Fig. 5.4F**). The sound leg produces greater work than the prosthetic leg during single support in late adaptation ($t=3.753$, $p=0.004$, **Fig. 5.4B**).

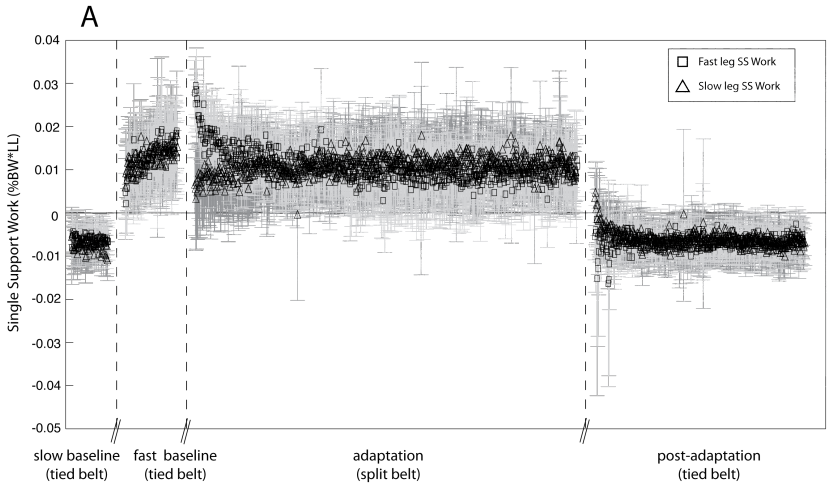
A
Fast leg SS Work
Slow leg SS Work
Single Support Work (%BW*LL)
slow baseline (tied belt)
fast baseline (tied belt)
adaptation (split belt)
post-adaptation (tied belt)

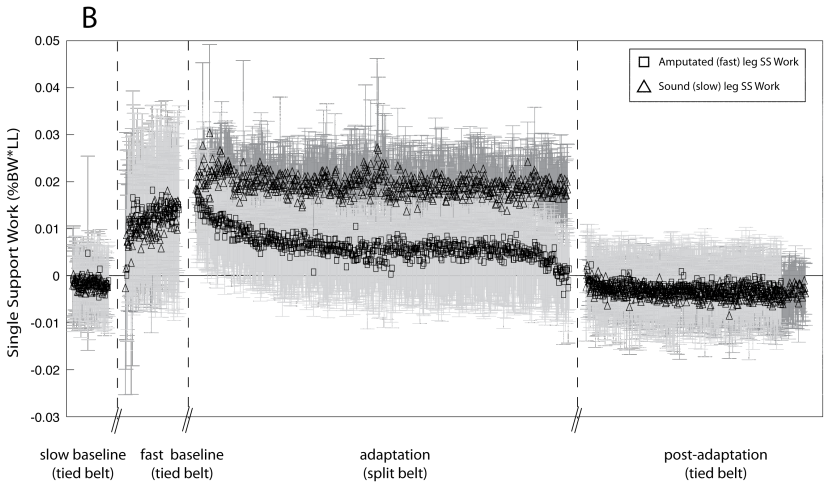
B
Amputated (fast) leg SS Work
Sound (slow) leg SS Work
Single Support Work (%BW*LL)
slow baseline (tied belt)
fast baseline (tied belt)
adaptation (split belt)
post-adaptation (tied belt)

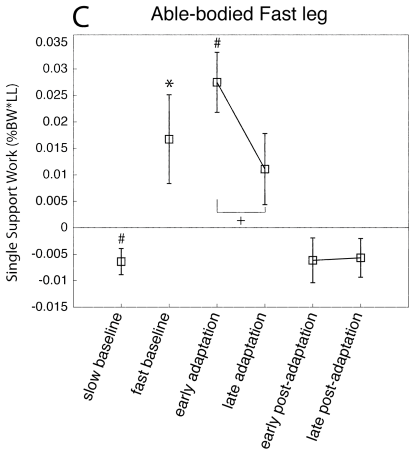
C
Able-bodied Fast leg
Single Support Work (%BW*LL)
slow baseline
fast baseline
early adaptation
late adaptation
early post-adaptation
late post-adaptation

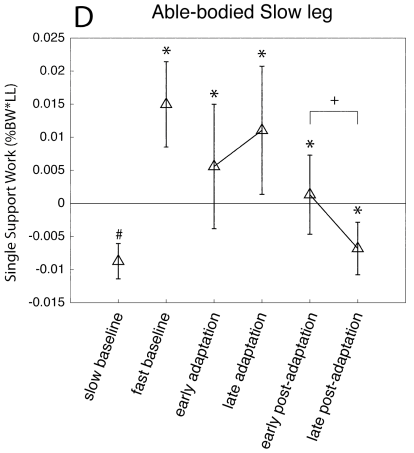
D
Able-bodied Slow leg
Single Support Work (%BW*LL)
slow baseline
fast baseline
early adaptation
late adaptation
early post-adaptation
late post-adaptation

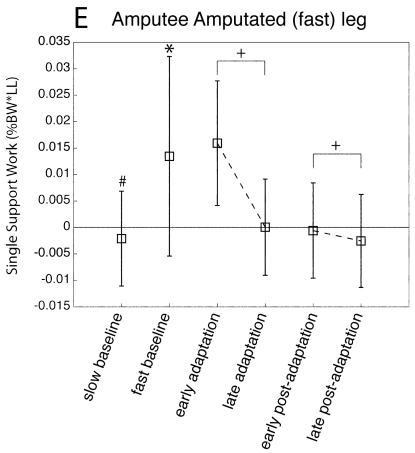
E
Amputee Amputated (fast) leg
Single Support Work (%BW*LL)
slow baseline
fast baseline
early adaptation
late adaptation
early post-adaptation
late post-adaptation

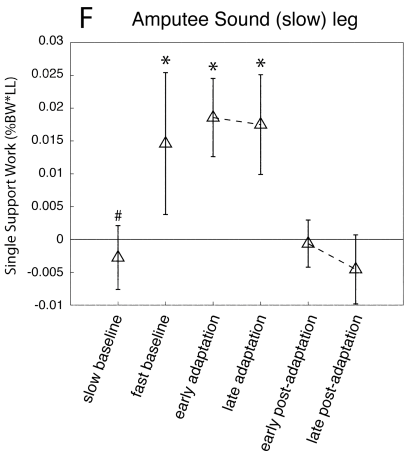
F
Amputee Sound (slow) leg
Single Support Work (%BW*LL)
slow baseline
fast baseline
early adaptation
late adaptation
early post-adaptation
late post-adaptation

Figure 5.4: Single support work for able-bodied subjects (top row) and subjects with an amputation (bottom row). **A**) Single support work for each step in the fast (squares) and slow (triangle) leg. Each symbol is again mean and standard deviation for a single step across all subjects. **B**) Single support work error for each step in the amputated (fast, squares) and sound (slow, triangles). **C-F**) Data sampled from different stages of adaptation. **C** and **D** represent data sampled from **A**, and **E** and **F** are sampled from **B**. Each symbol represents data averaged across five steps for that particular stage (see Methods for detail). The # symbol indicates significant differences ($p<0.05$) from fast baseline as determined from pairwise comparisons following a repeated measures ANOVA. Asterisks (*) indicate significant differences ($p<0.05$) from slow baseline. Bar and plus signs (+) indicate significant differences ($p<0.05$) across adaptation or post-adaptation stages (i.e. early adaptation compared to late adaptation). Only relevant statistical differences are represented (i.e. fast leg adaptation stages were only compared to fast baseline, see Methods for detail). **C**) Single support work of the fast leg in able-bodied subjects. **D**) Single support work of the slow leg in able-bodied subjects. **E**) Single support work of the amputated (fast) leg in subjects with an amputation. **F**) Single support work of the sound (slow) leg in subjects with an amputation.

5.3.3 Fast Leg Ankle Work Timing Adaptation

Able-bodied Subjects

The timing of fast leg positive ankle work production appears to change over the course of adaptation to walking on a split belt treadmill (**Fig. 5.5A**). During both fast and slow baseline walking, ankle work in the fast leg occurs predominantly during double support, though non-zero single support work does occur during fast baseline walking. However, in early adaptation, a two-sided paired t-test revealed that there is a no significant difference between positive, propulsive ankle work generated during single support versus that generated during double support ($t=-1.271$, $p=0.244$). In late adaptation, the ankle does significantly more positive, propulsive work during double support than during single support (paired one-sided t-test: $p=0.001$, $\alpha=0.025$ with Bonferroni correction). A regression analysis also revealed a moderate negative linear correlation ($y=-1.49x+4e-4$, $R^2=0.47$) between double support positive ankle work and single support positive ankle work (**Fig. 5.6A**).

Subjects with an Amputation

Subjects with an amputation appeared to have less capable of altering when their prosthetic ankle generated positive joint work (**Fig. 5.5B**). Positive prosthetic ankle work was qualitatively greater during double support than during single support throughout all stages of the experimental protocol. A one-sided paired t-test revealed that positive ankle work was greater in double support than in single support in both early ($t=2.785$, $p=0.014$, $\alpha=0.025$ with Bonferroni correction) and late ($t=6.128$, $p<0.001$, $\alpha=0.025$) adaptation. A linear regression analysis revealed no significant correlation between double support positive ankle work and single support positive ankle work ($y=-0.16x+0$, $R^2=0.09$; **Fig. 5.6B**).

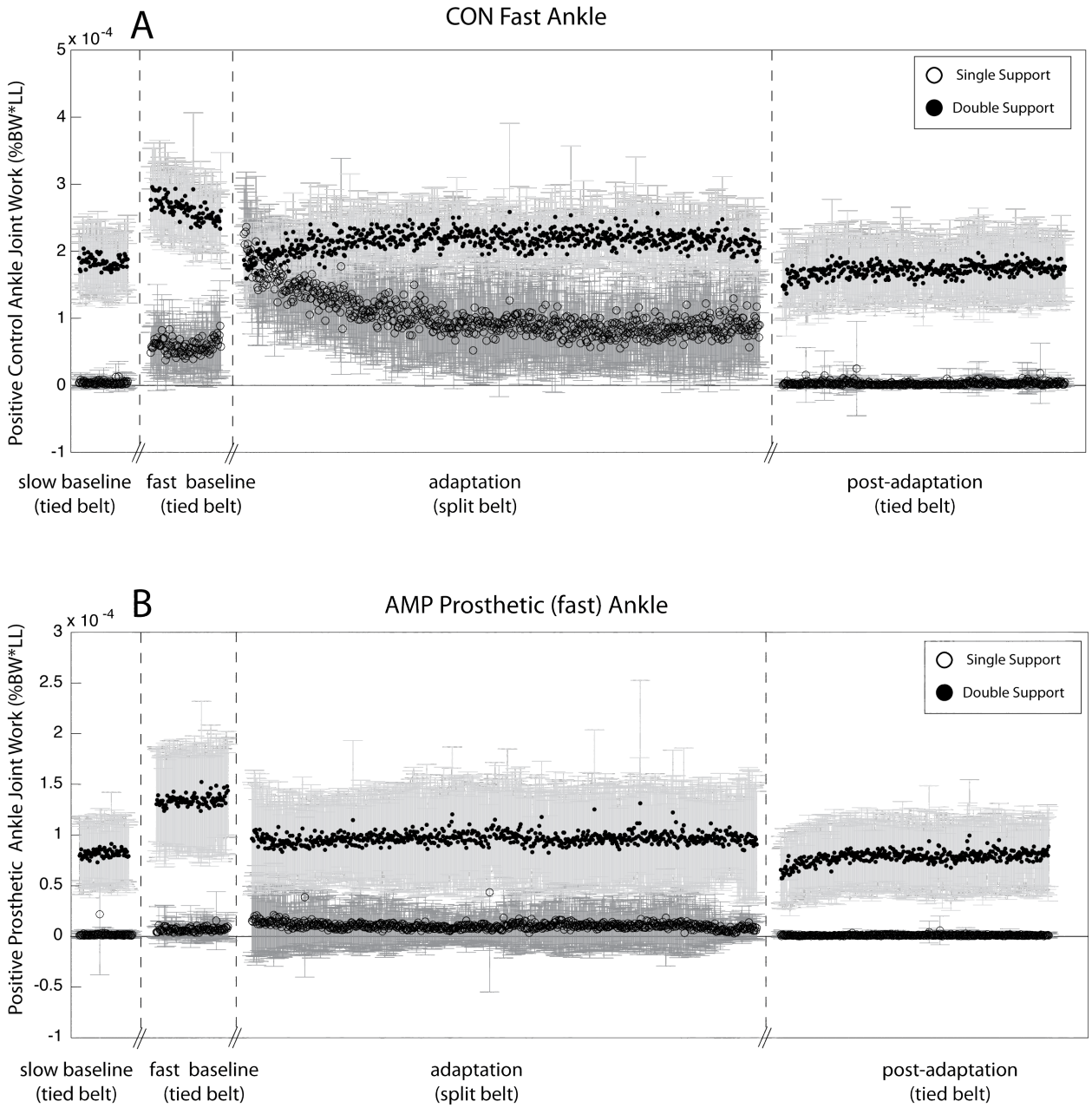

Figure 5.5: Adaptation of positive ankle work timing in the fast leg of able-bodied (**A**) and the amputated (fast) leg of subjects with an amputation (**B**). Positive ankle work in fast able-bodied legs (**A**) are primarily only seen in double support in both slow and fast baseline trials. During adaptation, positive ankle work in single support (open circles) slowly falls to close to zero, while positive ankle work in double support (closed circles) concurrently increases over the course of adaptation. Ankle work appears to shift to occur later in the gait cycle over the course of adaptation. Positive ankle work occurs mostly during double support throughout post-adaptation. Amputated leg (**B**) positive ankle work magnitudes are larger in double support than single support in all periods of the experimental protocol.

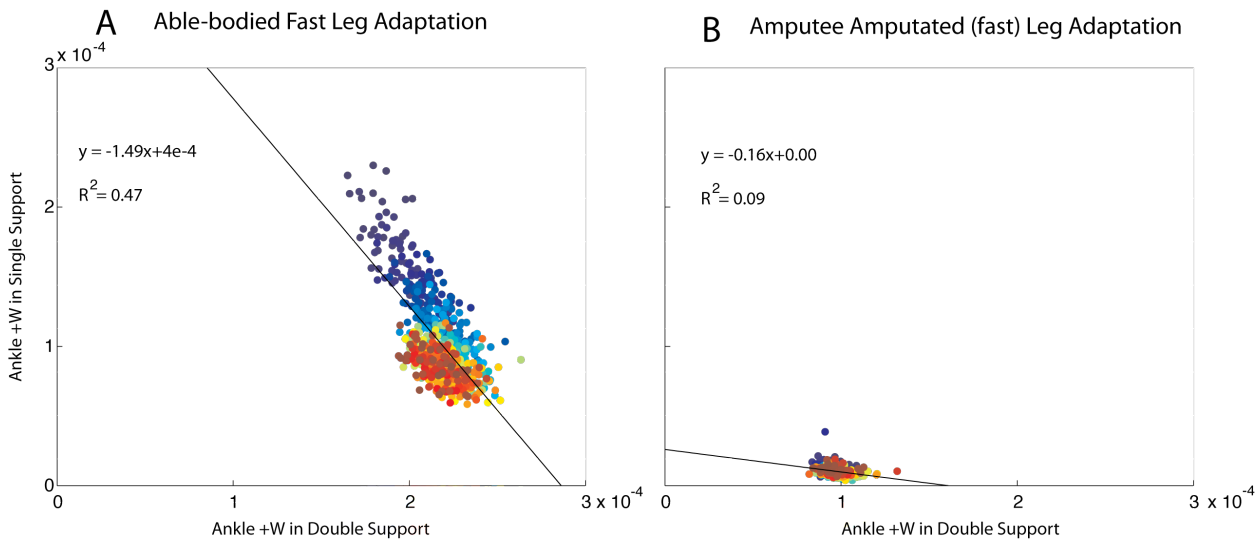

Figure 5.6: Linear relationship between positive ankle work in double support (x-axis) and single support (y-axis) during adaptation in the fast legs of able-bodied subjects (**A**) and the amputated (fast) legs of subjects with an amputation (**B**). Each dot represent the relationship between mean double support and single support positive ankle work across subjects. The colors indicate the progression through adaptation, where darker blues are early adaptation and hotter reds are late adaptation. Lines represent the best linear fit, and the insets show the characteristics of this fit.

5.3.4 Ankle-Knee Work Adaptation

Able-bodied Subjects

A linear regression analysis revealed a weak positive correlation between fast leg positive ankle work and total knee work (y=0.54x-1e-4, R^2=0.57; **Fig. 5.7A**). Knee work was less than zero in early adaptation (cool colored markers, beginning with dark blue) and rose to positive values by late adaptation. As the ankle produced more positive (plantar-flexion) work during double support, the knee transitioned from absorbing work to also generating positive work by the end of adaptation.

Subjects with an Amputation

The relationship between double support positive prosthetic ankle work and total knee work on the amputated leg was best described with a vertical line (x=9.77e-5, R^2=1, **Fig. 5.7B**), indicating that knee work varied independently of prosthetic ankle work.

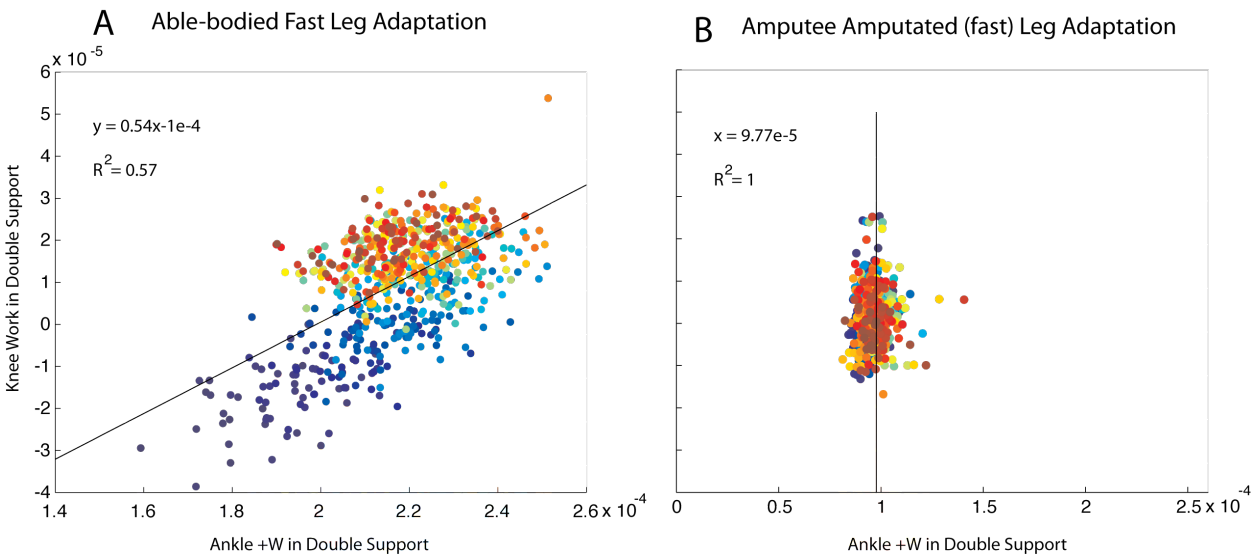

Figure 5.7: Linear relationship between positive ankle work (x-axis) and total knee work (y-axis) in double support during adaptation in the fast legs of able-bodied subjects (**A**) and the amputated (fast) legs of subjects with an amputation (**B**). Each dot represent the relationship between mean positive ankle work and total knee work across subjects. The colors indicate the progression through adaptation, where darker blues are early adaptation and hotter reds are late adaptation. Lines represent the best linear fit, and the insets show the characteristics of this fit.

5.4 Discussion

We investigated the role of distal feedback and motor control in regulating adaptation of leg and joint work by comparing locomotor adaptation of able walkers and walkers with an amputation. We discovered that able-bodied subjects used a predictive strategy to adapt negative leading leg work, while trailing leg propulsive work was adapted in a manner consistent with reactive, feedback regulated control. Able-bodied subjects also adapted the timing of ankle work production to occur later in the gait cycle over the course of adaptation possibly to facilitate use of more efficient power production mechanisms. Changes in ankle work production during leg power generation were accompanied by changes in total knee work, suggesting that coordinated ankle-knee covariation contributes to leg power adaptation. Subjects with an amputation adapted negative leading leg work errors in a similar predictive manner as control subjects on both their amputated and sound sides. Unlike the control subjects, however, walkers with

an amputation did not demonstrate significant adaptation of positive, propulsive work in their amputated leg, instead altering sound leg work. The absence of neuromechanical ankle-knee coupling in subjects with an amputation also affected individual ankle and knee joint work adaptation. The loss of distal sensory feedback and motor control does not affect predictive control mechanisms, but limits the ability to adapt reactive responses during split-belt treadmill walking.

5.4.1 Able-bodied Subjects Adapt Leading Leg Work Predictively and Trailing Leg Work Reactively

Able-bodied subjects adapted leg work errors differently depending on when in the gait cycle the work was produced. Individual legs generate different amounts of work at different stages of the gait cycle. During double support, one leg leads and produces negative, absorptive work, while the other leg trails and generates positive, propulsive work (Donelan, Kram et al. 2002a; Donelan, Kram et al. 2002b; Kuo 2002; Collins 2008; Collins and Kuo 2010). Negative leading leg work errors were adapted in a manner consistent with a predictive adaptation strategy. Both fast and slow leg leading leg work error demonstrated initial deviations from baseline values in early adaptation, showing clear initial perturbation in response to the introduction of split-belt walking (**Fig. 5.2C&E**). Leading leg negative work error in the slow leg demonstrated a significant negative aftereffect, showing a clear pattern of predictive adaptation (**Fig. 5.2C**). The fast leg negative work error did not demonstrate significant negative aftereffects (**Fig. 5.2E**), but the trend of the mean values followed a pattern that would be expected for a negative aftereffect, suggesting that greater aftereffects may have been cropped with the data the

period in which subjects were holding the safety handrail. Predictive adaptation occurs when behavior cannot be informed by the preceding gait period, but must be anticipated, requiring internalization of the conditions and updating the action with each step, presumably via cerebellar function (Kawato, Furukawa et al. 1987; Lam, Anderschitz et al. 2006; Morton and Bastian 2006; Smith, Ghazizadeh et al. 2006; Izawa, Rane et al. 2008; Jayaram, Tang et al. 2012; Ogawa, Kawashima et al. 2014). Because the period of leading leg negative work is immediately preceded by swing phase when little force feedback is present, production of negative work is seemingly anticipated and updated with each step. Leading leg work is therefore likely regulated by more predictive mechanisms rather than by online feedback, similarly to the pattern observed for anterior-posterior braking forces (Ogawa, Kawashima et al. 2014).

Positive trailing leg work in both the fast and slow legs of able-bodied subjects adapted in a pattern consistent with a reactive, feedback regulated adaptation strategy. Trailing leg work errors during double support deviated from baseline throughout adaptation, did not return to baseline values, and did not demonstrate negative after effects in either the fast or slow legs (**Fig. 5.2D&F**). Although not significant, the mean slow leg positive work error was initially much smaller than baseline in early post-adaptation, which suggests the presence of an aftereffect. However, this early post-adaptation error was similar to the error recorded in adaptation, rather than deviating in the opposite direction. This slow leg aftereffect is therefore not a negative aftereffect, but rather indicates a persistent change that remains present in post-adaptation. These patterns are consistent with control in which current behavior is monitored and adjusted online with each step, rather than predicted, internalized, and then updated with time

(Kawato, Furukawa et al. 1987; Morton and Bastian 2006; Reisman, Wityk et al. 2007; Ogawa, Kawashima et al. 2014). Trailing leg work can be adjusted based on force sensory information collected and integrated during the preceding single limb stance phase of gait, so positive, propulsive work adaptation is controlled using a reactive strategy. These results are also consistent with previously published work showing that leading leg kinetics are adapted with a predictive strategy while trailing leg kinetic adaptation are reactively regulated (Cho, Thajchayapong et al. 2013; Ogawa, Kawashima et al. 2014; Thajchayapong, Cho et al. 2014).

5.4.2 Able-bodied Subjects Adjust Timing of Ankle Work Production

While leg-level work changed quickly at the onset of adaptation, trailing leg joint-level work demonstrated additional, more gradual adaptation patterns. Specifically, the timing of positive, propulsive ankle work production was evenly distributed between single support and double support gait phases in early adaptation, but was gradually shifted to occur more during double support over the course of adaptation (**Fig. 5.5A**). Delaying ankle work production may improve mechanical efficiency of walking. As intra-leg work distribution is shifted from hip to primarily ankle work production throughout adaptation (Oh, Baek et al. 2012; Cho, Thajchayapong et al. 2013; Park and Park 2013; Thajchayapong, Cho et al. 2014), the timing of ankle power production becomes more influential in economizing walking mechanics. Delaying the onset of ankle work production may indicate that able-bodied subjects change the mechanism used to generate ankle power over the course of adaptation. Specifically, representative subject data (**Fig. 5.8**) shows that delayed onset of ankle power production is

accompanied by a longer period of foot flat (ankle angle=0), which may indicate either Achilles tendon loading or more efficient muscle fascicle length function, either of which would result in more efficient power production and walking mechanics (Zajac, Neptune et al. 2002; Zajac, Neptune et al. 2003; Ishikawa, Komi et al. 2005; Neptune and Sasaki 2005; Cronin, Avela et al. 2013; Zelik, Huang et al. 2014).

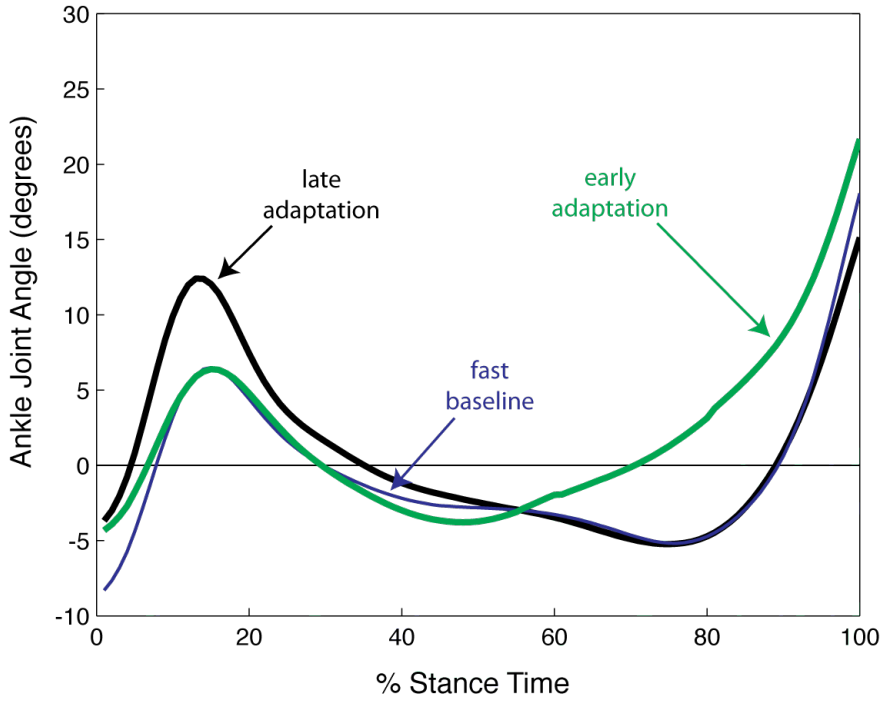

Figure 5.8: Representative able-bodied fast leg included ankle joint angle during stance at different stages in adaptation. Zero degrees is neutral ankle position determined from quiet standing in this individual. Positive values indicate plantar flexion, and negative values are dorsiflexion. Over the course of adaptation, from early (green) to late (black) adaptation, the ankle angle demonstrates a return to a fast baseline (blue) pattern, with longer foot flat (later initiation of plantar-flexion movement).

5.4.3 Able-bodied Knee Work Follows Ankle Work During Power Production

Previous work demonstrated that ankle-knee covariation during peak power production allows for more robust leg force application during steady-state walking (Chapter 3). Such robust leg force control likely also enables resilient responses to unexpected gait perturbations and could presumably aid adaptation to walking in a novel environment. The able-bodied subjects demonstrated a clear linear relationship between

ankle and knee power during double support when leg power is generated. Total knee work transitions from absorbing (negative) to producing (positive) work as the magnitude of ankle work produced during double support increases (**Fig. 5.7A**). While counterintuitive, simultaneously increasing knee and ankle work can result in more consistent leg power as the knee redirects, rather than absorbs, ankle work to affect center-of-mass dynamics and leg power production more efficiently. Utilizing covariance between the ankle and knee joint may facilitate motor learning by expanding the possible leg force equivalent joint torque combinations and enabling action exploration. Such exploitation of inter-joint coordination has been observed in throwing actions (Muller and Sternad 2004; Yang and Scholz 2005; Yang, Scholz et al. 2007; Muller and Sternad 2009; Cohen and Sternad 2012; Abe and Sternad 2013), pointing tasks (Domkin, Laczko et al. 2002; Domkin, Laczko et al. 2005; Yang, Scholz et al. 2007), and reaching behaviors (Wu, Miyamoto et al. 2014), and may also be present in locomotor adaptation.

5.4.4 Subjects with an Amputation Adapt Predictive Mechanisms but have Limited Reactive Adaptation in their Amputated Leg

Leading leg work in both the amputated and sound legs of subjects with an amputation demonstrated characteristic predictive adaptation patterns (**Fig. 5.3C&E**). Similarly to the slow legs of able-bodied subjects, aftereffects in neither the amputated (fast) or sound (slow) legs reached significant differences from baseline, but both trended towards displaying negative aftereffects. Since we cropped out portions of the adaptation trial due to handrail holding (see Methods), we may have eliminated significant post-adaptation baseline differences. The absence of significant negative aftereffects does not

disprove the presence of predictive regulation, but rather indicates that significant de-adaptation may have occurred before the handrail was released. That able-bodied subjects also demonstrated trends rather than significant negative aftereffects in fast leg negative work error suggests that holding the handrail may have obscured some adaptation patterns and should be avoided in future work. Despite this limitation, lack of distal sensory feedback and motor control does not seem to affect predictive adaptation mechanisms in either the sound or amputated legs of subjects with an amputation. The presence of predictive adaptation patterns in subjects with an amputation is likely due to the fact that our participants were otherwise healthy individuals with no known neurological damage. As a result, they were able to maintain adaptation patterns that were controlled by their intact central nervous system (Morton and Bastian 2006; Jayaram, Tang et al. 2012). These subjects with an amputation likely updated some internal representation of braking leg dynamics with sensory feedback from the hip or other more proximal structures not affected by transtibial amputation (Ogawa, Kawashima et al. 2014)).

Subjects with an amputation demonstrated asymmetric adaptation patterns for trailing leg propulsive work in their sound and amputated legs. Sound legs demonstrated very similar reactive adaptation patterns as the slow legs of able-bodied subjects. Sound leg positive work error initially deviated from baseline in early adaptation and demonstrated a persistent aftereffect in early post-adaptation. Amputated legs, however, showed no significant changes ($p>0.05$) in response to the experimental, split belt treadmill perturbation. The amputated leg positive work demonstrated a qualitative trend to be smaller than fast baseline values (negative error), which may indicate that subjects

with an amputation partially adjusted amputated leg positive work to desired values but our small sample size obscured these results. However, additional evidence from comparisons with able-bodied adaptation patterns suggest that the amputated leg has limited ability to reactively adapt trailing leg propulsive work.

Subjects with an amputation demonstrate significant asymmetry between simultaneous sound leg negative work and amputated leg positive work errors (**Fig. 5.3B**) that is not present in able-bodied subjects (**Fig. 5.2B**). Sound leg negative work error initially deviates from baseline in early adaptation and rises throughout adaptation (**Fig. 5.3E**), reducing the asymmetry between the amputated leg propulsive work and sound leg braking work over the course of adaptation. The sound leg appears to predictively update its negative work to reduce that asymmetry, while the amputated leg does not change. The amputated leg does not deviate from baseline as much as the sound leg in early adaptation either because it: (i) lacks the sensory feedback and/or motor control necessary to adapt at all or (ii) has become highly sensitive to changes due to its deficit and adapts much more rapidly than the sound leg. However, subjects with an amputation not only lack sufficient sensory feedback but are also are capable of changing leg work output. Subjects with an amputation were able to adjust amputated leg positive work output between the slow and fast baseline trials. It therefore appears that subjects with an amputation are capable of making necessary leg work changes, but are unable to sense that a change must be made. Subjects with an amputation appear to accommodate this deficit by instead altering sound leg work. The sensory loss associated with transtibial amputation, therefore, appears to substantially limit the ability of these subjects to adapt using online, reactive strategies.

5.4.5 Subjects with an Amputation Adapt Primarily Using their Sound Leg

Subjects with an amputation appear to rely on adjusting sound leg work production to compensate for lack of amputated leg propulsive work adaptation. The sound leg changes single support work production in a pattern consistent with reactive adaptation (**Fig. 5.4C**). Reactive adaptation was also seen in slow leg single support work of able-bodied subjects (**Fig. 5.4A&D**) and has been observed in vertical ground reaction forces (Mawase, Haizler et al. 2013). However, single support work production was symmetric in able-bodied subjects, but remained asymmetric in subjects with an amputation throughout adaptation (**Fig. 5.4A&B**). Single support work of the sound leg in subjects with an amputation was significantly larger ($p<0.025$) than the amputated leg, suggesting that subjects with an amputation were accelerating during single support with each step, possibly to compensate for insufficient propulsive work of the amputated leg in the previous step (Houdijk, Pollmann et al. 2009; Oh, Baek et al. 2012; Park and Park 2013). It may be possible that sound leg single support work adapts reactively to compensate for the lack of reactive adaptation in the amputated leg's propulsive work. Such asymmetric work production during single support, likely overtaxes sound leg hip power production and could lead to future overuse injuries in their contralateral leg as a result of long term prosthetic use.

5.4.6 Subjects with an Amputation Lack Substantial Joint Level Adaptation

Positive prosthetic ankle work production occurred primarily during double support in all test conditions (**Fig. 5.5B**). Prosthetic ankles demonstrated some positive

work during single support and adaptation trials, but magnitudes never reached those produced during double support. This pattern of work production is likely a physical limitation of the prosthetic device. Due to its design, the prosthetic foot-ankle mechanism must be deflected during loading in single support in order to recoil and provide propulsive work in double support. As such, positive ankle work appears to be relegated to double support phase only.

Knee work production in the amputated leg demonstrated variability independent of work done by the prosthetic ankle (**Fig. 5.7B**), suggesting that knee work in the amputated leg is controlled independently of prosthetic ankle work. Control of the amputated leg knee work, therefore, appears to be decoupled from prosthetic ankle work during adaptation. Ankle-knee decoupling may lead to less robust adaptation and perturbation responses, which could help explain why individuals with amputations are more prone to falls and have poorer obstacle avoidance performance during walking than comparable able-bodied subjects (Miller, Deathe et al. 2001; Miller, Speechley et al. 2001; Curtze, Hof et al. 2010; Curtze, Hof et al. 2012; Houdijk, van Ooijen et al. 2012). Independent control of knee work in the amputated leg may serve to achieve some other goal during walking of individuals with an amputation, but focused investigation of this possibility is required before such a conclusion can be determined.

5.4.7 Functional Implications of Amputation on Adaptive Walking Ability

The work presented here demonstrates a functional implication of distal sensori-motor loss due to amputation. The lack of distal sensory feedback, ankle motor control, and inter-joint coordination associated with amputation substantially affects the nervous

system and appears to limit the ability of these individuals to reactively adapt to novel environmental conditions, consistent with previous evidence suggesting that reactive adaptation is primarily regulated by feedback mechanisms (Nielsen and Sinkjaer 2002; Lam, Anderschitz et al. 2006; Morton and Bastian 2006; Smith, Ghazizadeh et al. 2006; Choi, Vining et al. 2009; Hohne, Stark et al. 2011; Jayaram, Tang et al. 2012). Furthermore, ankle-knee covariation appears to contribute to robust adaptation possibly by enabling action exploration in able-bodied individuals. Loss of this inter-joint coordination in subjects with an amputation likely makes responding to environmental challenges more difficult because they have less robust leg level control. Limited reactive adaptation and robust leg control make it more difficult for these individuals to sense and respond to external perturbations and may help explain why individuals with amputations are more prone to falls (Miller, Deathe et al. 2001; Miller, Speechley et al. 2001; Curtze, Hof et al. 2010; Curtze, Hof et al. 2012). Individuals with an amputation instead appear to rely on flexible adaptation of their sound leg to make corrective adjustments to environmental perturbations, putting them more at risk for overuse injuries on their sound side. Rehabilitation protocols may, therefore, benefit by incorporating extensive fall and injury prevention training for individuals with amputations.

Restoring or enhancing sensory feedback may help improve adaptive ability and perturbation response in individuals with amputations or other sensori-motor deficits, such as seen in peripheral neuropathy. Amputation removes globular skin on the plantar foot surface, eliminating a surface rich in sensory receptors. Individuals with lower-limb amputations may be able to distinguish and integrate feedback from their residual limb's interaction with their prosthesis via the socket. Indirect sensory information provided via

the socket interface could potentially be used to inform and enhance feedback regulated adaptation and perturbation responses. However, sensory receptors in the residual limb may not be sensitive enough to discriminate meaningful sensory feedback. Applying vibratory stimulus beneath the prosthetic foot improves postural stability, presumably by enhancing sensory feedback from the prosthetic foot's interaction with the ground (Rusaw, Hagberg et al. 2012). Enhancement of residual limb sensory feedback using vibration either beneath the foot or at the socket interface could potentially increase detectable sensory feedback, improve reactive adaptation, and reduce the risk of falls in this population.

Holding of the safety handrail in early adaptation and post-adaptation obscured some of our results. Handrail holding was necessary for safety, especially for the walkers with an amputation, with sudden introduction of split belt environment. This challenge and safety concern could be eliminated or minimized by gradually introducing participants to the split belt environment. Gradual introduction is less demanding on cognitive control and mediolateral balance regulation while preserving motor learning patterns (Sawers and Hahn 2013; Sawers, Kelly et al. 2013; Sawers, Kelly et al. 2013). Gradual introduction could therefore provide a viable methodology for obtaining more reliable data early in the adaptation and post-adaptation trial periods. This type of intervention could also be used to investigate responses in more impaired populations, like individuals with above-knee amputations and less mobile individuals in general. Ultimately gradual introduction of split-belt treadmill training is a safer and more feasible rehabilitation intervention and deserves further development for future implementation.

5.5 Conclusion

We studied locomotor adaptation of able and impaired individuals walking on a split-belt treadmill. Negative work done by the leading leg during step-to-step transitions is adapted predictively. Work generated by the leading leg is anticipated and slowly updated with each step, showing clear adaptation patterns in both able-bodied walkers and walkers with an amputation. Trailing leg positive work, however, is reactively adapted. Changes to the propulsive work are made online during each step, changing rapidly when presented with the novel split-belt walking environment. Loss of active ankle motor control and distal sensory feedback due to transtibial amputation limits reactive adaptation. Individuals with an amputation instead make corrective responses with their contra-lateral sound legs. The exact mechanism responsible for inhibiting reactive responses remains unclear, but is likely related to reduced sensory feedback.

Loss of sensory feedback and motor control also appears to obstruct inter-joint coordination. Ankle and knee work profiles adapt together in able-bodied individuals, and are likely enabled by previously observed ankle-knee covariation (Chapter 3). The robust leg control facilitated by ankle-knee covariation and inherent motor abundance may enable action exploration for able-bodied individuals to seek more economic walking mechanics. This pattern of coupled ankle-knee responses is not present in amputated legs and indicates less robust walking mechanics in these individuals.

Individuals with an amputation appear less able to robustly respond to environmental perturbations, possibly explaining why individuals with amputations are more prone to falls. Rehabilitation protocols could potentially be improved with more focused practice of inter-joint coordination, reactive response to unexpected

perturbations, and sound leg injury prevention. Ultimately, this work is the first to investigate the evolution of short-term adaptation of subjects with an amputation in response to split-belt treadmill walking. Future work may explore possible rehabilitation strategies to enhance reactive motor learning in individuals with amputations, possibly through implementation of gradual split-belt treadmill training, and could attempt to isolate the effect of sensory feedback on short-term adaptation in split-belt treadmill walking.

CHAPTER 6

CONCLUSIONS

Human locomotion is a complex task that is achieved through coordinated efforts at various levels of the neuromuscular control hierarchy. This control schema enables able-bodied humans to robustly respond to small perturbations during steady-state walking and successfully respond to large disturbances when confronted with novel walking environments. This ability to flexibly adapt to changing or unpredictable environmental demands may be impaired by morphological constraints, such as amputation. Identifying controlled task variables in able and impaired locomotion could inform gait rehabilitation strategies by providing specific variables for monitoring and focused improvement. Furthermore, quantifying differences in able and impaired adaptation patterns may inform expectations for the rate or pattern of progression throughout gait rehabilitation. The main purpose of my dissertation was to identify kinetic locomotor control strategies present in able human walking, understand how these control strategies are altered when the locomotor system is constrained by an amputation, and measure how able and impaired populations may alter these kinetics differently when perturbed by a novel walking environment. The major results and possible implications of these experimental studies are summarized below.

6.1 Major Findings

6.1.1 Hierarchical Task Goals in Able-bodied Walking

The first aim of my dissertation was to identify hierarchical task goals that likely contribute to robust human locomotion. Dynamic walking principles suggest that mechanically efficient step-to-step transitions are essential for economic bipedal walking and that targeted control of particular influential variables during these transitions could enable stereotypical walking mechanics (Kuo 2002; Donelan, Kram et al. 2002a; Donelan, Kram et al. 2002b; Kuo, Donelan et al. 2005; Ruina, Bertram et al. 2005; Kuo 2007; Collins 2008; Collins and Kuo 2010). Specifically, consistent net vertical force trajectories and trailing leg power production during these transitions contribute to continuous and mechanically efficient step-to-step transitions. I applied an uncontrolled manifold analysis to specifically test how lower level elemental variable coordination contributed to the consistency of these variables. In Chapter 2 (Toney and Chang 2013), I discovered that individual leg forces combine to generate consistent net vertical force trajectories over many steps. In Chapter 3, I found that force along the trailing leg was modulated with each step to make step-to-step corrections that maintain consistent peak trailing leg power. I also observed that variable ankle torque timing is the primary driver for leg force modulation, while knee torques covary with the ankle to refine the effect of ankle torque timing variability on leg force application and ultimately center of mass dynamics.

6.1.2. Effect of Amputation on Motor Control

The second aim of my dissertation was to determine how the locomotor control mechanisms identified in able-bodied walking (Chapters 2 and 3) change in response to the morphological constraint of amputation. Transtibial amputation effectively removes direct ankle motor control and disrupts much of the sensory feedback available to intact human walkers. Transtibal amputation, therefore, effectively constrains the locomotor system by removing active control of and sensory feedback from a single degree-of-freedom. In Chapter 4, I applied the uncontrolled manifold analysis to data collected from steady state walking of individuals with an amputation to test how this morphological constraint affects locomotor control. I discovered that replacing active ankle function with a passive prosthetic device does not affect center-of-mass or leg level dynamics. Subjects with an amputation were still able to stabilize vertical net force trajectories and produce consistent, albeit reduced, peak trailing leg power. Transtibial amputation did not appear to affect the ability of these subjects to modulate trailing leg force, suggesting that the ankle mechanism used in able-bodied individuals is a mostly passive mechanism. However, the ankle-knee covariation observed in able-bodied walkers was absent in the subjects with a transtibial amputation. This finding suggests that the elimination of active joint torque control and distal sensory feedback due to amputation disrupts inter-joint coordination, a deficit that is not apparently recovered in experienced walkers with amputations. The absence of ankle-knee coupling may result in less robust walking mechanics in amputees and may explain why such individuals are more prone to falls and why they often rely on their contralateral sound leg to respond to postural and environmental perturbations (Miller, Deathe et al. 2001; Miller, Speechley et al. 2001;

Vrieling, van Keeken et al. 2007; Curtze, Hof et al. 2010; Curtze, Hof et al. 2012; Nederhand, Van Asseldonk et al. 2012).

Observations from walking of individuals with an amputation speak to the importance of passive, biomechanical structures to stereotypical walking dynamics, but the limitations of these subjects show the importance of neural contributions to robust and adaptable walking behavior. Subjects with an amputation used a passive device to generate similar walking mechanics as well as motor control patterns of center-of-mass and leg-level variables as able-bodied subjects, which suggests that passive, biomechanical control mechanisms are sufficient to generate stereotypical walking mechanics, independent of active, neural control. The lack of active ankle neural control due to amputation, however, impedes the ability of these subjects to robustly respond to a novel environment, suggesting that neural control mechanisms are needed for active responses to unexpected perturbations. These potential different contributions of neural and biomechanical motor control to human walking are also evident in the performance of passive dynamic walking robots. These robots can reproduce stereotypical walking patterns without any kind of controller, but they are highly unstable and especially sensitive to initial conditions (McGeer 1990; Garcia, Chatterjee et al. 1998; Garcia, Chatterjee et al. 2000). Neural control mechanisms, therefore, appear to provide supplementary control that enables adaptive responses to novel environments or unexpected perturbations. Biomechanical mechanisms therefore provide the foundation for bipedal walking, while neural processes provide additional control that enables more robust and flexible bipedal walking.

6.1.3 Motor Control Adaptation to Split-belt Treadmill Walking

The third aim of this dissertation work was to compare short-term adaptation strategies utilized by able and impaired walkers. I was able to measure short-term adaptation in walking by employing a split-belt treadmill intervention in which one leg steps at twice the speed of the other (Chapter 5). This intervention presents a novel environment that sufficiently perturbs walking mechanics while preserving the basic characteristics of bipedal walking. Previous work has demonstrated that able-bodied individuals adapt to the split belt treadmill paradigm by changing some variables very rapidly (reactive adaptation) and other variables more slowly and with persistent negative aftereffects (predictive adaptation) (Kawato, Furukawa et al. 1987; Lam, Anderschitz et al. 2006; Morton and Bastian 2006; Smith, Ghazizadeh et al. 2006; Reisman, Wityk et al. 2007; Izawa, Rane et al. 2008; Choi, Vining et al. 2009; Ogawa, Kawashima et al. 2014). Predictive adaptation is indicative of motor control in which an internal representation of that variable's action is gradually updated with each step and requires intact cerebellar function (Lam, Anderschitz et al. 2006; Morton and Bastian 2006; Smith, Ghazizadeh et al. 2006; Jayaram, Tang et al. 2012). Reactive mechanisms rely more on distal feedback and independent reflex pathways that update actions online, almost immediately upon introduction of the perturbation (Nielsen and Sinkjaer 2002; Morton and Bastian 2006; Reisman, Wityk et al. 2007; Choi, Vining et al. 2009; Ogawa, Kawashima et al. 2014). I discovered that, similarly to braking and propulsive anterior-posterior forces (Ogawa, Kawashima et al. 2014), leading leg negative work error was adapted in a predictive manner, while trailing leg positive work error demonstrated more reactive control in able-bodied individuals.

Evaluation of joint work profiles revealed a trend for intact individuals to adopt more efficient walking mechanics over the course of adaptation exposure. While trailing leg work adaptation was rapid, evolution of more mechanically efficient ankle work timing was slow and is consistent with the idea that more gradual adaptation occurs in an effort to seek more economical solutions to the presented environment (Huang, Kram et al. 2012; Cho, Thajchayapong et al. 2013; Finley, Bastian et al. 2013; Thajchayapong, Cho et al. 2014). Later onset and production of ankle work within the gait cycle suggests that able-bodied humans adapt their ankle work and power timing to take advantage of more economic ankle power production strategies, utilizing either Achilles tendon energy storage and return (Ishikawa, Komi et al. 2005; Cronin, Avela et al. 2013; Zelik, Huang et al. 2014); Chapter 3) or more efficient muscle fascicle lengths (Zajac, Neptune et al. 2002; Zajac, Neptune et al. 2003; Neptune and Sasaki 2005). Adopting such a mechanism for power generation may lead to more mechanically efficient walking mechanics that rely on mostly passive mechanisms (Zelik, Huang et al. 2014).

I also observed that ankle and knee work appeared to adapt together over the course of adaptation to split belt treadmill walking (Chapter 5, **Fig. 5.7**). Coupled adaptation of ankle and knee work magnitudes suggests that the ankle-knee covariation observed in steady state walking (Chapter 3, **Fig. 3.8**) persists in perturbed environments and may contribute to maintaining robust adaptation responses. Multiple studies have demonstrated that humans can exploit the structure of underlying elemental variability to explore task space and adapt to improve performance (Domkin, Laczko et al. 2002; Muller and Sternad 2004; Domkin, Laczko et al. 2005; Yang and Scholz 2005; Hu and Sternad 2007; Yang, Scholz et al. 2007; Muller and Sternad 2009; Cohen and Sternad

2012; Abe and Sternad 2013; Wu, Miyamoto et al. 2014). Covariance of knee and ankle torques may enable able-bodied walkers to attempt various ankle torque timing strategies while mitigating the possibility of task failure (tripping or falling) through coupled, stabilizing knee action. While the underlying neural and/or mechanical physiological mechanism regulating ankle-knee coupling remains uncertain (Nichols 1999; Wilmink and Nichols 2003; Stahl and Nichols 2011), ankle-knee joint torque coupling appears to play a functional role in locomotor adaptation.

6.1.4 Lack of Sensory Feedback and Ankle Motor Control due to Amputation Limits Adaptation Ability

In Chapter 5, I also presented results from the adaptation of subjects with a transtibial amputation to walking on the split belt treadmill. Subjects with an amputation lack the sensory feedback, active ankle motor control, and ankle-knee covariance (Chapter 4) that able-bodied subjects use to adapt to walking on the split belt treadmill. As such, I expected walkers with an amputation to demonstrate different adaptation patterns than those observed in the able-bodied control subjects. Leg work adaptation patterns suggest that subjects with an amputation have a limited ability to adapt reactive, feedback regulated parameters of their amputated leg and that inter-joint ankle-knee covariation was absent. Reactive feedback mechanisms are regulated through online corrections mediated by distal reflex pathways (Nielsen and Sinkjaer 2002; Lam, Anderschitz et al. 2006; Morton and Bastian 2006; Smith, Ghazizadeh et al. 2006; Choi, Vining et al. 2009; Hohne, Stark et al. 2011; Jayaram, Tang et al. 2012). Disruption or

complete removal of these pathways due to amputation appears to limit the adaptability of these parameters even in experienced walkers with an amputation.

Rather than modifying central organization and utilizing a more predictive control mechanism, experienced subjects with an amputation appear to shift control up the hierarchy and make adaptive changes with the contra-lateral sound leg. A similar pattern has been observed in balance or postural perturbation and recovery in this population (Vrieling, van Keeken et al. 2007; Curtze, Hof et al. 2012; Nederhand, Van Asseldonk et al. 2012). Reorganizing motor control in this way, likely limits the bilateral motor redundancy in individuals with amputations since the amputated leg is no longer as easily modifiable as in able-bodied subjects. This likely affects whole body stabilization ability, and may explain why individuals with amputations fall more often and demonstrate asymmetric balance recovery strategies (Miller, Deathe et al. 2001; Miller, Speechley et al. 2001; Vrieling, van Keeken et al. 2007; Curtze, Hof et al. 2010; Curtze, Hof et al. 2012; Nederhand, Van Asseldonk et al. 2012).

6.2 Implications for Rehabilitation and Gait Training

My analysis of able-bodied walking has identified implicit gait goals and controlled variables that are important for achieving steady-state walking mechanics typical of an intact population (Chapters 2 and 3). Specifically, controlled ankle torque production and coupled ankle-knee function are important for sufficiently powered and robust locomotion. Ensuring adequate knee strength and implementing training tools to encourage coordinating knee angle (as an observable correlate for knee torque) with ankle function could help patients with amputations achieve walking patterns more robust

to unexpected perturbations. Results from Chapters 3 and 5 also suggest that walking economy may be improved by utilizing passive physiological structures. Impaired individuals often walk with greater metabolic and mechanical cost so enhancing or improving utilization of passive structures, such as a prosthetic foot, could reduce the metabolic cost of walking. Overall, these results demonstrate that functional improvements may not be solely relegated to increasing strength of individual muscles or joints but that improving inter-joint coordination within a leg can aid robust walking mechanics and may reduce fall risk.

Differences in adaptation patterns between subjects with an amputation and able-bodied subjects revealed from split-belt walking in Chapter 5 suggest that individuals with amputations may require more intensive training regimens to effectively alter walking mechanics even after they appear subjectively similar to able-bodied individuals. It is also especially important to train these individuals to walk on unusual or unpredictable surfaces to better mimic what they may encounter in daily living. More practice adapting to different walking conditions may enhance reactive adaptation capabilities and reduce fall risk. Additionally, individuals with an amputation seem to adapt primarily using their sound leg, putting them more at risk for overuse injuries. It may therefore be beneficial to provide preventative therapy to individuals with new amputations to prevent injury on their intact side. Work in stroke patients has demonstrated the potential for split-belt treadmill walking to provide therapy to reduce asymmetries in walking mechanics. Such an intervention may be possible in individuals with amputations, especially since my data shows that they are capable of walking in the split-belt environment. Retention and transfer studies will be necessary before any

therapeutic intervention involving split-belt walking could be introduced into rehabilitation practice for individuals with amputations.

6.3 Future Studies and Limitations

6.3.1 Alternative Task Goals in Able and Impaired Locomotion

I focused my analysis of task goals specifically on the contribution of joint torques and leg forces to whole body kinetics. It is likely that other controlled variables and task goals contribute to the complex task of bipedal walking and deserve further investigation. For example, kinematic variables (joint angles, leg length, and leg orientation) contribute to consistency of hopping locomotion, specifically in aerial phase and at mid stance (Auyang, Yen et al. 2009; Auyang 2010; Auyang and Chang 2013). Controlled foot placement is important in precision stepping (Rosenblatt, Hurt et al. 2014), and may play an important role in regulating initial contact and swing phase in human walking.

Others have also suggested that whole body angular momentum regulation is the primary goal of continuous human walking (Herr and Popovic 2008; Robert, Bennett et al. 2009; Bennett, Russell et al. 2010; Gruben and Boehm 2012). In fact, Robert et. al. found that segmental angular momenta combined to stabilize whole body angular momentum during single leg stance and modulate whole body angular momentum during step-to-step transitions (2009). It is possible that controlling whole body angular momentum is a primary task goal of able-bodied walking and walking with an amputation (Silverman and Neptune 2011; Curtze, Hof et al. 2012), and the leg force and net force regulation I discovered contribute to this higher hierarchical task. This potential organization of the task hierarchy of walking deserves additional future analysis in both able-bodied and impaired human walking.

6.3.2 Limitation of Applying the Uncontrolled Manifold Analysis to a Population with an Amputation

My implementation and interpretation of the UCM analysis assumes that all included elemental variables are controlled either individually or coordinated together to contribute to whole leg function. Amputation, however, effectively removes active control of the ankle joint. I deliberately included the ankle joint torque in my UCM analysis of subjects with an amputation for consistency with previously published kinetic UCM analysis during locomotion (Yen, Auyang et al. 2009; Yen and Chang 2010; Yen 2011; Toney and Chang 2013). Additionally, because each of my recruited subjects wore an energy storage and return (ESAR) prosthetic device, they retain indirect control of prosthetic ankle output by controlling how the device is loaded preceding push off. The prosthetic ankle still effects leg force output, so including its contribution to whole leg force is consistent with the idea that all contributing variables should be considered when applying the UCM analysis.

Including the prosthetic ankle joint torque in this analysis, however, may not accurately represent the neuromechanical control contributing to leg force generation and efficient walking mechanics. Subjects with an amputation lack direct sensory feedback of the prosthetic foot's interaction with the ground. Contact between the residual limb and the socket may however provide indirect sensory information about the foot-ground interaction. It is therefore feasible that subjects with an amputation have learned to incorporate the force and/or moment at the residual limb-socket interface into their motor control schema. Control of socket kinetics has been observed during cycling of individuals with amputations (Childers, Prilutsky et al. 2014) and may also contribute to consistent walking mechanics of individuals with amputations. The UCM analysis could be used to evaluate how socket forces and moments contribute to end point force or to test whether socket kinetics are actually controlled goal variables during walking with an

amputation. Such a systematic investigation into motor control of individuals with amputations could lead to significant insight about how these individuals interact with their prosthetic device.

6.3.3 Use of Experienced Subjects with an Amputation

The subjects with an amputation that participated in this study were specifically recruited for being good, experienced walkers. Because this was the first time subjects with an amputation have been studied using a split-belt walking paradigm, I wanted to ensure that those subjects recruited could adequately complete the study. Over the course of rehabilitation, subjects with ampuations improve balance perturbation response, walking velocity, knee kinematics, and obstacle avoidance (Barnett, Vanicek et al. 2009; Barnett, Polman et al. 2013; Barnett, Vanicek et al. 2013), suggesting that early training can modify behavioral outcomes. It is possible that individuals with more acute injuries may demonstrate different, less robust motor control patterns or may be more sensitive to split-belt treadmill intervention than those individuals with a longer time since amputation. Amputation causes lasting changes in cortical representations of the amputated limb (Elbert and Rockstroh 2004), which may partially explain why these individuals did not demonstrate predictive control of their amputated leg work. Individuals with more acute injuries may have residual amputated leg cortical representation that could be exploited for training to predictively control amputated leg kinetics. Also, more acute individuals may not have blunted their distal feedback yet and may be able to alter their reactive mechanisms more readily than individuals with more chronic amputations. Overall, individuals with more acute amputations may retain more readily plastic neural mechanisms that could prove beneficial for rehabilitation training, especially if the intervention is introduced soon after the initial surgery. A longitudinal study specifically investigating kinetic motor control and leg work production would be necessary to fully characterize this possibility.

Despite their advanced walking ability, three out of four subjects were unable to complete the split belt paradigm with their amputated leg on the slow belt. This limitation is likely because of the extended stance time of the slow leg. Subjects with an amputation typically adopt asymmetric stance times in steady state walking where they spend more time on their sound than on their amputated leg, likely because they lack substantial medio-lateral stability on their amputated side to remain in single limb stance for an extended duration. Unfortunately, this limited the scope of my split belt intervention as I was only able to collect and analyze data in which the subjects with an amputation walked with their amputated leg on the fast belt. While this limited set of data yielded interesting and informative results, it is possible that the mirrored leg orientation could yield additional insights. Such an experiment could be accomplished by increasing the mean treadmill speed but maintaining an asymmetric speed ratio (i.e. 1:1.5 speed ration in which the slow belt is fast enough to not to elicit uncomfortable mechanics/stance times/responses). This challenge could also be mitigated by gradual introduction of the split belt condition (Sawers and Hahn 2012; Sawers 2012; Sawers and Hahn 2013; Sawers, Kelly et al. 2013).

6.3.4 Gradual vs. Sudden Split-belt Treadmill Introduction

Like many training paradigms, split-belt treadmill walking can be introduced suddenly or gradually. Sudden introduction, which I utilized in Chapter 5, elicits large initial errors and allowed me to study how walkers respond to an unexpected perturbation. However, safety concerns required that subjects hold a handrail for the first 30 seconds of the sudden perturbation, which obscured some of the adaptation patterns. Gradual introduction reduces the postural stability challenge of treadmill walking and could eliminate the necessity for handrail holding (Sawers 2012; Sawers and Hahn 2013; Sawers, Kelly et al. 2013; Sawers, Kelly et al. 2013). If the time course of adaptation changes can be observed in gradual introduction, gradual training could enable better

characterization of initial adaptation without the handrail holding complication. Gradual introduction may also be more feasible for implementation in a rehabilitation setting because it may enable less skilled (or otherwise impaired) walkers to attempt this intervention. Gradual introduction of split belt treadmill walking also improved retention and transfer, making it a more desirable rehabilitation training tool for long-term rehabilitation objectives.

6.3.5 Prosthetic Design

All participants with an amputation in this research wore ESAR prosthetic feet. These devices store and return some energy, though their power production is smaller than the ankle power produced by intact individuals (Winter and Sienko 1988; Hermodsson, Ekdahl et al. 1994; Sanderson and Martin 1997; Zmitrewicz, Neptune et al. 2006; Su, Gard et al. 2007; Kovac, Medved et al. 2009; Ventura, Klute et al. 2011; Ferris, Aldridge et al. 2012). The results from Chapters 4 and 5 suggest that using a passive device to replace ankle function does not disrupt leg-level function in steady state walking, but eliminates the ankle-knee covariation important for robust walking mechanics in steady-state and split-belt walking. Systematic prosthetic design and testing is limited, rarely considering more than the aesthetic characteristics of an individuals' gait. Recent academic work has begun to characterize the possible improvements associated with powered ankle mechanisms (Ferris, Aldridge et al. 2012; Grabowski and D'andrea 2013), device weight (Selles, Bussmann et al. 1999; Selles, Korteland et al. 2003; Grabowski and D'andrea 2013; Smith and Martin 2013), and ankle energetic return characteristics (Zmitrewicz, Neptune et al. 2006; Ventura, Klute et al. 2011; Zelik, Collins et al. 2011; Fey, Klute et al. 2013; Major, Twiste et al. 2014). However, few if any of these investigations consider facilitating inter-joint coordination with the device itself or through targeted training. While changes in knee power and torque magnitude have been seen in response to powered prostheses use (Ferris, Aldridge et al. 2012;

Grabowski and D'andrea 2013), no consideration has been given to the relationship between ankle and knee torque timing coordination, which appears important for achieving robust walking mechanics and enabling more stable/robust locomotor adaptation. Subjects with amputations are able to learn specific EMG firing patterns in their residual tibialis anterior (Alcaide-Aguirre, Morgenroth et al. 2013), suggesting that advanced design could exploit residual and possibly non-functional lower limb musculature. Advanced prosthetic design could consider physically coupling knee function to powered ankle timing, or possibly adjusting timing of ankle power application in response to knee behavior, allowing individuals with amputations to drive and control powered ankle force generation through knee action. The possibility of coupling knee and ankle action is especially relevant after above knee amputations when simultaneous knee and ankle control is necessary. Inter-joint coordination should be carefully developed in possible future implementation of powered ankle and microprocessor knees for individuals with above-knee amputations.

6.3.5 Enhancing Sensory Feedback to Affect Locomotor Adaptation

The results from locomotor adaptation of individuals with an amputation suggests but does not prove that extinguishing sensory feedback impairs reactive adaptation mechanisms. Truly testing the effect of distal feedback sensors on locomotor adaptation, rather than combined with the effects of distal motor control, requires specific elimination of sensory feedback in able-bodied controls. Hohne et. al. observed that able-bodied individuals with reduced plantar surface cutaneous sensation after injection of an anaesthetic solution demonstrated increased margins of stability and base of support in response to an unexpected gait perturbation (2011). Another study reduced skin temperature and found greater variability in step parameters (Sawa, Doi et al. 2013). Together, these two studies suggest that cutaneous feedback contributes to locomotor stability and step-to-step variability. Applying a UCM analysis to evaluate inter-joint

variance structure in able-bodied subjects with muted cutaneous feedback would specifically identify how function joint torque organization may incorporate cutaneous feedback information from distal end effectors.

As discussed above (Section 6.3.2), individuals with amputations maintain indirect sensory feedback from the ground via the residual limb-socket interface. Loss of glabrous skin mechanoreceptors with amputation, however, diminishes their sensitivity to external stimuli. Individuals with amputations may be able to improve reactive adaptation if sensory feedback from the residual limb were enhanced. Vibratory stimulus beneath prosthetic feet can improve postural response (Rusaw, Hagberg et al. 2012). Future prosthetic design could potentially incorporate intra-socket vibration to amplify distal sensory feedback and improve motor control. Implementation of feedback enhancement early in rehabilitation may be critical to maintain central representation of the affected leg and promote integration of the artificial prosthetic device into the predictive motor control system.

6.4 Final Thoughts

This dissertation work focused on quantifying differences in motor control patterns of able-bodied walkers and walkers with an amputation. While the results presented identified some ways that walkers with amputations differ from able-bodied individuals, much more work is necessary in order to more fully understand the effects amputation and prosthetic device use have on an individual. Amputation is a highly traumatic assault on the human body. Significant advancements have been made on the cutting edge of prosthetic design, but few of these hyper-advanced devices are used daily. There still exists a chasm between technological development and patient delivery. Some of this separation results from our poor understanding of how individuals with amputations control, interact, and learn with their device. I hope that future work will

consider the wearer as well as the technology in an effort to promote symbiotic relationships between individuals with amputations and the devices they depend on.

APPENDIX A

DETAILS OF THE UNCONTROLLED MANIFOLD CALCULATIONS

The human body often has many more degrees-of-freedom than strictly necessary to execute a desired task. For example, there are many possible joint-torque combinations, but only a relatively small subset results in a particular leg-force generated against the ground. The uncontrolled manifold describes this subset of elemental joint-torques that produce the same leg-force. Motor control of this leg-force requires coordination of the multitude of options this motor abundance provides, where successful performance is achieved through the selective stabilization of variables critical for task success, i.e., goal variables. The uncontrolled manifold (UCM) analysis statistically evaluates the variance across repeated movements to identify patterns of elemental variable combinations that determine the consistency of goal variable execution. For example, leg-forces combining to stabilize net-force will exhibit a non-random structure to their variance over many step cycles. Similarly, joint-torque combinations acting to stabilize leg-force would also exhibit non-random variance structure. In this way, the uncontrolled manifold analysis provides insight into the neuromechanical control of these locomotor movements.

Specifically, the UCM approach quantifies the alignment of variance in elemental variables with the variability in goal variable execution. The formal analysis relies on the derivation of a Jacobian describing how small deviations in local-variables affect the hypothesized task-level goal variable. Elemental variance that lies along the null space of

this Jacobian is considered goal-equivalent (GEV) because these small deviations have zero effect on the goal variable. All remaining elemental variance orthogonal to the null space has a detrimental effect on goal variable execution and is thus termed non goal-equivalent variance (NGEV). By comparing the relative amounts of each variance type, we can quantify whether elemental variance is organized to result in stable, consistent or inconsistent goal variable execution.

A1.1 Inter-leg (2DOF) stabilization of vertical net-forces

As an example, let us examine the formal analysis of how vertical leg-force (F_v^{leg}) variance structure contributes to stable net vertical force (F_v^{net}) generation. The proposed manifold for inter-leg coordination linearly sums the individual leg-forces to equal the net-force acting on the whole body (Eq. A1.1), resulting in a 1x2 Jacobian (Eq. A1.2):

$$F_v^{lead} + F_v^{trail} = F_v^{net} \qquad \textbf{(Eq. A1.1)}$$

The Jacobian matrix (J) contains the partial derivatives of the mathematical relationship relating the elemental variables (F_v^{lead} and F_v^{trail}) to the goal variable (F_v^{leg}):

$$J = \begin{bmatrix} 1 & 1 \end{bmatrix} \qquad \textbf{(Eq. A1.2)}$$

The Jacobian quantifies how small changes in elemental variables affect the goal variable. Because walking is a well-practiced and repetitive behavior, average leg-force trajectory ($F_v^{lead}+F_v^{trail}$) captures desired combinations of elemental leg-forces to generate the appropriate net force. The null space ($\vec{\varepsilon}$) of J relative to the mean leg-force trajectory ($\vec{\Theta}^0$) describes the goal-equivalent manifold (linearized UCM) in which a small leg-force deviation has no effect on F_v^{net} (Eq. A1.3):

$$0 = J\left(\vec{\Theta}^0\right)\cdot \vec{\varepsilon} \quad \textbf{(Eq. A1.3)}$$

We next decompose the leg-force residual differences from mean behavior ($\vec{X}^0$) into components parallel (Eq. A1.4) and orthogonal (Eq. A1.5) to this manifold at each time point in the gait cycle:

$$\vec{X}_{\parallel} = \sum_{i=1}^{n} \vec{\varepsilon}_i \cdot \left(\vec{X} - \vec{X}^0\right) \quad \textbf{(Eq. A1.4)}$$

$$\vec{X}_{\perp} = \left(\vec{X} - \vec{X}^0\right) - \vec{X}_{\parallel} \quad \textbf{(Eq. A1.5)}$$

Thus, total variance per degree of freedom within the linearized manifold is estimated as Goal Equivalent (GEV, Eq. A1.6) and the normalized variance outside of this manifold is estimated as Non-Goal Equivalent Variance (NGEV, Eq. A1.7), where n is the number of local variables (or local degrees-of-freedom) and d are the global degrees of freedom:

$$GEV = \frac{\sum X_{\parallel}^2}{(n-d)\cdot N_{steps}} \quad \textbf{(Eq. A1.6)}$$

$$NGEV = \frac{\sum X_{\perp}^2}{d\cdot N_{steps}} \quad \textbf{(Eq. A1.7)}$$

Alternatively, we can more efficiently calculate GEV and NGEV directly from the Jacobian (J) and Covariance matrix (C) as shown in Equations 8-9. The covariance matrix characterizes all elemental variance at a particular time point in the gait cycle. The diagonal components of C represent each leg force's individual variance independent of the contralateral leg force. Examining the trace of C captures total elemental variance

(TOTV) without requiring iterative comparison of each point to the mean leg force trajectory:

$$GEV = \frac{trace(null(J)^T \cdot C \cdot null(J))}{n - d} \quad \textbf{(Eq. A1.8)}$$

$$NGEV = \frac{trace((J \cdot J^T)^{-1} \cdot J \cdot C \cdot J^T)}{d} \quad \textbf{(Eq. A1.9)}$$

Inter-subject comparisons are made using the Index of Motor Abundance (IMA), a difference metric normalized to total local variance that indicates selective use of redundancy to stabilize whole leg function (Eqs. A1.10-11).

$$IMA = \frac{(GEV - NGEV)}{TOTV} \qquad \textbf{(Eq. A1.10)}$$

$$TOTV = \frac{trace(C)}{n} \qquad \textbf{(Eq. A1.11)}$$

IMA values greater than zero (IMA>0) indicate non-random structuring of individual leg-force variance over many gait cycles that act to minimize variance in (i.e., stabilize) net-force goal variable performance across many steps.

A1.2 Inter-leg (2DOF) de-stabilization of anterior-posterior leg-force

Applying the UCM analysis to other potential locomotor goals follows the same analysis presented above, but requires a specific Jacobian derivation for each tested goal. The proposed manifold for inter-leg stabilization of anterior-posterior leg-forces is also an arithmetic sum (Eq. A1.12) and results in a Jacobian (Eq. A1.13) identical to that for vertical net-force stabilization:

$$F_{ap}^{lead} + F_{ap}^{trail} = F_{ap}^{net} \qquad \textbf{(Eq. A1.12)}$$

$$J = \begin{bmatrix} 1 & 1 \end{bmatrix} \qquad \textbf{(Eq. A1.13)}$$

In this case, however, the leading leg forces will all be negative as they are directed along the leg opposite the direction of progression to apply braking forces to slow center-of-mass progression. We therefore expected leg-force combinations to move anterior-posterior net-force away from the proposed manifold, thus destabilizing anterior-posterior net-force for step-to-step modulation to maintain walking speed.

A1.3 Intra-leg (3DOF) stabilization of vertical leg-force

Calculating the effect of joint-torques to leg-force is based on principles from robotics control. Mapping joint-torques to leg force requires a two dimensional planar manifold within three dimensional joint-torque space. This manifold is found by solving for the basis vector of joint torques (ε_k) that solve the general equation:

$$0 = \left[(J \cdot M^{-1} \cdot J^T)^{-1} \cdot J \cdot M^{-1}\right] \cdot A \cdot \varepsilon_k \qquad \textbf{(Eq. A1.14)}$$

In this general equation, the term $\left[(J \cdot M^{-1} \cdot J^T)^{-1} \cdot J \cdot M^{-1}\right]$ is the transpose of the dynamically consistent generalized inverse of $\boldsymbol{J}$ and provides end point force when multiplied by segmental torques (Khatib 1987). In this case, $\boldsymbol{J}$ is the kinematic Jacobian matrix calculated from the geometric relationship of joint angles to end point position relative to a global reference frame. When joint angles are mapped to the vertical component of end point position, $\boldsymbol{J}$ is:

$$J = \left[-l_1 \cos(\theta_1) \quad -l_2 \cos(\theta_2) \quad -l_3 \cos(\theta_3)\right] \qquad \textbf{(Eq. A1.15)}$$

$\boldsymbol{M}$ is the mass matrix of the full dynamical equation of motion where l refers to calculated segment length and m to segment mass. $\boldsymbol{I}$ is the segment rotational inertia from the segment's distal end, and d is the fractional distance from the segment's distal end to its center-of-mass estimated from an anthropometric model (Winter 1980). θ

represents the segment angle of the segment relative to the horizontal in the sagittal plane. For each of these variables, subscripts denote the relevant leg segment (1=foot, 2=shank, 3=thigh):

$$M = \begin{bmatrix} l_1^2(m_2+m_3)+I_1 & l_1(l_2m_3+m_2l_2d_2)\cos(\theta_1-\theta_2) & l_1m_3l_3d_3\cos(\theta_1-\theta_3) \\ l_1(l_2m_3+m_2l_2d_2)\cos(\theta_1-\theta_2) & l_2^2m_3+I_2 & l_2m_3l_3d_3\cos(\theta_2-\theta_3) \\ l_1m_3l_3d_3\cos(\theta_1-\theta_3) & l_2m_3l_3d_3\cos(\theta_2-\theta_3) & I_3 \end{bmatrix}$$

(**Eq. A1.16**)

A converts joint torques to segmental torques as required by the general equation (**Eq. A1.14**) above:

$$A = \begin{bmatrix} 1 & 0 & 0 \\ -1 & 1 & 0 \\ 0 & -1 & 1 \end{bmatrix} \quad \textbf{(Eq. A1.17)}$$

The remaining calculation of GEV, NGEV, and IMA required to apply the UCM analysis to this potential goal, follows the same analysis presented above (section A1.1), using this appropriately derived Jacobian relating joint-torques to vertical leg-force generation.

A1.4 Intra-leg (3DOF) stabilization of anterior-posterior leg-force

Calculating the manifold for joint-torques to anterior-posterior leg-force is identical to that of the manifold for vertical leg-force presented above but with a different kinematic Jacobian matrix. In this case, the geometrical relationship between joint-angles and anterior-posterior leg position within global Cartesian space is:

$$J = \begin{bmatrix} l_1\sin(\theta_1) & l_2\sin(\theta_2) & l_3\sin(\theta_3) \end{bmatrix} \quad \textbf{(Eq. A1.18)}$$

The remaining analysis for applying the UCM follows the procedure described above (section A1.1) with the Jacobian appropriately derived relating joint-torques to anterior-posterior leg-force.

REFERENCES

Abe, M. O. and D. Sternad (2013). "Directionality in distribution and temporal structure of variability in skill acquisition." Frontiers in Human Neuroscience **7**.

Af Klint, R., N. Mazzaro, et al. (2010). "Load Rather Than Length Sensitive Feedback Contributes to Soleus Muscle Activity During Human Treadmill Walking." Journal of Neurophysiology **103**(5): 2747-2756.

Alcaide-Aguirre, R. E., D. C. Morgenroth, et al. (2013). "Motor control and learning with lower-limb myoelectric control in amputees." Journal of Rehabilitation Research and Development **50**(5): 687-698.

Auyang, A. G. and Y. H. Chang (2013). "Effects of a Foot Placement Constraint on Use of Motor Equivalence during Human Hopping." PloS One **8**(7).

Auyang, A. G., J. T. Yen, et al. (2009). "Neuromechanical stabilization of leg length and orientation through interjoint compensation during human hopping." Experimental Brain Research **192**(2): 253-264.

Auyang, A. G.-Y. (2010). Robistness and hierarchical control of performance variables through coordinataion during human locomotrion. Applied Physiology, Georgia Institute of Technology.

Barnett, C., R. Polman, et al. (2013). "Longitudinal kinematic and kinetic adaptations to obstacle crossing in recent lower limb amputees." Prosthetics and Orthotics International.

Barnett, C., N. Vanicek, et al. (2009). "Kinematic Gait Adaptations in Unilateral Transtibial Amputees During Rehabilitation " Prosthetics and Orthotics International **33**.

Barnett, C. T., N. Vanicek, et al. (2013). "Postural responses during volitional and perturbed dynamic balance tasks in new lower limb amputees: A longitudinal study." Gait & Posture **37**(3): 319-325.

Bastian, A. J. (2008). "Understanding sensorimotor adaptation and learning for rehabilitation." Current Opinion in Neurology **21**: 628-633.

Bauman, J. M. and Y. H. Chang (2013). "Rules to limp by: joint compensation conserves limb function after peripheral nerve injury." Biology Letters **9**(5).

Bennett, B. C., S. D. Russell, et al. (2010). "Angular momentum of walking at different speeds." Human Movement Science **29**: 114-124.

Bernstein, N. (1967). The Co-ordination and Regulation of Movements, Pergamon Press Ltd.

Beurskens, R., J. M. Wilken, et al. (2014). "Dynamic stability of individuals with transtibial amputation walking in destabilizing environments." Journal of Biomechanics **47**: 1675-1681

.

Boeltz, T., M. Ireland, et al. (2013). "Effects of treadmill training on functional recovery following peripheral nerve injury in rats." Journal of Neurophysiology **109**(11): 2645-2657.

Bonnet, X., C. Villa, et al. (2014). "Mechanical work performed by individual limbs of transfemoral amputees during step-to-step transitions: Effect of walking velocity." Proceedings of the Institution of Mechanical Engineers Part H-Journal of Engineering in Medicine **228**(1): 60-66.

Bosco, G. and R. E. Poppele (2000). "Reference Frames for Spinal Proprioception: Kinematics Based or Kinetics Based?" Journal of Neurophysiology **83**: 2946-2955.

Bosco, G., R. E. Poppele, et al. (2000). "Reference Frames for Spinal Proprioception: Limb Endpoint Based or Joint-Level Based?" Journal of Neurophysiology **83**: 2931-2945.

Buckley, J. G., A. R. De Asha, et al. (2013). "Understanding adaptive gait in lower-limb amputees: insights from multivariate analyses." Journal of Neuroengineering and Rehabilitation **10**.

Cabel, D. W., P. Cisek, et al. (2001). "Neural activity in primary motor cortex related to mechanical loads applied to the shoulder and elbow during a postural task." Journal of Neurophysiology **86**(4): 2102-2108.

Capaday, C. (2002). "The special nature of human walking and its neural control." Trends in Neurosciences **25**(7): 370-376.

Cavagna, G. A. and M. Kaneko (1977). "Mechanical Work and Efficiency in Level Walking and Running." Journal of Physiology-London **268**(2): 467-481.

Chang, Y.-H., A. G. Auyang, et al. (2009). "Whole limb kinematics are preferentially conserved over individual joint kinematics after peripheral nerve injury." The Journal of Experimental Biology **212**: 3511-3521.

Childers, W. L., B. I. Prilutsky, et al. (2014). "Motor adaptation to prosthetic cycling in people with trans-tibial amputation." Journal of Biomechanics **in press**.

Cho, G., M. Thajchayapong, et al. (2013). Adaptation of Step-to-step Mechanical Work on Center O Mass During Split-belt Treadmill Walking. American Society of Biomechanics, Omaha, NE.

Choi, J. T. and A. J. Bastian (2007). "Adaptation reveals independent control networks for human walking." Nature Neuroscience **10**(8): 1055-1062.

Choi, J. T., E. P. G. Vining, et al. (2009). "Walking flexibility after hemispherectomy: split-belt treadmill adaptation and feedback control." Brain **132**: 722-733.

Chvatal, S. A. and L. H. Ting (2012). "Voluntary and Reactive Recruitment of Locomotor Muscle Synergies during Perturbed Walking." Journal of Neuroscience **32**(35): 12237-12250.

Chvatal, S. A. and L. H. Ting (2013). "Common muscle synergies for balance and walking." Frontiers in Computational Neuroscience **7**.

Chvatal, S. A., G. Torres-Oviedo, et al. (2011). "Common muscle synergies for control of center of mass and force in nonstepping and stepping postural behaviors." Journal of Neurophysiology **106**(2): 999-1015.

Cohen, R. G. and D. Sternad (2012). "State space analysis of timing: exploiting task redundancy to reduce sensitivity to timing." Journal of Neurophysiology **107**(2): 618-627.

Collins, S., A. Ruina, et al. (2005). "Efficient Bipedal Robots Based on Passive-Dynamic Walkers." Science **307**: 1082-1085.

Collins, S. H. (2008). Dynamic Walking Principles Applied to Human Gait. Mechanical Engineering University of Michigan.

Collins, S. H. and A. D. Kuo (2010). "Recycling Energy to Restore Impaired Ankle Function during Human Walking." PloS One **5**(2).

Cronin, N. J., J. Avela, et al. (2013). "Differences in contractile behaviour between the soleus and medial gastrocnemius muscles during human walking." Journal of Experimental Biology **216**(5): 909-914.
Curtze, C., A. L. Hof, et al. (2010). "Balance recovery after an evoked forward fall in unilateral transtibial amputees." Gait & Posture **32**(3): 336-341.
Curtze, C., A. L. Hof, et al. (2012). "The relative contributions of the prosthetic and sound limb to balance control in unilateral transtibial amputees." Gait & Posture **36**(2): 276-281.
Czerniecki, J. M., A. P. Turner, et al. (2012). "Mobility Changes in Individuals With Dysvascular Amputation From the Presurgical Period to 12 Months Postamputation." Archives of Physical Medicine and Rehabilitation **93**(10): 1766-1773.
Daley, M. A. and A. A. Biewener (2006). "Running over rough terrain reveals limb control for intrinsic stability." Proceedings of the National Academy of Sciences of the United States of America **103**(42): 15681-15686.
Daley, M. A., G. Felix, et al. (2007). "Running stability is enhanced by a proximo-distal gradient in joint neuromechanical control." Journal of Experimental Biology **210**(3): 383-394.
Davies, B. and D. Datta (2003). "Mobility outcome following unilateral lower limb amputation." Prosthetics and Orthotics International **27**: 186-190.
Detrembleur, C., J. M. Vanmarsenille, et al. (2005). "Relationship between energy cost, gait speed, vertical displacement of centre of body mass and efficiency of pendulum-like mechanism in unilateral amputee gait." Gait & Posture **21**(3): 333-340.
Dietz, V., W. Zijlstra, et al. (1994). "Human neuronal interlimb coordination during split-belt locomotion." Exp Brain Res **101**: 513-520.
Domkin, D., J. Laczko, et al. (2005). "Joint angle variability in 3D bimanual pointing: uncontrolled manifold analysis." Exp Brain Res **163**: 44-57.
Domkin, D., J. Laczko, et al. (2002). "Structure of joint variability in bimanual pointing tasks." Experimental Brain Research **143**(1): 11-23.
Donelan, J. M., R. Kram, et al. (2002). "Mechanical work for step-to-step transitions is a major determinant of the metabolic cose of human walking." The Journal of Experimental Biology **205**: 3717-3727.
Donelan, J. M., R. Kram, et al. (2002). "Simultaneous positive and negative external mechanical work in human walking." Journal of Biomechanics **35**: 117-124.
Donelan, J. M., R. Kram, et al. (2002a). "Mechanical work for step-to-step transitions is a major determinant of the metabolic cost of human walking." Journal of Experimental Biology **205**(23): 3717-3727.
Donelan, J. M., R. Kram, et al. (2002b). "Simultaneous positive and negative external mechanical work in human walking." Journal of Biomechanics **35**(1): 117-124.
Donker, S. F. and P. J. Beek (2002). "Interlimb coordination in prosthetic walking: effects of asymmetry and walking velocity." Acta Psychologica **110**(2-3): 265-288.
Elbert, T. and B. Rockstroh (2004). "Reorganization of human cerebral cortex: The range of changes following use and injury." Neuroscientist **10**(2): 129-141.

Faist, M., C. Hoefer, et al. (2006). "In humans Ib facilitation depends on locomotion while suppression of Ib inhibition requires loading." Brain Research **1076**: 87-92.
Farris, D. J. and G. S. Sawicki (2012). "Human medial gastrocnemius force-velocity behavior shifts with locomotion speed and gait." Proceedings of the National Academy of Sciences of the United States of America **109**(3): 977-982.
Ferris, A. E., J. M. Aldridge, et al. (2012). "Evaluation of a Powered Ankle-Foot Prosthetic System During Walking." Archives of Physical Medicine and Rehabilitation **93**(11): 1911-1918.
Fey, N. P., G. K. Klute, et al. (2013). "Altering prosthetic foot stiffness influences foot and muscle function during below-knee amputee walking: A modeling and simulation analysis." Journal of Biomechanics **46**(4): 637-644.
Finley, J. M., A. J. Bastian, et al. (2013). "Learning to be economical: the energy cost of walking tracks motor adaptation." Journal of Physiology-London **591**(4): 1081-1095.
Garcia, M., A. Chatterjee, et al. (2000). "Efficiency, speed, and scaling of two-dimensional passive-dynamic walking." Dynamics and Stability of Systems **15**(2): 75-99.
Garcia, M., A. Chatterjee, et al. (1998). "The simplest walking model: Stability, complexity, and scaling." Journal of Biomechanical Engineering-Transactions of the Asme **120**(2): 281-288.
Gates, D. H., B. J. Darter, et al. (2012). "Comparison of walking overground and in a Computer Assisted Rehabilitation Environment (CAREN) in individuals with and without transtibial amputation." Journal of Neuroengineering and Rehabilitation **9**.
Gates, D. H., J. B. Dingwell, et al. (2012). "Gait characteristics of individuals with transtibial amputations walking on a destabilizing rock surface." Gait & Posture **36**(1): 33-39.
Gates, D. H., S. J. Scott, et al. (2013). "Frontal plane dynamic margins of stability in individuals with and without transtibial amputation walking on a loose rock surface." Gait & Posture **38**(4): 570-575.
Geertzen, J. H. B., J. D. Martina, et al. (2001). "Lower limb amputation Part 2: Rehabilitation - a 10 year literature review." Prosthetics and Orthotics International **25**: 14-20.
Ghez, C. and R. Sainburg (1995). "Proprioceptive Control of Interjoint Coordination." Canadian Journal of Physiology and Pharmacology **73**(2): 273-284.
Goldberg, E. J., P. S. Requejo, et al. (2008). "The effect of direct measurement versus cadaver estimates of anthropometry in the calculation of joint moments during above-knee prosthetic gait in pediatrics." Journal of Biomechanics **41**(3): 695-700.
Gorniak, S., V. Zatsiorsky, et al. (2009). "Hierarchical control of static prehension: II. Multi-digit synergies." Experimental Brain Research **194**(1): 1-15.
Gorniak, S. L., V. M. Zatsiorsky, et al. (2007). "Emerging and disappearing synergies in a hierarchically controlled system." Experimental Brain Research **183**(2): 259-270.

Grabowski, A. M. and S. D'andrea (2013). "Effects of a powered ankle-foot prosthesis on kinetic loading of the unaffected leg during level-ground walking." Journal of Neuroengineering and Rehabilitation **10**.

Gruben, K. G. and W. L. Boehm (2012). "Force direction pattern stabilizes sagittal plane mechanics of human walking." Human Movement Science **31**(3): 649-659.

Hak, L., J. H. v. Dieen, et al. (2014). "Walking in an Unstable Environment: Strategies Used by Transtibial Amputees to Prevent Falling During Gait." Arch Phys Med Rehabil **in press**.

Hermodsson, Y., C. Ekdahl, et al. (1994). "Gait in male trans-tibial amputees: a comparative study with healthy subjects in relation to walking speed." Prosthetics and Orthotics International **18**: 68-77.

Herr, H. and M. Popovic (2008). "Angular momentum in human walking." The Journal of Experimental Biology **211**: 467-481.

Hohne, A., C. Stark, et al. (2011). "Effects of reduced plantar cutaneous afferent feedback on locomotor adjustments in dynamic stability during perturbed walking." Journal of Biomechanics **44**: 2194-2200.

Houdijk, H., E. Pollmann, et al. (2009). "The energy cost for the step-to-step transition in amptuee walking." Gait & Posture **30**(1): 35-40.

Houdijk, H., M. W. van Ooijen, et al. (2012). "Assessing Gait Adaptability in People With a Unilateral Amputation on an Instrumented Treadmill With a Projected Visual Context." Physical Therapy **92**(11): 1452-1460.

Hu, X. and D. Sternad (2007). Internal variability constrained to task irrelevant direction in skill acquisition and control. Neuroscience, SanDiego, CA, Society for Neuroscience.

Huang, H. J., R. Kram, et al. (2012). "Reduction of Metabolic Cost during Motor Learning of Arm Reaching Dynamics." Journal of Neuroscience **32**(6): 2182-2190.

Ishikawa, M., P. V. Komi, et al. (2005). "Muscle-tendon interaction and elastic energy usage in human walking." Journal of Applied Physiology **99**(2): 603-608.

Izawa, J., T. Rane, et al. (2008). "Motor adaptation as a process of reoptimization." Journal of Neuroscience **28**(11): 2883-2891.

Jayaram, G., B. Tang, et al. (2012). "Modulating locomotor adaptation with cerebellar stimulation." Journal of Neurophysiology **107**(11): 2950-2957.

Jensen, L., T. Prokop, et al. (1998). "Adaptational effects during human split-belt walking: influence of afferent input." Experimental Brain Research **118**(1): 126-130.

Kawato, M., K. Furukawa, et al. (1987). "A Hierarchical Neural-Network Model for Control and Learning of Voluntary Movement." Biological Cybernetics **57**(3): 169-185.

Kepple, T. M., K. L. Siegel, et al. (1997). "Relative contributions of the lower extremity joint moments to forward progression and support during gait." Gait & Posture **6**(1): 1-8.

Khatib, O. (1987). "A Unified Approach for Motion and Force Control of Robot Manipulators - the Operational Space Formulation." Ieee Journal of Robotics and Automation **3**(1): 43-53.

Kovac, I., V. Medved, et al. (2009). "Ground Reaction Force Analysis in Traumatic Transtibial Amputee Gait." Coll. Antropol. **33**(Suppl. 2): 107-114.
Kuo, A. (2002). "Energetics of Actively Powered Locomotion Using the Simplest Walking Model." Journal of Biomechanical Engineering **124**: 113-120.
Kuo, A. (2007). "The six determinants of gait and the inverted pendulum analogy: A dynamic walking perspective." Human Movement Science **26**: 617-656.
Kuo, A. D. (2002). "Energetics of actively powered locomotion using the simplest walking model." Journal of Biomechanical Engineering-Transactions of the Asme **124**(1): 113-120.
Kuo, A. D., J. M. Donelan, et al. (2005). "Energetic Consequences of Walking Like an Inverted Pendulum: Step-to-Step Transisitons." Exercise and Sport Sciences Reviews **33**(2): 88-98.
Kuo, A. D., J. M. Donelan, et al. (2005). "Energetic consequences of walking like an inverted pendulum: Step-to-step transitions." Exercise and Sport Sciences Reviews **33**(2): 88-97.
Kurtzer, I., J. A. Pruszynski, et al. (2006). "Primate upper limb muscles exhibit activity patterns that differ from their anatomical action during a postural task." Journal of Neurophysiology **95**(1): 493-504.
Kurz, M. J., T. N. Judkins, et al. (2008). "A passive dynamic walking robot that has a deterministic nonlinear gait." Journal of Biomechanics **41**: 1310-1316.
Lam, T., M. Anderschitz, et al. (2006). "Contribution of feedback and feedforward strategies to locomotor adaptations." Journal of Neurophysiology **95**(2): 766-773.
Latash, M., F. Fanion, et al. (2003). Coordination of multielement motor systems based on motor abundance. Progress in Motor Control: effects of age, disorder, and rehabilitation. M. Latash and M. Levin. Champagne, IL, Human Kinetics. **3:** 97-124.
Latash, M. L. (2012). "The bliss (not the problem) of motor abundance (not redundancy)." Experimental Brain Research **217**(1): 1-5.
Latash, M. L., J. F. Scholz, et al. (2001). "Structure of motor variability in marginially redundant multifinger force production tasks." Exp Brain Res **141**: 153-165.
Latash, M. L., J. F. Scholz, et al. (2002). "Finger coordination during discrete and oscillatory force production tasks." Exp Brain Res **146**: 419-432.
Lin-Chan, S.-J., D. H. Nielsen, et al. (2003). "The Effects of Added Prosthetic Mass on Physiologic Responses and Stride Frequency During Multiple Speeds of Walking in Persons With Transtibial Amputation." Arch Phys Med Rehabil **84**: 1865-1871.
Loeb, G. E., I. E. Brown, et al. (1999). "A hierarchical foundation for models of sensorimotor control." Experimental Brain Research **126**(1): 1-18.
Major, M. J., M. Twiste, et al. (2014). "The effects of prosthetic ankle stiffness on ankle and knee kinematics, prosthetic limb loading, and net metabolic cost of trans-tibial amputee gait." Clinical Biomechanics **29**(1): 98-104.
Martin, T. A., J. G. Keating, et al. (1996). "Throwing while looking through prisms .2. Specificity and storage of multiple gaze-throw calibrations." Brain **119**: 1199-1211.
Mawase, F., T. Haizler, et al. (2013). "Kinetic adaptation during locomotion on a split-belt treadmill." Journal of Neurophysiology **109**(8): 2216-2227.

McGeer, T. (1990). "Passive Dynamic Walking." International Journal of Robotics Research **9**(2): 62-82.
McKay, J. L. and L. H. Ting (2012). "Optimization of Muscle Activity for Task-Level Goals Predicts Complex Changes in Limb Forces across Biomechanical Contexts." PLoS Computational Biology **8**(4).
Miller, D. I. (1987). "Resultant Lower-Extremity Joint Moments in Below-Knee Amputees during Running Stance." Journal of Biomechanics **20**(5): 529-541.
Miller, W. C., A. B. Deathe, et al. (2001). "The influence of falling, fear of falling, and balance confidence on prosthetic mobility and social activity among individuals with a lower extremity amputation." Archives of Physical Medicine and Rehabilitation **82**(9): 1238-1244.
Miller, W. C., M. Speechley, et al. (2001). "The prevalence and risk factors of falling and fear of falling among lower extremity amputees." Archives of Physical Medicine and Rehabilitation **82**(8): 1031-1037.
Morton, S. M. and A. J. Bastian (2006). "Cerebellar Contributions to Locomotor Adaptations during Splitbelt Treadmill Walking." The Journal of Neuroscience **26**(36): 9107-9116.
Muller, H. and D. Sternad (2004). "Decomposition of Variability in the Execution of Goal-Oriented Tasks: Three Components of Skill Improvement." Journal of Experimental Psychology: Human Perception and Performance **30**(1): 212-233.
Muller, H. and D. Sternad (2009). "Motor Learning: Changes in the Structure of Variability in a Redundant Task." Progress in Motor Control **629**: 439-456.
Munin, M. C., M. C. Espejo-DeGuzman, et al. (2001). "Predictive factors for successful early prosthetic ambulation among lower-limb amputees." Journal of Rehabilitation Research and Development **38**(4): 379-384.
Nederhand, M. J., E. H. F. Van Asseldonk, et al. (2012). "Dynamic Balance Control (DBC) in lower leg amputee subjects; contribution of the regulatory activity of the prosthesis side." Clinical Biomechanics **27**(1): 40-45.
Neptune, R. R., S. A. Kautz, et al. (2001). "Contributions of the individual ankle plantar flexors to support, forward progression and swing initiation during walking." Journal of Biomechanics **34**(11): 1387-1398.
Neptune, R. R. and K. Sasaki (2005). "Ankle plantar flexor force production is an important determinant of the preferred walk-to-run transition speed." Journal of Experimental Biology **208**(5): 799-808.
Nguyen, T. C. and K. J. Reynolds (2014). "The effect of variability in body segment parameters on joint moment using Monte Carlo simulations." Gait & Posture **39**(1): 346-353.
Nichols, T. R. (1999). "Receptor mechanisms underlying heterogenic reflexes among the triceps surae muscles of the cat." Journal of Neurophysiology **81**(2): 467-478.
Nielsen, J. b. and T. Sinkjaer (2002). "Afferent feedback in the control of human gait." Journal of Electromyography and Kinesiology **12**: 213-217.
Nolan, L., A. Wit, et al. (2003). "Adjustments in gait symmetry with walking speeds in trans-femoral and trans-tibial amputees." Gait & Posture **17**: 142-151.
Ogawa, T., N. Kawashima, et al. (2014). "Predictive control of ankle stiffness at heel contact is a key element of locomotor adaptation during split-belt treadmill walking in humans." Journal of Neurophysiology **111**(4): 722-732.

Oh, K., J. Baek, et al. (2012). "Gait strategy changes with acceleration to accommodate the biomechanical constraint on push-off propulsion." Journal of Biomechanics **45**(16): 2920-2926.
Park, H. W. and S. Park (2013). "Increase of push-off propulsion to compensate heel strike loss during step-to-step transition is limited at faster gait speeds." International Journal of Precision Engineering and Manufacturing **14**(5): 825-829.
Powers, C. M., S. Rao, et al. (1998). "Knee kinetics in trans-tibial amputee gait " Gait & Posture **8**: 1-7.
Prokop, T., W. Berger, et al. (1995). "Adaptational and Learning-Processes during Human Split-Belt Locomotion - Interaction between Central Mechanisms and Afferent Input." Experimental Brain Research **106**(3): 449-456.
Reisman, D. S., A. J. Bastian, et al. (2010). "Neurophysiologic and Rehabilitation Insights From the Split-Belt and Other Locomotor Adaptation Paradigms." Physical Therapy **90**(2): 187-195.
Reisman, D. S., H. J. Block, et al. (2005). "Interlimb Coordination During Locomotion: What Can be Adapted and Stored?" Journal of Neurophysiology **94**: 2403-2415.
Reisman, D. S., R. Wityk, et al. (2007). "Locomotor adaptation on a split-belt treadmill can improve walking symmetry post-stroke." Brain **130**: 1861-1872.
Robert, T., B. C. Bennett, et al. (2009). "Angular momentum synergies during walking." Experimental Brain Research **197**(2): 185-197.
Roberts, T. J. (2002). "The integrated function of muscles and tendons during locomotion." Comparative Biochemistry and Physiology a-Molecular and Integrative Physiology **133**(4): 1087-1099.
Roberts, T. J. and E. Azizi (2011). "Flexible mechanisms: the diverse roles of biological springs in vertebrate movement." Journal of Experimental Biology **214**(3): 353-361.
Roberts, T. J. and R. L. Marsh (2003). "Probing the limits to muscle-powered accelerations: lessons from jumping bullfrogs." Journal of Experimental Biology **206**(15): 2567-2580.
Roemmich, R. T., E. L. Stegemoller, et al. (2012). "Lower extremity sagittal joint moment production during split-belt treadmill walking." Journal of Biomechanics **45**(16): 2817-2821.
Roper, J. A., E. L. Stegemoller, et al. (2013). "Oxygen consumption, oxygen cost, heart rate, and perceived effort during split-belt treadmill walking in young healthy adults." European Journal of Applied Physiology **113**(3): 729-734.
Rosenblatt, N. J., C. P. Hurt, et al. (2014). "An apparent contradiction: increasing variability to achieve greater precision?" Experimental Brain Research **232**(2): 403-413.
Ruina, A., J. E. A. Bertram, et al. (2005). "A collisional model of the energetic cost of support work qualitatively explains leg sequencing in walking and galloping, pseudo-elastic leg behavior in running and the walk-to-run transition." Journal of Theoretical Biology **237**: 170-192.
Rusaw, D., K. Hagberg, et al. (2012). "Can vibratory feedback be used to improve postural stability in persons with transtibial limb loss?" Journal of Rehabilitation Research and Development **49**(8): 1239-1253.

Rybak, I. A., K. Stecina, et al. (2006). "Modelling spinal circuitry involved in locomotor pattern generation: insights from the effects of afferent stimulation." Journal of Physiology-London **577**(2): 641-658.
Sagawa, Y., K. Turcot, et al. (2011). "Biomechanics and physiological parameters during gait in lower-limb amputees: A systematic review." Gait & Posture **33**: 511-526.
Sainburg, R. L., M. F. Ghilardi, et al. (1995). "Control of Limb Dynamics in Normal Subjects and Patients without Proprioception." Journal of Neurophysiology **73**(2): 820-835.
Sanderson, D. J. and P. E. Martin (1997). "Lower extremity kinematic and kinetic adaptations in unilateral below-knee amputees during walking." Gait & Posture **6**: 126-136.
Sangani, S. G., A. J. Starsky, et al. (2007). "Multijoint reflexes of the stroke arm: Neural coupling of the elbow and shoulder." Muscle & Nerve **36**(5): 694-703.
Sawa, R., T. Doi, et al. (2013). "Decreased skin temperature of the foot increases gait variability in healthy young adults." Gait & Posture **38**(3): 518-522.
Sawers, A. and M. E. Hahn (2012). "Regulation of whole-body frontal plane balance varies within a step during unperturbed walking." Gait & Posture **36**(2): 322-324.
Sawers, A. and M. E. Hahn (2013). "Gradual training reduces practice difficulty while preserving motor learning of a novel locomotor task." Human Movement Science **32**(4): 605-617.
Sawers, A., M. E. Hahn, et al. (2012). "Beyond componentry: How principles of motor learning can enhance locomotor rehabilitation of individuals with lower limb loss-A review." Journal of Rehabilitation Research and Development **49**(10): 1431-1441.
Sawers, A., V. E. Kelly, et al. (2013). "Effects of Gradual Versus Sudden Training on the Cognitive Demand Required While Learning a Novel Locomotor Task." Journal of Motor Behavior **45**(5): 405-414.
Sawers, A., V. E. Kelly, et al. (2013). "Gradual training reduces the challenge to lateral balance control during practice and subsequent performance of a novel locomotor task." Gait & Posture **38**(4): 907-911.
Sawers, A. B. (2012). A Gradual vs. Sudden Introduction to Novel Locomotor Task Requirements: Consequences for Motor Learning, Balance Control and Cognitive Demand. Rehabilitation Science, University of Washington.
Scholz, J. P. and G. Schoner (1999). "The uncontrolled manifold concept: Identifying control variables for a functional task." Exp Brain Res **126**: 289-306.
Scholz, J. P., G. Schoner, et al. (2000). "Identifying the control strucutre of multijoint coordination during pistol shooting." Exp Brain Res **135**: 382-404.
Schoner, G. and J. A. S. Kelso (1988). "Dynamic Pattern Generation in Behavioral and Neural Systems." Science **239**(4847): 1513-1520.
Selles, R. W., J. B. J. Bussmann, et al. (1999). "Effects of prosthetic mass and mass distribution on kinematics and energetics of prosthetic gait: A systematic review." Archives of Physical Medicine and Rehabilitation **80**(12): 1593-1599.
Selles, R. W., S. Korteland, et al. (2003). "Lower-Leg Inertial Properties in Transtibial Amputees and Control Subjects and Their Influence on the Swing Phase During Gait." Arch Phys Med Rehabil **84**: 569-577.

Shim, J. K., M. L. Latash, et al. (2003). "Prehension synergies: trial-to-trial variability and hierarchical organization of stable performance." Experimental Brain Research **152**(2): 173-184.
Shymway-Cook, A. and M. Woollacott (2001). Motor control: theory and practical applications. Philadelphia, Lippincott Williams & Wilki.
Silverman, A. K. and R. R. Neptune (2011). "Differences in whole-body angular momentum between below-knee amputees and non-amputees across walking speeds." Journal of Biomechanics **44**(3): 379-385.
Smith, J. D. and P. E. Martin (2013). "Effects of Prosthetic Mass Distribution on Metabolic Costs and Walking Symmetry." Journal of Applied Biomechanics **29**(3): 317-328.
Smith, M. A., A. Ghazizadeh, et al. (2006). "Interacting Adaptive Processes wth Difference Timescales Underlie Short-Term Motor Learning." PLoS Biology **4**(6): 1035-1043.
Stahl, V. A. and T. R. Nichols (2011). "Short-Term Effects of Muscular Denervation and Fasciotomy on Global Limb Variables during Locomotion in the Decerebrate Cat." Cells Tissues Organs **193**(5): 325-335.
Su, J. L. S. and J. B. Dingwell (2007). "Dynamic stability of passive dynamic walking on an irregular surface." Journal of Biomechanical Engineering-Transactions of the Asme **129**(6): 802-810.
Su, P.-F., S. A. Gard, et al. (2007). "Gait characteristics of persons with bilateral transtibial amputations." Journal of Rehabilitation Research and Development **44**(4): 491-502.
Svoboda, Z., M. Janura, et al. (2012). "Variability of kinetic variables during gait in unilateral transtibial amputees." Prosthetics and Orthotics International **36**.
Thajchayapong, M., G. Cho, et al. (2014). Changes in total mechanical work explain why metabolic cost tracks locomotor adaptation during split belt walking. World Congress of Biomechanics, Boston, MA.
Ting, L. H., C. C. Raasch, et al. (1998). "Sensorimotor state of the contralateral leg affects ipsilateral muscle coordination of pedaling." Journal of Neurophysiology **80**(3): 1341-1351.
Todorov, E. and M. I. Jordan (2002). "Optimal feedback control as a theory of motor coordination." Nature Neuroscience **5**(11): 1226-1235.
Toney, M. E. and Y. H. Chang (2013). "Humans robustly adhere to dynamic walking principles by harnessing motor abundance to control forces." Experimental Brain Research **231**(4): 433-443.
Vasudevan, E. V. L. and A. J. Bastian (2010). "Split-Belt Treadmill Adaptation Shows Different Functional Networks for Fast and Slow Human Walking." Journal of Neurophysiology **103**(1): 183-191.
Ventura, J. D., G. K. Klute, et al. (2011). "The effect of prosthetic ankle energy storage and return properties on muscle activity in below-knee amputee walking." Gait & Posture **33**: 220-226.
Verdaasdonk, B. W., H. F. J. M. Koopman, et al. (2009). "Energy efficient walking with central pattern generators: from passive dynamic walking to biologically inspired control." Biological Cybernetics **101**(1): 49-61.

Vrieling, A. H., H. G. van Keeken, et al. (2007). "Obstacle crossing in lower limb amputees." Gait & Posture **26**(4): 587-594.
Waters, R. L. and S. Mulroy (1999). "The energy expenditure of normal and pathologic gait." Gait & Posture **9**(3): 207-231.
Wilmink, R. J. H. and T. R. Nichols (2003). "Distribution of heterogenic reflexes among the quadriceps and triceps surae muscles of the cat hind limb." Journal of Neurophysiology **90**(4): 2310-2324.
Winter, D. A. (1980). "Overall Principle of Lower-Limb Support during Stance Phase of Gait." Journal of Biomechanics **13**(11): 923-927.
Winter, D. A. and S. E. Sienko (1988). "Biomechanics of Below-Knee Amputee Gait." Journal of Biomechanics **21**(5): 361-367.
Wu, H. G., Y. R. Miyamoto, et al. (2014). "Temporal structure of motor variability is dynamically regulated and predicts motor learning ability." Nature Neuroscience **17**(2): 312-321.
Wurdeman, S. R., S. A. Myers, et al. (2013). "Transtibial Amputee Joint Motion has Increased Attractor Divergence During Walking Compared to Non-Amputee Gait." Annals of Biomedical Engineering **41**(4): 806-813.
Yang, J.-F., J. P. Scholz, et al. (2007). "The role of kinematic redundancy in adaptation of reaching." Exp Brain Res **176**: 54-69.
Yang, J. F. and J. P. Scholz (2005). "Learning a throwing task is associated with differential changes in the use of motor abundance." Experimental Brain Research **163**(2): 137-158.
Yen, J. T., A. G. Auyang, et al. (2009). "Joint-level kinetic redundancy is exploited to control limb-level forces during human hopping." Experimental Brain Research **196**(3): 439-451.
Yen, J. T. and Y.-H. Chang (2010). "Rate-dependent control strategies stabilize limb forces during human locomotion." Journal of the Royal Society Interface **7**(46): 801-810.
Yen, J. T.-B. (2011). Force Control During Human Bouncing Gaits. Biomedical Engineering, Georgia Institute of Technology.
Zajac, F. E., R. R. Neptune, et al. (2002). "Biomechanics and muscle coordination of human walking - Part I: Introduction to concepts, power transfer, dynamics and simulations." Gait & Posture **16**(3): 215-232.
Zajac, F. E., R. R. Neptune, et al. (2003). "Biomechanics and muscle coordination of human walking Part II: Lessons from dynamical simulations and clinical implications." Gait & Posture **17**(1): 1-17.
Zelik, K. E., S. H. Collins, et al. (2011). "Systematic Variation of Prosthetic Foot Spring Affects Center-of-Mass Mechanics and Metabolic Cost During Walking." Ieee Transactions on Neural Systems and Rehabilitation Engineering **19**(4): 411-419.
Zelik, K. E., T. W. P. Huang, et al. (2014). "The role of series ankle elasticity in bipedal walking." Journal of Theoretical Biology **346**: 75-85.
Zmitrewicz, R. J., R. R. Neptune, et al. (2006). "The Effect of Foot and Ankle Prosthetic Components on Braking and Propulsive Impulses During Transtibial Amputee Gait." Arch Phys Med Rehabil **87**: 1334-1339.